Polar Biology
https://doi.org/10.1007/s00300-020-02736-w

ORIGINAL PAPER

Auditory biology of bearded seals (*Erignathus barbatus*)

Jillian M. Sills[1] · Colleen Reichmuth[1,2] · Brandon L. Southall[1,3] · Alex Whiting[4] · John Goodwin[4]

Received: 8 November 2019 / Revised: 13 August 2020 / Accepted: 18 August 2020

Abstract

Bearded seals (*Erignathus barbatus*) have a circumpolar Arctic distribution and are closely associated with unstable pack ice, spending nearly all of their lives in remote habitats. As a result, their biology and behavior remain largely unknown. With respect to sensory biology, bearded seals—like other marine mammals—rely on acoustic cues to support a range of vital behaviors. Acoustic monitoring from moored instrumentation has revealed a rich repertoire of underwater calls associated with the breeding season. However, the ability of bearded seals to perceive sound has never been investigated. In this study, species-typical auditory profiles were obtained from two young male bearded seals trained to cooperate in a go/no-go sound detection paradigm. Hearing thresholds were measured for underwater tonal sounds at frequencies between 0.1 and 61 kHz, in quiet conditions and in the presence of octave-band masking noise. The bearded seals displayed sensitive underwater hearing with peak sensitivity near 50 dB re 1 µPa and a broad frequency range of best hearing extending from approximately 0.3 to 45 kHz. Additionally, the two seals performed particularly well compared to other mammals when detecting target signals embedded within background noise; critical ratios ranged from 12 to 30 dB between 0.1 and 25.6 kHz. These findings improve understanding of the acoustic ecology of bearded seals, inform best management practices related to anthropogenic noise in Arctic habitats, and provide insight into comparative auditory capabilities within the lineage of phocid seals.

Keywords Bearded seal · Acoustic ecology · Audiogram · Hearing · Arctic · Noise

Introduction

True seals (family Phocidae) are amphibious carnivores comprising 18 extant species. Within the Phocidae lineage, the Phocinae subfamily includes 10 species inhabiting the North Pacific, North Atlantic, and circumpolar seas of the northern hemisphere, as well as some freshwater regions. The largest of these 'northern' phocids is the bearded seal (*Erignathus barbatus,* Erxleben 1777), which—as the earliest diverging lineage in the Phocinae subfamily—is sister to the remaining nine northern seals and is separated from these related species by 11 to 17 million years (Árnason et al. 2006; Higdon et al. 2007; Fulton and Strobeck 2010). Bearded seals have a pan-Arctic distribution and are closely associated with unstable pack ice, spending nearly all of their lives in remote habitats and moving in association with the seasonal advance and retreat of sea ice (Burns 1981; Simpkins et al. 2003; Frost et al. 2008). They are of particular interest due to their importance as a subsistence resource and their presumed vulnerability to the effects of climate change, including diminishing sea ice, increased environmental variability, and expanding human activities in their Arctic habitat. As a result of these factors, the Beringia and Okhotsk distinct population segments of bearded seals are listed as threatened under the Endangered Species Act.

Bearded seals are unique among the true seals. They demonstrate multiple ancestral traits relative to the rest of their subfamily, including the presence of four mammary teats rather than two (King 1964); the lack of a white lanugo upon parturition, which emerged later in the lineage and is presumably related to predator avoidance (Árnason et al. 2006); a genetic karyotype of $2n = 34$ rather than $2n = 32$

Electronic supplementary material The online version of this article (https://doi.org/10.1007/s00300-020-02736-w) contains supplementary material, which is available to authorized users.

✉ Jillian M. Sills
jmsills@ucsc.edu

[1] Long Marine Laboratory, Institute of Marine Sciences, University of California Santa Cruz, Santa Cruz, CA, USA

[2] Alaska SeaLife Center, Seward, AK, USA

[3] SEA, Inc., Aptos, CA, USA

[4] Native Village of Kotzebue, Kotzebue, AK, USA

Published online: 27 August 2020

chromosomes, a trait shared with all monachid (southern) seals but with only the hooded seal (*Cystophora cristata*) among northern phocids (Árnason et al. 2006); and smooth rather than beaded facial vibrissae, a feature present in only one other phocid—the monachid Hawaiian monk seal (*Neomonachus schauinslandi*) (King 1964; McHuron et al. 2020). Detailed anatomical investigations indicate that the skull morphology of bearded seals deviates from that of other seals. They have a notably wide, stout skull and a high, arched palate, features which may be adaptations for hydraulic jetting and suction feeding in these benthic foragers (King 1964; Burns and Frost 1979; Burns 1981; Marshall et al. 2008; Kienle and Berta 2016; Kienle et al. 2018). While they consume fish like other phocids, bearded seals are specialized suction feeders that tend to forage in shallow water (< 100 m) associated with pack ice, and rely predominantly on mollusks and crustaceans for sustenance (Lowry et al. 1980; Kingsley et al. 1985; Dehn et al. 2007; Cameron et al. 2010; Hamilton et al. 2018).

Bearded seals are known for their rich repertoire of underwater calls, apparently produced by males (Ray et al. 1969; Davies et al. 2006). In the cold, dark, and seasonally ice-covered waters of the Arctic, the eerie trills, moans, ascents, and sweeps of bearded seals are common (e.g., Van Parijs et al. 2001; Risch et al. 2007; Jones et al. 2014). Their often long-duration, high-amplitude underwater vocalizations can be detected above background noise tens of kilometers away (Cleator et al. 1989) and are present year-round in some locations, though they are associated primarily with the breeding season (e.g., Van Parijs et al. 2001; Hannay et al. 2013; MacIntyre et al. 2013; Jones et al. 2014; MacIntyre et al. 2015; Chou et al. 2020). Distinctive within their vocal repertoire are tonal downsweeps; only ribbon (*Histriophoca fasciata*) and Weddell seals (*Leptonychotes weddellii*) produce calls with similar features (Terhune 2018). However, as the ability of bearded seals to perceive sound has not been formally evaluated, it is difficult to understand how the auditory systems of these seals filter sound—including conspecific vocalizations—from the environment. Indigenous knowledge has shown that bearded seals are likely sensitive to the airborne sounds associated with subsistence hunting (J. Goodwin, unpublished data), but less is understood about their auditory sensitivity in water.

The hearing capabilities of other northern seals have been the focus of numerous investigations since the 1960s; recent examinations have revealed surprisingly acute sound reception capabilities in air along with a uniquely broad and highly sensitive range of hearing in water (see Reichmuth et al. 2013). Behavioral measures of underwater hearing ability are presently available for harbor (*Phoca vitulina*), ringed (*Pusa hispida*), spotted (*Phoca largha*), Caspian (*Pusa caspica*), and harp seals (*Pagophilus groenlandicus*) (see Southall et al. 2019). However, it is unknown whether these data for related species can accurately predict hearing abilities in bearded seals. Given the evolutionary, anatomical, and life history factors that isolate bearded seals from other northern seals, it is unclear what to expect in terms of their auditory capabilities. Similarities in hearing to other phocinae seals would imply that auditory adaptations common to all extant northern seals appeared 11 to 17 million years ago (Árnason et al. 2006; Higdon et al. 2007; Fulton and Strobeck 2010). Differences might provide insight into how hearing—specifically the expanded frequency range of sensitive underwater hearing—emerged within the true seal lineage. Such information would have relevance for species conservation and management, as well as for understanding selective pressures on hearing in seals.

Here, we present a series of behavioral experiments to evaluate species-typical underwater hearing capabilities in bearded seals. Auditory sensitivity curves were measured for two trained seals in quiet conditions across the frequency range of hearing to describe absolute (unmasked) auditory sensitivity. Hearing was then measured in the presence of controlled background noise; the resulting critical ratio measurements describe the frequency tuning of the auditory system, and can be used to conservatively assess the ability of bearded seals to detect sounds within environmental noise. This is particularly relevant as human activity—and its associated acoustic footprint—continues to expand rapidly in Arctic environments (for review, see Moore et al. 2012). This auditory research with bearded seals builds upon similar experiments conducted with spotted and ringed seals (Sills et al. 2014, 2015). Together, these three related studies provide fundamental knowledge about the auditory biology of seals and enable meaningful comparisons across individuals, environmental contexts, and species.

Materials and methods

Subjects

The subjects were young male bearded seals identified as *Siku* (NOA0010177) and *Noatak* (NOA0010270). These seals were collected in Kotzebue Sound, Alaska for participation in long-term research at Long Marine Laboratory at the University of California Santa Cruz. Subjects were 1 to 2 years old during testing, and both were apparently healthy individuals with no known ear injuries or ototoxic exposures. At the beginning of the study their body masses were 98 and 88 kg, respectively. Each seal typically received one-third to one-half of his daily diet (freshly thawed capelin and herring fish) for participation in experimental sessions, which were conducted once per day, 5 days per week. Diets were established to maintain healthy body condition and were not constrained for research purposes.

Testing environment

Testing was completed in two pools. Pool 1 was a circular, partially in-ground concrete pool 1.8 m deep and 7.6 m in diameter, which was lined with epoxy. Pool 2 was a circular, above-ground fiberglass pool 1.8 m deep and 9.1 m in diameter. Both pools were filled with filtered seawater of 11 to 18 °C. Bearded seal *Siku* completed all testing in Pool 1. Bearded seal *Noatak* completed low-frequency testing ($\leq$6.4 kHz absolute thresholds, $\leq$800 Hz masked thresholds) in Pool 1, with the remainder of his thresholds measured in Pool 2. This seal repeated testing for one absolute and one masked threshold in both pools to confirm that there was no difference in the measured values based on testing environment.

The experimental apparatus (*listening station*) was comprised of a water-filled PVC frame with a mounted chin rest, where the seal could reliably position his head at 1 m depth near the edge of the pool. The listening station included a light to denote the interval of each test trial, a response target that could be pressed upon detection of a signal, and an underwater camera that enabled a remote experimenter to view the seal in real time. The chin rest also included an embedded latency switch that the animal was trained to depress with his nose to initiate each trial; this switch was used to measure the time between signal onset and release of the switch as the subject moved to touch the response target.

Pools were made as quiet as possible during testing by eliminating water flow and activity in adjacent areas. To quantify ambient noise, measurements were taken each day at the center position of the seal's head during testing. A calibrated TC4032 low-noise hydrophone (0.01–80 kHz, $\pm$2.5 dB; Teledyne Reson, Slangerup, Denmark) with a Reson EC6073 input module was used with a battery-powered 2270 sound analyzer (sampling rate 48 kHz; Brüel & Kjær A/S, Nærum, Denmark) to record 1 min unweighted noise samples. Percentile statistics of 1/3-octave-band levels were calculated from 1 min L_{eq} values for frequencies from 0.04 to 20 kHz. For frequencies from 20 to 62 kHz, a battery-powered FR-2 Field Memory Recorder (sampling rate 192 kHz; Fostex Company, Tokyo, Japan) was used with the TC4032 hydrophone to obtain comparable measurements on a subset of testing days. Threshold-to-noise offsets for the underwater audiogram were calculated as the difference between hearing threshold and ambient noise spectral density level—calculated from the median of 1/3-octave-band 50th percentile measurements (L50)—at each test frequency.

Audiometric procedure

The seals were gradually trained for husbandry and research behaviors using operant conditioning and positive reinforcement. Prior to the start of this study, they learned to participate in a go/no-go sound detection task. At the start of a testing session, one seal was provided access to the pool. A trainer prompted the seal to dive to the chin rest and initiate a 4-s interval delineated by the trial light. The seal touched the response target with his nose if he detected a signal during the trial interval, and remained still on the chin rest if he did not. Correct responses—reporting the presence or absence of the signal as appropriate—were marked by a conditioned reinforcer (acoustic buzzer) followed by primary reinforcement (fish) provided by the trainer at the surface. If the seal made an error—reporting signal detection on a signal-absent trial (*false alarm*) or failure to report a signal on a signal-present trial (*miss*)—he was called to the surface by the trainer and then allowed to proceed to the next trial. The trainer was unaware of individual trial conditions and received instructions via headphones from an experimenter who was located nearby in an isolated room.

Hearing thresholds were estimated using an adaptive staircase procedure (Cornsweet 1962). Frequencies were tested to completion in a mixed order, and the first test frequency was remeasured at the end of the study. Within a given session, signal frequency was the same while amplitude varied. Signal-present and signal-absent trials were conducted in pseudorandom order, with 50–70% signal-present trials within a session that included 40 to 60 trials. A session began and ended with several supra-threshold trials that served to maintain behavioral control on the task. In between these warm-up and cool-down trials was a test phase, during which signal level was decreased by 2 dB following each correct detection and raised by 4 dB after each miss until five hit-to-miss transitions (descending misses) within 6 dB of one another were obtained. Sessions were repeated on successive days until performance stabilized and the average level of descending misses varied by less than 3 dB across three sessions. Threshold was calculated from signal-present trials in these sessions using probit analysis (Finney 1971) and defined as the sound pressure level (SPL) in dB re 1 µPa corresponding to the 50% correct detection rate. Specifically, a psychometric function was fit to the proportion of correct detections at each signal level, and an inverse prediction was applied to calculate threshold at the 50% correct detection level. Threshold criteria were met when 95% confidence intervals on the psychometric function were less than 4 dB. To ensure comparable response bias across threshold measurements, performance on signal-absent trials was also considered. False alarm rate was determined as the proportion of signal-absent trials on which the seal incorrectly reported detection of a signal; responses prior to signal presentation on signal-present trials were also scored as false alarms. Threshold criteria included a test phase false alarm rate—pooled for each frequency across the

three sessions used to calculate threshold—that was above 0 and below 0.3.

Reaction times for correct signal detections were automatically recorded as the time between tone onset and release of the latency switch. These data were used to generate latency-intensity curves at each frequency with a least-squares power function (Moody 1970) that modeled reaction time relative to signal amplitude. Reaction times were interpolated at threshold (0 dB sensation level, SL) and at 20 dB above threshold (20 dB SL).

Absolute (unmasked) hearing thresholds

Sessions were conducted in quiet conditions to measure absolute underwater hearing thresholds. Thresholds were measured across the range of hearing at 13 frequencies, in octave steps from 0.1 to 25.6 kHz, one half-octave step to 36.2 kHz, and quarter-octave steps to 60.9 kHz. Test stimuli were 500 ms frequency-modulated upsweeps with 10% bandwidth (±5% from center frequency) and 5% rise and fall times, generated using National Instruments (NI) LabVIEW software (National Instruments Corp., Austin, TX, USA) with the Hearing Test Program (HTP) virtual instrument (Finneran 2003). Signals were sent through an NI USB-6259 BNC M-series data acquisition module with an update rate of 500 kHz and bandpass filtered using a 3364 anti-aliasing filter (Krohn-Hite, Brockton, MA, USA). Finally, a PA5 digital attenuator (Tucker-Davis Technologies, Alachua, FL, USA) and sometimes a P1000 power amplifier (Hafler Professional, Tempe, AZ, USA) were in line prior to the transducer in the test pool. This was a J-11 moving coil transducer (Naval Undersea Warfare Center, Newport, RI, USA) for 0.1–6.4 kHz signals, a LL1424 HP projector with an AC1424HP bridging transformer box (Lubell Labs, Columbus, OH, USA) for 3.2 kHz signals in Pool 2, or a 1042 projecting hydrophone (International Transducer Corporation, Santa Barbara, CA, USA) for 12.8–60.9 kHz signals. The speakers were decoupled from the underwater listening station and suspended into the pool 5–8 m behind the subject, in a frequency-specific location determined by spatial mapping of the received sound field.

Mapping of the sound field was conducted prior to testing at each frequency to ensure acceptable variability (±3 dB) in the test stimulus in the region surrounding the position of the seal's head during testing. A signal of fixed level was recorded at 24 positions within a 14 × 14 × 14 cm grid centered on the daily calibration position (i.e., the center of the seal's head at the depth of his ears). During testing, signals were calibrated in this position before each session. Calibration signals were measured across a range of amplitudes and evaluated in the frequency domain to compare expected with received SPLs and confirm signal integrity. The TC4032 hydrophone was used for mapping and daily stimulus calibration, and signals were returned through the same filter, NI hardware, and HTP software used for signal generation. The sampling rate was always 500 kHz.

Masked hearing thresholds and critical ratios

Threshold measurements were also obtained in the presence of octave-band masking noise centered on the test frequency. The hearing test procedure was identical except for the addition of the masking noise, which was always the same level and always paired with the interval of the trial light. Critical ratios (CRs) were measured as the difference (in dB) between the SPL of the masked hearing threshold and the spectral density level of the octave-band noise masker at the center frequency of the masking band (Fletcher 1940; Scharf 1970).

Underwater masked hearing thresholds were measured at nine frequencies in octave steps, to obtain critical ratios between 0.1 and 25.6 kHz. The same underwater test signals, mapping and calibration procedures, software, and hardware chains described above were used to measure hearing in the presence of octave-band noise. Noise stimuli were gated (500 ms rise time), flat-spectrum noise maskers generated using AVS Audio Editor 7.1 (Online Media Technologies Limited, London, UK), flattened through amplitude compensation with Adobe Audition CS6 (Adobe Systems Incorporated, San Jose, CA, USA), and analyzed with SpectraPLUS (Pioneer Hill Software LLC, Poulsbo, WA, USA). The 0.1–12.8 kHz maskers were transmitted from the sound card of a computer through the P1000 amplifier (where they mixed with the test signals) to the J-11, LL1424 HP, or 1042 projector in the test pool. The 25.6 kHz masker was generated and filtered using MATLAB (MathWorks, Natick, MA, USA), and then projected from the computer through a Roland Quad-Capture USB 2.0 Audio Interface (sampling rate 192 kHz; Roland Corporation US, Los Angeles, CA, USA) before reaching the amplifier. The target spectral density level (dB re (1 μPa)^2/Hz) of the masking noise was 10 dB above the absolute hearing threshold measured at the relevant frequency for the same subject, and was held constant throughout testing.

All noise stimuli were mapped prior to testing: 1 min noise samples were received across nine positions in the 14 × 14 cm plane at the depth of the subject's ears at the listening station. The three 1/3-octave -band levels within each masker were assessed, with acceptable variability between all bands being ±3 dB across the mapping grid. Additionally, received levels measured across the grid in the center 1/3-octave band were required to be ±3 dB from the level received in the daily calibration position. Like the test signals, the maskers were calibrated just prior to each session. This ensured that the center 1/3-octave band was within 1 dB

Table 1 Underwater hearing thresholds obtained for two bearded seals (*Erignathus barbatus*) using psychophysical methods

Frequency (kHz)	Bearded seal *Siku*					Bearded seal *Noatak*				
	Threshold (dB re 1 µPa)	FA rate	Ambient noise [dB re (1 µPa)^2/Hz]	Latency (ms) at 0 dB SL	Latency (ms) at 20 dB SL	Threshold (dB re 1 µPa)	FA rate	Ambient noise [dB re (1 µPa)^2/Hz]	Latency (ms) at 0 dB SL	Latency (ms) at 20 dB SL
0.1	92	0.14	72	694	333	87	0.17	68	885	531
0.2	76	0.23	61	746	230	74	0.06	56	707	436
0.4	70	0.13	48	591	308	67	0.18	46	1058	418
0.8	60	0.19	45	531	323	59	0.17	43	768	282
1.6	57	0.05	40	656	286	59	0.20	40	968	368
3.2	51	0.21	35	566	277	58	0.26	35	568	275
6.4	52	0.18	30	712	256	56	0.10	30	949	344
12.8	52	0.07	29	711	303	53	0.15	30	525	257
25.6	54	0.18	31	607	303	53	0.18	26	526	240
36.2	57	0.13	30	576	279	58	0.09	26	627	238
43.1	65	0.16	26	455	248	64	0.19	24	361	249
51.2	101	0.08	24	366	221	97	0.21	23	420	319
60.9	110	0.22	25	349	213	111	0.21	22	398	168

The 50% detection thresholds are reported for each test frequency, along with false alarm (FA) rates during the testing phase (pooled across the three test sessions at each frequency, $n \geq 20$ signal-absent trials), corresponding ambient noise levels in the test pool, and interpolated reaction times at threshold (0 dB SL) and 20 dB SL. Noise levels are shown in units of power spectral density, calculated from the median of unweighted, 1/3-octave-band 50th percentile measurements (L50) that included each test frequency. All reported noise levels reflect the test enclosure where the work was completed for each subject. For both subjects, 95% confidence intervals were narrower than 4 dB for all reported thresholds. The psychometric functions associated with these hearing thresholds are provided as Online Resource 1, and the latency-intensity functions measured for each frequency are provided as Online Resource 2

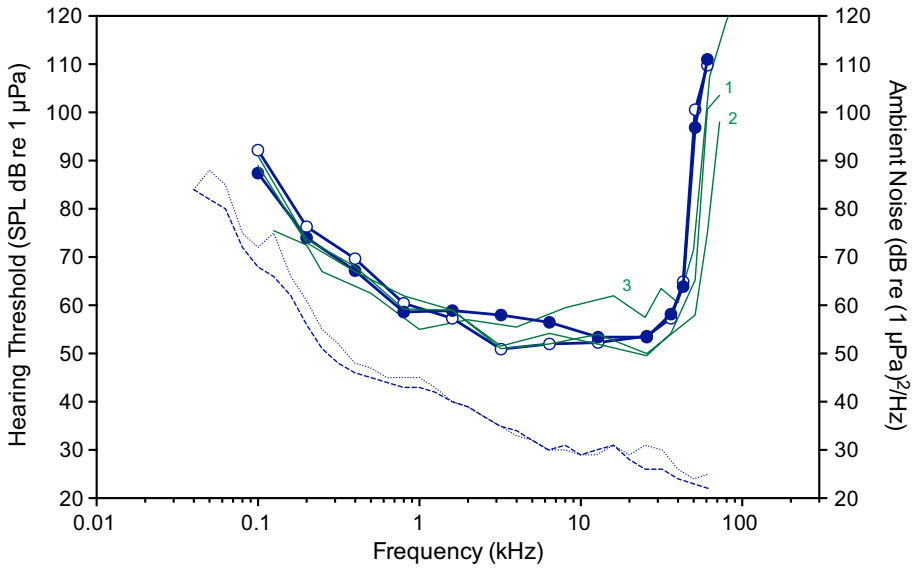

Fig. 1 Underwater audiograms for two bearded seals (*Erignathus barbatus*), *Noatak* (filled circles) and *Siku* (open circles), obtained using psychophysical methods**.** The 50% detection thresholds are shown for 13 frequencies between 0.1 and 60.9 kHz; these values are derived from psychometric functions plotted in Online Resource 1. Ambient noise in the relevant testing enclosure—depending on the animal and the test frequency—is plotted as a dashed line for *Noatak* and a dotted line for *Siku*, both corresponding to the right-hand *y*-axis. These ambient noise profiles comprise power spectral density levels (dB re (1 µPa)^2/Hz) derived from the median of unweighted 1/3-octave-band 50th percentile levels (L50) measured across all testing sessions. For comparison, recent behavioral audiograms are provided for ringed [*Pusa hispida*, 1, $n=1$ (Sills et al. 2015)], spotted [*Phoca largha*, 2, $n=2$ (Sills et al. 2014)], and harbor seals [*Phoca vitulina*, 3, $n=2$, (Kastelein et al. 2009)]

of its target level (the two surrounding bands were required to be within 3 dB of this target level).

Results

Underwater audiograms

Hearing thresholds measured in quiet conditions under water are provided in Table 1 for two bearded seals, along with corresponding false alarm rates, ambient noise levels, and interpolated response latencies at threshold (0 dB SL) and 20 dB above threshold (20 dB SL). The resulting audiograms and associated environmental noise floors are shown in Fig. 1 with representative auditory data for other northern seals. The psychometric functions associated with individual hearing thresholds are provided as Online Resource 1.

The two seals displayed sensitive hearing across a wide range of frequencies in water. The frequency of best hearing was 3.2 kHz for *Siku* and 12.8 kHz for *Noatak*, both falling within a relatively flat region at the base of the audiogram. Lowest measured thresholds were 51 and 53 dB re 1 µPa, respectively. The range of best hearing—within 20 dB of best sensitivity, as in Reichmuth et al. (2013)—was broad, extending from approximately 0.3 kHz (0.23 kHz for *Noatak*; 0.35 kHz for *Siku*) to 45 kHz, with functional hearing extending even more widely from below 0.1 kHz to at least 60 kHz. The audiograms exhibited the typical mammalian U-shape, with sharper roll-offs in sensitivity at high than at low frequencies. Sensitivity declined by approximately 35 dB within a quarter-octave above the range of best sensitivity.

Mean false alarm rates throughout testing were 0.15 and 0.17 for *Siku* and *Noatak*, respectively. Response bias was stable across frequencies and seals, indicating that the measured thresholds are directly comparable within and between seals, and to the comparative data shown in Fig. 1. Threshold-to-noise offsets in the testing pools ranged from 15 to 89 dB, and were greatest at high frequencies. Median response latencies at threshold and 20 dB SL were 591 and 279 ms for *Siku,* and 627 and 282 ms for *Noatak*. Reaction times were generally slower at low frequencies for both subjects, and this trend was more apparent near threshold than for supra-threshold stimuli. The latency-intensity functions measured for each frequency are provided as Online Resource 2.

Underwater critical ratio measurements

Underwater masked thresholds, masking noise spectral density levels, critical ratios, false alarm rates, and reaction time data are provided for the two bearded seals in Table 2. The critical ratio data are shown with representative values for northern seals in Fig. 2. Mean false alarm rate was 0.17 for

Table 2 Underwater critical ratio measurements obtained for two bearded seals (*Erignathus barbatus*)

Frequency (kHz)	Bearded seal *Siku*						Bearded seal *Noatak*					
	Masked threshold (dB re 1 µPa)	Masker level [dB re (1 µPa)^2/Hz]	Critical ratio (dB)	FA rate	Latency (ms) at 0 dB SL	Latency (ms) at 20 dB SL	Masked threshold (dB re 1 µPa)	Masker level [dB re (1 µPa)^2/Hz]	Critical ratio (dB)	FA rate	Latency (ms) at 0 dB SL	Latency (ms) at 20 dB SL
0.1	118	102	16	0.09	608	236	114	97	17	0.19	600	372
0.2	98	86	12	0.24	606	229	98	84	14	0.23	744	416
0.4	–	–	–	–	–	–	92	77	15	0.24	663	389
0.8	–	–	–	–	–	–	86	69	17	0.09	794	403
1.6	–	–	–	–	–	–	90	69	21	0.10	473	252
3.2	–	–	–	–	–	–	90	68	22	0.20	749	211
6.4	–	–	–	–	–	–	91	66	25	0.26	687	246
12.8	–	–	–	–	–	–	90	63	27	0.12	580	179
25.6	–	–	–	–	–	–	93	63	30	0.08	704	273

In addition to the critical ratio at each frequency, also provided are the spectral density level for each flat-spectrum, octave-band masker; masked hearing threshold; false alarm (FA) rate (pooled across the three test sessions at each frequency, $n \geq 24$ signal-absent trials); and interpolated reaction times at threshold (0 dB SL) and 20 dB SL. For both subjects, 95% confidence intervals were narrower than 4 dB for all masked thresholds

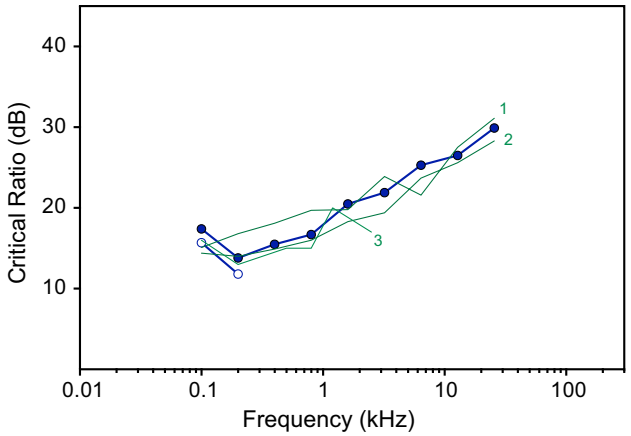

Fig. 2 Underwater critical ratios for two bearded seals (*Erignathus barbatus*), *Noatak* (filled circles) and *Siku* (open circles), measured in the presence of octave-band masking noise. Critical ratios are plotted for *Noatak* at nine frequencies and for *Siku* at two frequencies. Also shown are critical ratio measurements for ringed [*Pusa hispida*, 1, $n=2$, (Sills et al. 2015)], spotted [*Phoca largha*, 2, $n=2$, (Sills et al. 2014)], and harbor seals [*Phoca vitulina*, 3, $n=1$, (Southall et al. 2000)]

both seals during masking trials, similar to that during standard audiometric testing. Median response latencies at threshold and 20 dB SL were 607 and 233 ms for *Siku*, and 687 and 273 ms for *Noatak*. Critical ratios ranged from 14 dB at 0.2 kHz to 30 dB at 25.6 kHz for *Noatak*, increasing linearly by about 2 dB per octave. At 0.1 kHz his critical ratio was higher, with a measured value of 17 dB. *Siku* completed testing at two frequencies, with critical ratios of 16 dB at 0.1 kHz and 12 dB at 0.2 kHz, reflecting the same increase at the lowest frequency tested.

Discussion

The bearded seals in this study exhibited acute underwater hearing abilities, with their lowest measured threshold of 51 dB re 1 µPa approaching the peak sensitivity of fully aquatic cetaceans at much higher frequencies (see Erbe et al. 2016). The bandwidth of hearing within 20 dB of this minimum threshold was broad, ranging from 0.3 to 45 kHz, while the full range of hearing extended from at least 0.1 to 60 kHz. Such a wide range of sensitive hearing is exceptional among mammals, although comparable to the reported auditory capabilities of other northern seals (Terhune 1988; Kastelein et al. 2009; Reichmuth et al. 2013; Sills et al. 2014, 2015).

It is essential to consider the measured thresholds in relation to background (ambient) noise levels in the testing environment. Threshold-to-noise offsets at each frequency can be compared to critical ratios to determine whether noise

may have influenced threshold measurements. In this study, it is possible that hearing was constrained by background noise between 0.8 and 25.6 kHz, as threshold-to-noise offsets were similar in magnitude to critical ratios at the same frequencies. Therefore, despite the relatively low hearing thresholds reported for these bearded seals, threshold values in this range should be viewed as conservative estimates of auditory sensitivity—i.e., greater than or equal to absolute (unmasked) hearing thresholds—for this species. Below 0.8 and above 25.6 kHz, environmental noise was adequately low to verify the measurement of absolute thresholds. Thus, the low- and high-frequency margins of the audiograms were confirmed to reflect the true sensitivity of the seals' auditory systems.

With respect to hearing in the presence of surrounding noise, northern seals are capable of detecting sounds at lower signal-to-noise ratios than most mammals tested at similar frequencies (Southall et al. 2000, 2003; Sills et al. 2014, 2015). The bearded seals in this study identified target signals in noisy backgrounds at signal-to-noise ratios as low as 12 dB (at 0.2 kHz). Like spotted, ringed, and harbor seals, bearded seals apparently have an enhanced ability—relative to terrestrial mammals (Fay 1988)—to extract signals from noise across a wide range of frequencies. However, the critical ratios measured for the two bearded seals increased predictably above 0.2 kHz at a rate similar to that of most mammals (Fay 1988). The slight increase in critical ratio for both bearded seals at the lowest frequency tested (0.1 kHz) is similar to that observed in some other marine and terrestrial mammals (Richardson et al. 1995; Erbe et al. 2016). Unlike auditory specialists such as echolocating bats (e.g., Long 1977), bearded seals do not exhibit enhanced detection abilities at any particular frequencies.

Interpolated reaction times obtained for the two bearded seals in quiet and noisy conditions complement the threshold and critical ratio values at each frequency. The reported patterns (slower latencies at low frequencies, especially near threshold) are similar to those obtained previously for spotted and ringed seals, although the absolute response times were generally slower for the larger bearded seals (Sills et al. 2014, 2015). As expected, response times for equivalent sensation levels were the same whether they were measured in quiet or in the presence of controlled noise. The reaction times measured at threshold in the present study thus serve to validate the masked thresholds and corresponding critical ratio values reported for each frequency. The ancillary measurement of auditory reaction times provides information about perceptual loudness and serves as a useful metric for comparing signals of different frequencies and amplitudes received under different noise conditions.

Considered from a comparative perspective, the hearing ability of bearded seals is similar to that of related species, but entirely unique relative to patterns of terrestrial hearing in carnivores and aquatic hearing in other marine mammals. The biological significance of such broadly sensitive underwater hearing in seals is unknown. The bandwidth of best hearing in bearded seals overlaps their reported vocal range in water, with the spectral content of conspecific calls falling between 0.08 and 22 kHz (Cleator et al. 1989; Van Parijs et al. 2001). However, their vocalizations extend at least two octaves lower in frequency while the range of best hearing extends about an octave higher. The wide span of sensitive hearing (> 7 octaves) described for this species—with the ability to detect sounds across an even greater bandwidth—suggests that bearded seals attend to other features of the soundscape in addition to conspecific vocalizations. They can listen for auditory cues to orient themselves within the three-dimensional environment (e.g., to find the surface, breathing holes, or the ice edge) or to identify the presence of predators or prey (Elsner et al. 1989; Wartzok et al. 1992; Schusterman et al. 2000; Miksis-Olds and Madden 2014). High-frequency hearing in particular may support their ability to locate the position of biologically relevant sound sources (Heffner and Heffner 2008; Nummela and Thewissen 2008), especially when other sensory cues are unavailable. While the adaptive significance of an expanded, sensitive audiogram remains unresolved, it is likely that the derived high-frequency auditory capabilities of seals in water are enabled by efficient bone and tissue conduction of waterborne sounds (Møhl 1968; Repenning 1972; Ramprashad 1975; Hemilä et al. 2006; Nummela 2008; Kastelein et al. 2018) and an inner ear capable of resolving higher frequencies than the auditory systems of any other marine or terrestrial carnivores (Ruggero and Temchin 2002; Hemilä et al. 2006).

From a more applied perspective, the auditory data now available for bearded seals confirm that, despite notable differences in evolutionary history, anatomy, and ecology, all ten northern seal species can be considered together as one functional hearing group. For management purposes, this indicates that it is reasonable to pool available data for phocinae species in order to evaluate the potentially harmful effects of noise on hearing. The bearded seal audiograms reported here are also consistent with the updated *phocid carnivores in water* weighting proposed by Southall et al. (2019). Auditory research with otariid pinnipeds (fur seals and sea lions) has confirmed a single functional hearing group spanning all 14 species in that family—from the most basal to the most recent and across the extremes of body size (Mulsow et al. 2012). It is not yet apparent whether a single grouping is appropriate for all phocid seals (i.e., including both the Phocinae and Monachinae subfamilies), as suggested by Finneran (2016), the US National Marine Fisheries Service (2018), and Southall et al. (2019). However, similarities in high-frequency roll-offs described for phocinae seals and the monachid northern elephant seal

(Kastak and Schusterman 1999) indicate that adaptations of the basilar membrane to enable neural encoding of high frequencies may have emerged more than 16 million years ago (see Higdon et al. 2007) and are likely common to most (if not all) phocid carnivores.

As human activities expand in Arctic waters, this work provides new information to enable scientists and regulators to better predict the effects of continued degradation of acoustic habitat on bearded seals. For example, the masking experiment described herein enables us to directly quantify how noise affects the ability of these seals to perceive relevant sounds. While critical ratios were measured in the presence of continuous, spectrally flattened background noise, these values can be applied (with some limitations) to understand signal detection in more complex acoustic environments (see, e.g., Dooling et al. 2013; Cunningham et al. 2014; Erbe et al. 2016; Sills et al. 2017a). Although only underwater critical ratios were measured, these data can be used to predict the effects of noise both above and below the water's surface (see Renouf 1980; Turnbull and Terhune 1990; Southall et al. 2003; Sills et al. 2014, 2015), which is an important consideration for amphibious seals. Ultimately, these audiograms and critical ratios can be used—in conjunction with noise measurements from representative environments and descriptions of biologically relevant sounds—to estimate the physical range over which free-ranging bearded seals can communicate with conspecifics or listen for predators or prey under different noise conditions (see, e.g., Erbe et al. 2016, Hannay et al. 2016; Sills et al. 2017b; Pine et al. 2018). Such integrated analyses shed light on the complex acoustic world of bearded seals, about which new information is emerging but much remains to be discovered.

Conclusions

This study takes a perceptual, whole-animal approach to address a key knowledge gap regarding auditory sensitivity in bearded seals and, in doing so, provides valuable insight into the acoustic ecology of these marine mammals. Bearded seals display acute underwater hearing capabilities across a broad range of frequencies, with the ability to detect underwater sounds as quiet as 51 dB re 1 µPa. The fact that bearded seals—as the evolutionarily outgroup within the Phocinae subfamily—have comparable hearing to more recently derived seals indicates that it is reasonable to extrapolate auditory capabilities across this lineage. It remains unclear whether southern, monachid seals also fit into this functional grouping. Additional data are needed to determine whether all true seals have similar auditory capabilities, which has relevance both in terms of understanding the evolution of underwater hearing in seals and for informing best management practices related to noise pollution in the habitats on which they rely.

Acknowledgements We are grateful to C. Casey, D. Casper, J. Gallahorn, P. Goodwin, and B. Long for their efforts during acquisition and acclimation of the two bearded seals in Kotzebue, AK and at the Alaska SeaLife Center in Seward, AK. We also thank A. Sloan and J. Skidmore of the National Marine Fisheries Service; L. Quakenbush, K. Frost, and M. Nelson of the Alaska Department of Fish and Game; P. Boveng of the National Marine Mammal Laboratory; and T. Moran of the U.S. Fish & Wildlife Service for advice, logistical support, and permit coordination in Kotzebue, AK. Drs. D. Casper, C. Goertz, and K. Woodie provided veterinary care for the bearded seals, and J. Finneran of the U.S. Navy Marine Mammal Program generously provided access to the custom LabVIEW software used to measure auditory thresholds. We thank J. Byl and two anonymous reviewers for their comments on this manuscript. This work was made possible by the dedicated husbandry and research teams at the Alaska SeaLife Center and the Long Marine Laboratory at the University of California Santa Cruz; we especially thank C. Casey, H. Hermann-Sorensen, S. Knaub, J. Sullivan, B. Long, R. Nichols, L. Polasek, A. Rouse, B. Ruscher-Hill, R. Sattler, and D. Woodie for their efforts. We are grateful to L. Brzuzy, C. Rea, J. Campbell, K. Broker, and G. Wolinsky, who helped us with problem solving and administrative needs. Portions of this research were presented at the 22nd Biennial Conference on the Biology of Marine Mammals, the Joint 6th International Meeting on the Effects of Sound in the Ocean on Marine Mammals and 3rd Programme Review Meeting of the E&P Sound & Marine Life Joint Industry Programme, and the 5th International Conference on the Effects of Noise on Aquatic Life.

Funding This study was funded by the International Association of Oil and Gas Producers, through their E&P Joint Industry Programme on Sound and Marine Life (award 22-07-23). Supplemental funding for the bearded seal acquisition effort was provided through the Northwest Arctic Borough Science Committee.

Compliance with ethical standards

Conflicts of interest The authors declare that they have no conflicts of interest.

Ethical approval All applicable international, national, and institutional guidelines for the care and use of animals were followed. Studies involving animals were conducted in accordance with the ethical standards of the Institutional Animal Care and Use Committee at the University of California Santa Cruz. Research was further authorized under research permits 14535 and 18902 issued by the National Marine Fisheries Service of the United States, in consultation with the Ice Seal Committee.

References

Árnason U, Gullberg A, Janke A, Kullberg M, Lehman N, Petrov EA, Väinölä R (2006) Pinniped phylogeny and a new hypothesis for their origin and dispersal. Mol Phylogenet Evol 41:345–354

Burns JJ, Frost KJ (1979) The natural history and ecology of the bearded seal, Erignathus barbatus. Department of Fish and Game, Alaska

Burns JJ (1981) Bearded seal Erignatus barbatus Erxleben, 1777. In: Ridgway SH, Harrison RJ (eds) Handbook of marine mammals, vol 2: seals, vol 2. Academic Press, New York, pp 145–170

Cameron MF, Bengtson JL, Boveng PL, Jansen JK, Kelly BP, Dahle SP, Logerwell EA, Overland JE, Sabine CL, Waring GT, Wilder JM (2010) Status review of the bearded seal (*Erignathus barbatus*). US Department of Commerce, NOAA Tech Memo NMFS-AFSC-211

Chou E, Antunes R, Sardelis S, Stafford KM, West L, Spagnoli C, Southall BL, Robards M, Rosenbaum H (2020) Seasonal variation in Arctic marine mammal acoustic detection in the northern Bering Sea. Mar Mamm Sci 36:522–547

Cleator HJ, Stirling I, Smith TG (1989) Underwater vocalizations of the bearded seal (*Erignathus barbatus*). Can J Zool 67:1900–1910

Cornsweet TN (1962) The staircase-method in psychophysics. Am J Psychol 75:485–491

Cunningham KC, Southall BL, Reichmuth C (2014) Auditory sensitivity in complex listening scenarios. J Acoust Soc Am 136:3410–3421

Davies CE, Kovacs KM, Lydersen C, van Parijs SM (2006) Development of display behavior in young captive bearded seals. Mar Mamm Sci 22:952–965

Dehn LA, Sheffield GG, Follmann EH, Duffy LK, Thomas DL, O'Hara TM (2007) Feeding ecology of phocid seals and some walrus in the Alaskan and Canadian Arctic as determined by stomach contents and stable isotope analysis. Polar Biol 30:167–181

Dooling RJ, Blumenrath SH, Smith E, Fristrup K (2013) Evaluating anthropogenic noise effects on animal communication. In: NoiseCon2013, 26–28 August 2013, Denver, CO

Elsner R, Wartzok D, Sonafrank NB, Kelly BP (1989) Behavioral and physiological reactions of arctic seals during under-ice pilotage. Can J Zool 67:2506–2513

Erbe C, Reichmuth C, Cunningham K, Lucke K, Dooling R (2016) Communication masking in marine mammals: A review and research strategy. Mar Pollut Bull 103:15–38

Fay RR (1988) Hearing in vertebrates: a psychophysics databook. Hill-Fay Associates, Winnetka

Finneran JJ (2003) An integrated computer-controlled system for marine mammal auditory testing. SPAWAR Systems Center, San Diego

Finneran JJ (2016) Auditory weighting functions and TTS/PTS exposure functions for marine mammals exposed to underwater noise (Technical Report 3026). SPAWAR Systems Center, San Diego

Finney DJ (1971) Probit analysis, 3rd edn. Cambridge University Press, Cambridge

Fletcher H (1940) Auditory patterns. Rev Mod Phys 12:47–65

Frost KJ, Whiting A, Cameron MF, Simpkins MA (2008) Habitat use, seasonal movements and stock structure of bearded seals in Kotzebue Sound, Alaska. Tribal Wildlife Grants Program, Fish and Wildlife Service, Tribal Wildlife Grants Study U-4-IT. Final report from the Native Village of Kotzebue, Kotzebue, AK, for U.S. Fish and Wildlife Service, Anchorage, AK

Fulton TL, Strobeck C (2010) Multiple fossil calibrations, nuclear loci and mitochondrial genomes provide new insight into biogeography and divergence timing for true seals (Phocidae, Pinnipedia). J Biogeogr 37:814–829

Hamilton CD, Kovacs KM, Lydersen C (2018) Individual variability in diving, movement and activity patterns of adult bearded seals in Svalbard, Norway. Sci Rep 8:16988

Hannay DE, Delarue J, Mouy X, Martin BS, Leary D, Oswald JN, Vallarta J (2013) Marine mammal acoustic detections in the northeastern Chukchi Sea, September 2007–July 2011. Cont Shelf Res 67:127–146

Hannay DE, Matthews MN, Schlesinger A, Hatch L, Harrison J (2016) Lost listening area assessment of anthropogenic sounds in the Chukchi Sea. J Acoust Soc Am 140:3072–3073

Heffner HE, Heffner RS (2008) High-frequency hearing. In: Dallos P, Oertel D, Hoy R (eds) Handbook of the senses: audition. Elsevier, New York, pp 55–60

Hemilä S, Nummela S, Berta A, Reuter T (2006) High-frequency hearing in phocid and otariid pinnipeds: an interpretation based on inertial and cochlear constraints. J Acoust Soc Am 120:3463–3466

Higdon JW, Bininda-Emonds OR, Beck RM, Ferguson SH (2007) Phylogeny and divergence of the pinnipeds (Carnivora: Mammalia) assessed using a multigene dataset. BMC Evol Biol 7:216

Jones JM, Thayre BJ, Roth EH, Mahoney M, Sia I, Merculief K, Jackson C, Zeller C, Clare M, Bacon A, Weaver S, Gentes Z, Small RJ, Stirling I, Wiggins SM, Hildebrand JA (2014) Ringed, bearded, and ribbon seal vocalizations North of Barrow, Alaska: seasonal presence and relationship with sea ice. Arctic 67:203–222

Kastak D, Schusterman RJ (1999) In-air and underwater hearing sensitivity of a northern elephant seal (*Mirounga angustirostris*). Can J Zool 77:1751–1758

Kastelein RA, Wensveen PJ, Hoek L, Verboom WC, Terhune JM (2009) Underwater detection of tonal signals between 0.125 and 100 kHz by harbor seals (*Phoca vitulina*). J Acoust Soc Am 125:1222–1229

Kastelein RA, Helder-Hoek L, Terhune JM (2018) Hearing thresholds, for underwater sounds, of harbor seals (*Phoca vitulina*) at the water surface. J Acoust Soc Am 143:2554–2563

Kienle SS, Berta A (2016) The better to eat you with: the comparative feeding morphology of phocid seals (Pinnipedia, Phocidae). J Anat 228:396–413

Kienle SS, Hermann-Sorensen H, Costa DP, Reichmuth C, Mehta RS (2018) Comparative feeding strategies and kinematics in phocid seals: suction without specialized skull morphology. J Exp Biol 221(Pt 5):jeb179424

King JE (1964) Seals of the world. British Museum, Natural History, London

Kingsley MCS, Stirling I, Calvert W (1985) The distribution and abundance of seals in the Canadian high Arctic, 1980–82. Can J Fish Aquat Sci 42:1189–1210

Long GR (1977) Masked auditory thresholds from the bat, *Rhinolophus ferrumequinum*. J Comp Physiol 116:247–255

Lowry LF, Frost KJ, Burns JJ (1980) Feeding of bearded seals in the Bering and Chukchi Seas and trophic interaction with Pacific walruses. Arctic 33:330–342

MacIntyre KQ, Stafford KM, Berchok CL, Boveng PL (2013) Year-round acoustic detection of bearded seals (*Erignathus barbatus*) in the Beaufort Sea relative to changing environmental conditions, 2008–2010. Polar Biol 36:1161–1173

MacIntyre KQ, Stafford KM, Conn PB, Laidre KL, Boveng PL (2015) The relationship between sea ice concentration and the spatiotemporal distribution of vocalizing bearded seals (*Erignathus barbatus*) in the Bering, Chukchi, and Beaufort Seas from 2008 to 2011. Prog Oceanogr 136:241–249

Marshall CD, Kovacs KM, Lydersen C (2008) Feeding kinematics, suction and hydraulic jetting capabilities in bearded seals (*Erignathus barbatus*). J Exp Biol 211:699–708

McHuron EA, Williams T, Costa DP, Reichmuth C (2020) Contrasting whisker growth dynamics within the phocid lineage. Mar Ecol Prog Ser 634:231–236

Miksis-Olds JL, Madden LE (2014) Environmental predictors of ice seal presence in the Bering Sea. PLoS ONE 9:e106998

Møhl B (1968) Hearing in seals. In: Harrison RJ, Hubbard C, Peterson RS, Rice CE, Schusterman RJ (eds) The behaviour and physiology of pinnipeds. Appleton-Century-Crofts, New York, pp 172–195

Moody DB (1970) Reaction time as an index of sensory function. In: Stebbins WC (ed) Animal psychophysics: the design and conduct of sensory experiments. Appleton-Century-Crofts, New York, pp 227–302

Moore SE, Reeves RR, Southall BL, Ragen TJ, Suydam RS, Clark CW (2012) A new framework for assessing the effects of anthropogenic sound on marine mammals in a rapidly changing Arctic. Bioscience 62:289–295

Mulsow J, Houser DS, Finneran JJ (2012) Underwater psychophysical audiogram of a young male California sea lion (*Zalophus californianus*). J Acoust Soc Am 131:4182–4187

National Marine Fisheries Service (2018) 2018 revisions to: Technical guidance for assessing the effects of anthropogenic sound on marine mammal hearing (version 2.0): Underwater acoustic thresholds of permanent and temporary threshold shifts. NOAA Technical Memorandum NMFS-OPR-59, U. S. Dept. of Commerce, NOAA

Nummela S (2008) Hearing in aquatic mammals. In: Thewissen JGM, Nummela S (eds) Sensory evolution on the threshold: adaptations in secondarily aquatic vertebrates. University of California Press, Berkeley, pp 211–224

Nummela S, Thewissen JGM (2008) The physics of sound in air and water. In: Thewissen JGM, Nummela S (eds) Sensory evolution on the threshold: adaptations in secondarily aquatic vertebrates. University of California Press, Berkeley, pp 175–181

Pine MK, Hannay DE, Insley SJ, Halliday WD, Juanes F (2018) Assessing vessel slowdown for reducing auditory masking for marine mammals and fish of the western Canadian Arctic. Mar Pollut Bull 135:290–302

Ray C, Watkins WA, Burns JJ (1969) The underwater song of *Erignathus barbatus* (bearded seal). In: Zoologica. New York Zoological Society, New York, pp 79–83

Ramprashad F (1975) Aquatic adaptations in the ear of the harp seal *Pagophilus groenlandicus* (Erxleben, 1777). Rapp P-v Réun Cons Int Explor Mer 169:102–111

Reichmuth C, Holt MM, Mulsow J, Sills JM, Southall BL (2013) Comparative assessment of amphibious hearing in pinnipeds. J Comp Physiol A 199:491–507

Renouf D (1980) Masked hearing thresholds of harbour seals (*Phoca vitulina*) in air. J Aud Res 20:263–269

Repenning CA (1972) Underwater hearing in seals: functional morphology. In: Harrison RJ (ed) Functional anatomy of marine mammals, vol 1. Academic Press, London, pp 307–331

Richardson WJ, Greene CR, Malme CI, Thomson DH (1995) Marine mammals and noise. Academic Press, San Diego

Risch D, Clark CW, Corkeron PJ, Elepfandt A, Kovacs KM, Lydersen C, Stirling I, Van Parijs SM (2007) Vocalizations of male bearded seals, *Erignathus barbatus*: classification and geographical variation. Anim Behav 73:747–762

Ruggero MA, Temchin AN (2002) The roles of the external, middle, and inner ears in determining the bandwidth of hearing. Proc Natl Acad Sci USA 99:13206–13210

Scharf B (1970) Critical bands. In: Tobias JV (ed) Foundations of modern auditory theory, vol 1. Academic Press, New York, pp 159–202

Schusterman RJ, Kastak D, Levenson DH, Reichmuth CJ, Southall BL (2000) Why pinnipeds don't echolocate. J Acoust Soc Am 107:2256–2264

Sills JM, Southall BL, Reichmuth C (2014) Amphibious hearing in spotted seals (*Phoca largha*): underwater audiograms, aerial audiograms and critical ratio measurements. J Exp Biol 217:726–734

Sills JM, Southall BL, Reichmuth C (2015) Amphibious hearing in ringed seals (*Pusa hispida*): underwater audiograms, aerial audiograms and critical ratio measurements. J Exp Biol 218:2250–2259

Sills JM, Southall BL, Reichmuth C (2017a) The influence of temporally varying noise from seismic air guns on the detection of underwater sounds by seals. J Acoust Soc Am 141:996–1008

Sills JM, Reichmuth C, Whiting A (2017b) Acoustic habitat utilized by ice-living seals: hearing and masking in natural noise environments. J Acoust Soc Am 141:4002

Simpkins MA, Hiruki-Raring LM, Sheffield G, Grebmeier JM, Bengtson JL (2003) Habitat selection by ice-associated pinnipeds near St. Lawrence Island, Alaska in March 2001. Polar Biol 26:577–586

Southall BL, Schusterman RJ, Kastak D (2000) Masking in three pinnipeds: underwater, low-frequency critical ratios. J Acoust Soc Am 108:1322–1326

Southall BL, Schusterman RJ, Kastak D (2003) Auditory masking in three pinnipeds: aerial critical ratios and direct critical bandwidth measurements. J Acoust Soc Am 114:1660–1666

Southall BL, Finneran JJ, Reichmuth C, Nachtigall PE, Ketten DR, Bowles AE, Ellison WT, Nowacek DP, Tyack PL (2019) Marine mammal noise exposure criteria: updated scientific recommendations for residual hearing effects. Aquat Mamm 45:125–232

Terhune JM (1988) Detection thresholds of a harbour seal to repeated underwater high-frequency, short-duration sinusoidal pulses. Can J Zool 66:1578–1582

Terhune JM (2018) The underwater vocal complexity of seals (Phocidae) is not related to their phylogeny. Can J Zool 97:232–240

Turnbull SD, Terhune JM (1990) White noise and pure tone masking of pure tone thresholds of a harbour seal listening in air and underwater. Can J Zool 68:2090–2097

Van Parijs SM, Kovacs KM, Lydersen C (2001) Spatial and temporal distribution of vocalizing male bearded seals: implications for male mating strategies. J Mammal 138:905–922

Wartzok D, Elsner R, Stone H, Kelly BP, Davis RW (1992) Under-ice movements and the sensory basis of hole finding by ringed and Weddell seals. Can J Zool 70:1712–1722

JASA ARTICLE

Evaluating temporary threshold shift onset levels for impulsive noise in seals[a)]

Jillian M. Sills,[1,b)] Brandi Ruscher,[2] Ross Nichols,[2] Brandon L. Southall,[3] and Colleen Reichmuth[1]

[1]*Institute of Marine Sciences, Long Marine Laboratory, University of California Santa Cruz, Santa Cruz, California 95060, USA*

[2]*Department of Ocean Sciences, University of California Santa Cruz, Santa Cruz, California 95064, USA*

[3]*Southall Environmental Associates, Inc., 9099 Soquel Drive, Suite 8, Aptos, California 95003, USA*

ABSTRACT:

The auditory effects of single- and multiple-shot impulsive noise exposures were evaluated in a bearded seal (*Erignathus barbatus*). This study replicated and expanded upon recent work with related species [Reichmuth, Ghoul, Sills, Rouse, and Southall (2016). J. Acoust. Soc. Am. **140**, 2646–2658]. Behavioral methods were used to measure hearing sensitivity before and immediately following exposure to underwater noise from a seismic air gun. Hearing was evaluated at 100 Hz—close to the maximum energy in the received pulse, and 400 Hz—the frequency with the highest sensation level. When no evidence of a temporary threshold shift (TTS) was found following single shots at 185 dB re 1 μPa^2 s unweighted sound exposure level (SEL) and 207 dB re 1 μPa peak-to-peak sound pressure, the number of exposures was gradually increased from one to ten. Transient shifts in hearing thresholds at 400 Hz were apparent following exposure to four to ten consecutive pulses (cumulative SEL 191–195 dB re 1 μPa^2 s; 167–171 dB re 1 μPa^2 s with frequency weighting for phocid carnivores in water). Along with these auditory data, the effects of seismic exposures on response time, response bias, and behavior were investigated. This study has implications for predicting TTS onset following impulsive noise exposure in seals. © *2020 Acoustical Society of America*.

https://doi.org/10.1121/10.0002649

(Received 16 July 2020; revised 25 September 2020; accepted 28 October 2020; published online 24 November 2020)

[Editor: Klaus Lucke] Pages: 2973–2986

I. INTRODUCTION

Over recent decades, the expansion of human activities in marine environments has resulted in an influx of noise throughout many of the world's oceans (McDonald *et al.*, 2006; Hildebrand, 2009). Oil and gas development, commercial shipping, and military operations often contribute significantly to underwater soundscapes. One of the many concerns arising from increased levels of underwater noise is the potential for noise-induced hearing loss in marine mammals—animals which rely on underwater sound for important life functions such as orientation, predator and prey detection, and communication.

Various studies have evaluated auditory sensitivity in marine mammals following exposure to noise (see, e.g., Finneran, 2015; Southall *et al.*, 2019, for recent reviews). Temporary changes in hearing (temporary threshold shifts, TTSs) are typically used as the primary measure of auditory effect in these controlled experiments. While such studies have largely focused on continuous (long-duration) fatiguing noise, there is growing interest in the effects of impulsive noise on marine mammal hearing. Impulsive noise is widespread in the marine environment and generated from a range of sources, including air guns used for seismic exploration and oil and gas production; short, intense pulses associated with underwater explosions (e.g., military operations and seal bombs used in fisheries); and impact pile driving for wind development projects, oil platforms and offshore energy installations, and construction in bays and harbors (Hildebrand, 2009). Impulsive sources in noise exposure studies have included playbacks of impact pile driving sounds (Kastelein *et al.*, 2015; Kastelein *et al.*, 2018) and actual or simulated seismic air guns (Lucke *et al.*, 2009; Finneran *et al.*, 2015; Reichmuth *et al.*, 2016; Kastelein *et al.*, 2017).

TTS research with impulsive noise has focused on odontocete cetaceans with specialized high-frequency hearing. However, pinnipeds (seals, sea lions, and walruses) and mysticete whales are likely more vulnerable to such exposures, as the energy content of anthropogenic impulsive noise primarily falls below 1 kHz (Richardson *et al.*, 1995). In particular, phocid (true) seals have the most sensitive low-frequency hearing of any marine mammal group tested to date (see Reichmuth *et al.*, 2013; Erbe *et al.*, 2016). Three studies have investigated the effects of impulsive underwater noise on pinniped hearing (Finneran *et al.*, 2003; Reichmuth *et al.*, 2016; Kastelein *et al.*, 2018). Of these, none demonstrated TTS onset—defined as threshold shift $\geq$6 dB (see Southall *et al.*, 2007; Finneran, 2016; National Marine Fisheries Service, 2018; Southall *et al.*, 2019)—following exposure to single or multiple pulses. Therefore, there is insufficient information available to determine TTS

[a)]Portions of this work were presented in "Auditory studies with bearded seals: sound sensitivity and the effects of noise," 5th International Conference of the Effects of Noise on Aquatic Life, Den Haag, Netherlands, July 2019 and in "Auditory detection, masking, and temporary threshold shift in bearded seals (*Erignathus barbatus*)," 6th International Meeting on the Effects of Sound in the Ocean on Marine Mammals, Den Haag, Netherlands, September 2018.

[b)]Electronic mail: jmsills@ucsc.edu, ORCID: 0000-0002-3110-4844.

onset conditions for any pinniped exposed to impulsive noise, which complicates efforts to manage noise effects on free-ranging individuals.

In the absence of direct data, current regulatory guidance (Finneran, 2016; National Marine Fisheries Service, 2018) is derived from the initial approach developed by Southall *et al.* (2007), supplemented by newer data available for pinnipeds through 2016 (see Southall *et al.*, 2019). For the phocid carnivores in water (PCW) hearing group, TTS onset following impulsive noise exposures in water is predicted to occur at a peak sound pressure level of 212 dB re 1 μPa (corresponding to a nominal peak-to-peak sound pressure of 218 dB re 1 μPa) and a cumulative weighted sound exposure level[1] (SEL) of 170 dB re 1 μPa^2 s. However, these TTS onset values have not been empirically confirmed.

To inform regulatory guidance for seals and provide insight into appropriate noise-exposure guidelines for other marine mammals with presumed sensitive low-frequency hearing, we conducted a series of auditory experiments investigating TTS in seals. Due to the pervasiveness of seismic noise worldwide (e.g., Gedamke and McCauley, 2010; Nieukirk *et al.*, 2012), this work focused on exposure to impulsive noise from seismic air guns. We initially evaluated underwater hearing in spotted (*Phoca largha*) and ringed (*Pusa hispida*) seals following exposure to single pulses from a small sleeve air gun (Reichmuth *et al.*, 2016). In that study, behavioral audiometric testing was completed with trained seals at 100 Hz—approximately 1/2-octave above the peak energy of the broadband noise—in exposure conditions with received, unweighted SEL extending from 165 to 181 dB re 1 μPa^2 s (corresponding peak-to-peak sound pressures from 190 to 207 dB re 1 μPa). While the upper end of this SEL range reached the predicted *M*-weighted TTS-onset level from early noise exposure criteria (Southall *et al.*, 2007), no TTS was observed in these seals.

Here, we expand upon this prior work with a set of three experiments to investigate TTS onset and the frequency-dependent effects of impulsive noise exposure. This work was completed primarily with one bearded seal trained for behavioral measurements of underwater hearing. Given underlying uncertainty about the auditory effects of impulsive noise, progressive testing toward predicted TTS-onset conditions proceeded conservatively. Experiment 1 began by replicating the single-shot exposure parameters used by Reichmuth *et al.* (2016) and extending these to higher target levels (received SEL up to 186 dB re 1 μPa^2 s; here, and for the remainder of this manuscript, SEL values are unweighted except when stated otherwise). When TTS onset was not identified at the primary test frequency of 100 Hz, experiment 2 evaluated hearing at a second frequency before and after exposure to the same received levels. This additional testing was completed at 400 Hz—the frequency of maximum sensation level, or greatest difference between the air gun exposure spectrum and the frequency-specific hearing threshold of the subject. This approach was based on other auditory studies with marine mammals, which suggest that maximum threshold shift may be observed at the frequency with the greatest offset between auditory sensitivity and fatiguing noise level (e.g., Kastak *et al.*, 1999; Kastak *et al.*, 2005; Kastak *et al.*, 2007; Lucke *et al.*, 2009; Kastelein *et al.*, 2017).

In experiment 3, single-shot received SEL was maintained at a relatively constant exposure level (~185 dB re 1 μPa^2 s) while the number of consecutive exposures was increased from one to ten. Using multiple-pulse exposures had several advantages over continuing to increase SEL by raising the amplitude of single shots. First, these exposure sequences—with repetition rates comparable to real-world air gun arrays—simulated more realistic exposure scenarios in which free-ranging seals encounter multiple pulses while diving. Second, this method enabled the generation of impulsive sounds with characteristics more representative of distant seismic sources as opposed to the more complex acoustic conditions of larger single pulses in an enclosed tank. Finally, holding single-shot amplitude constant while increasing the cumulative exposure level avoided concerns for direct physiological harm (non-auditory effects) as a result of intense exposures at close range. While peak sound pressure level did not reach predicted TTS onset conditions for any single impulse, the received cumulative sound exposure level (cSEL) for the ten-shot exposure series reached the updated PCW-weighted level for predicted TTS onset in seals (Southall *et al.*, 2019).

These auditory experiments yield improved predictions regarding TTS onset in seals following exposure to broadband noise from seismic air guns, and inform regulatory guidelines regarding impulsive noise in the marine environment.

II. MATERIALS AND METHODS

A. General methods

The primary goal was to identify the onset of repeatable, recoverable TTS (defined as threshold shifts $\geq$6 dB) in seals following exposure to impulsive underwater noise. The audiometric procedure involved four standard steps: (1) measurement of a pre-exposure hearing threshold at the target frequency; (2) voluntary exposure to calibrated air gun impulse(s), with number of pulses and received level determined by experiment and condition number; (3) measurement of a post-exposure hearing threshold at the target frequency within minutes of the exposure event; and in the event of a threshold shift, (4) measurement of a recovery hearing threshold at the target frequency 24 hours following exposure. The study design included both actual (air gun) exposures and control (no noise) exposures during each experimental condition.

1. Test subject

The subject was a subadult male bearded seal identified as *Noatak* (NOA0010270), who was 3–4 years old during testing. This seal's underwater hearing was evaluated previously with psychoacoustic methods (Sills *et al.*, 2020); the resulting audiogram demonstrated sensitive auditory

https://doi.org/10.1121/10.0002649

capabilities comparable to those of the related harbor (*Phoca vitulina*; Reichmuth *et al.*, 2013; Erbe *et al.*, 2016), spotted (Sills *et al.*, 2014), and ringed seals (Sills *et al.*, 2015). This bearded seal was maintained at a healthy body weight throughout training and data collection and received one-third to one-half of his prescribed diet (freshly thawed capelin and herring fish) during daily audiometric sessions. Research was conducted up to five days per week with a maximum of one exposure series per day; actual exposures could occur on consecutive days as long as hearing had returned to normal following exposure. Testing was conducted voluntarily with the subject's behavior under conditioned control, established by positive reinforcement training. The seal's participation in this study was approved by the Institutional Animal Care and Use Committee at the University of California Santa Cruz under authorization from the U.S. National Marine Fisheries Service (permit 18902) and the Ice Seal Committee.

2. Environment and apparatuses

Audiometric testing was conducted in a circular, partially in-ground pool (1.8 m deep, 7.6 m diameter) filled with ambient seawater (11 °C–17 °C).

Hearing thresholds were measured at the *listening station*, which was built from water-filled, acoustically transparent polyvinyl chloride (PVC). The listening station included a chin rest that positioned the seal's ears within a calibrated sound field at 1 m depth, 0.75 m from the edge of the pool. A response target, which the seal could press to indicate detection of a signal, was located 20 cm to the left of the chin rest. At the front of the chin rest was a switch that the seal depressed to initiate each trial, which enabled the automatic measurement of response time as the interval between signal onset and release of the switch. The listening station also included a light to indicate the duration of each individual trial and an underwater camera to provide a remote experimenter with a real-time view of the seal.

Exposure (and mock-exposure) events were conducted at the *exposure station*. This water-filled PVC station was suspended near the center of the test pool from an acoustically isolated steel pipe spanning the pool's diameter. The exposure station included a chin rest to position the seal's ears at 1 m depth, a TC4013 (Teledyne Reson A/S, Slangerup, Denmark) hydrophone (±3 dB response from 0.001 to 170 kHz, nominal sensitivity −211 dB re 1 V/μPa) coupled to the chin rest to quantify received exposure levels, a horizontal PVC bar that assisted the seal in maintaining his position, and an underwater camera to enable remote monitoring by the experimenter during all exposures. When positioned at the exposure station, the seal was 1 m from and on axis with the air gun.

3. Ambient noise measurements

Ambient noise measurements were made twice daily, as in Reichmuth *et al.* (2016), prior to each pre-exposure session and each noise exposure/post-exposure test sequence. One-minute, unweighted noise measurements were obtained for frequencies from 0.01 to 20 kHz with a Reson TC4032 low-noise hydrophone (±2.5 dB response from 0.01 to 80 kHz; nominal sensitivity −170 dB re 1 V/μPa with a frequency-specific sensitivity adjustment based on recent calibration). The hydrophone was mounted in the underwater testing enclosure and paired with a Reson EC6073 input module, Reson EC6069 battery module, and battery-powered 2270 sound analyzer (Brüel and Kjær A/S, Nærum, Denmark). Pre- and post-exposure 1/3-octave band levels containing the signal frequency were compared daily to ensure similar ambient noise backgrounds during pre- and post-exposure hearing tests.

These ambient noise measurements were pooled across the entire study ($n = 150$) to characterize background noise. Spectral density levels [dB re (1 μPa)^2/Hz] were determined from 1/3-octave band levels. Median spectral density values were used to represent typical ambient conditions across all sessions and evaluate whether audiometric thresholds could have been constrained by background noise. To describe the variance in background noise, percentile statistics (L10, L50, and L90) for 1/3-octave bands were calculated from equivalent continuous noise levels (Leq). Median (L50) noise levels were also compared for pre- versus post-exposure sessions to evaluate whether differences could have influenced estimates of threshold shift.

B. Experiment 1: The effect of single-shot exposures on hearing near the frequency of maximum exposure level

Experiment 1 evaluated hearing sensitivity at 100 Hz following escalating levels of single-shot exposures. This frequency was chosen to occur near the region of maximum energy for the broadband exposures (30–80 Hz). The single impulses received at close range to the source were intended to represent the acoustic conditions an animal would experience at farther distances from an operational array within a non-reverberant environment—to the greatest extent possible within the bounds of the experimental enclosure. As this was a continuation of work completed recently with spotted and ringed seals, many of the relevant methodological details can be found in Reichmuth *et al.* (2016).

At the beginning of experiment 1, *baseline audiometric testing* was conducted to determine a reference threshold at 100 Hz by confirming previous threshold measurements for the same subject, to describe typical variation in thresholds at 100 Hz, and to establish additional expertise in the subject. *Air gun exposure testing* then occurred over five successive noise exposure conditions (C1–C5). Conditions C1–C4 replicated previous testing with spotted and ringed seals (Reichmuth *et al.*, 2016) with a target SEL range of 165–181 dB re 1 μPa^2 s. Condition C5 extended SEL to 186 dB re 1 μPa^2 s. Corresponding received peak-to-peak sound pressure and peak sound pressure level ranges (dB re 1 μPa) for each of the testing conditions are provided in Table I, along with additional details of the experimental design.

TABLE I. Study parameters for single-shot exposure testing during experiments 1 and 2, showing the operating volume (in.^{3}) and pressure (psi) of the air gun, the horizontal distance from the air gun to the exposure station where the seal was located, the single-shot unweighted target SEL range (dB re 1 μPa^2 s), the corresponding received peak-to-peak sound pressure range (dB re 1 μPa), and the number of replicate audiometric testing sequences (n) conducted with the bearded seal subject under each condition at 100 and 400 Hz. Control conditions (full test sequences with mock noise exposures) were conducted in the same configuration as corresponding exposure sessions and interspersed with these exposures at a ratio of 1:4.

Exposure condition	Impulsive sound source	Air gun volume (in.^{3})	Air gun pressure (psi)	Distance (m)	Target exposure (dB SEL)	Corresponding exposure (dB peak-to-peak)	Replicate series at 100 Hz (n)	Replicate series at 400 Hz (n)
C1	Sleeve gun	10	30	1	165–168	190–193	4	—
C2	Sleeve gun	10	50	1	169–172	194–197	8	—
C3	Sleeve gun	10	70	1	173–176	199–202	8	—
C4	Sleeve gun	10	110	1	178–181	204–207	8	8
C5	BOLT	5	500	1.5	183–186	206–209	4	4
Control							8	3
Total							40	15

1. Audiometric signal generation and calibration

The signals used to evaluate hearing were 500 ms frequency-modulated upsweeps centered on 100 Hz, with narrow (10%) bandwidth and 5% linear rise and fall times. Signals were generated with the Hearing Test Program (HTP; Finneran, 2003) in LabVIEW [National Instruments (NI) Corp., Austin, TX] and sent through an NI 6259 data acquisition module, a 3364 bandpass filter (Krohn-Hite, Brockton, MA), a PA5 digital attenuator (Tucker-Davis Technologies, Alachua, FL), and a P1000 power amplifier (Hafler Professional, Tempe, AZ) prior to reaching a submerged J-11 low-frequency transducer (Naval Undersea Warfare Center, Newport, RI). Audiometric signals were calibrated prior to each session using the Reson TC4032 hydrophone at the position corresponding to the center of the subject's head while on the listening station. Measured signals were compared with expected sound pressure levels (SPLs) and evaluated in time and frequency domains to ensure signal quality. Spatial mapping of the received sound field was conducted at the start of the study to confirm acceptable variability ($\pm$3 dB) in the test stimulus within a 14 $\times$ 14 $\times$ 14 cm grid centered on the listening station.

2. Impulse noise generation and calibration

Two noise sources were used to generate impulsive stimuli. A custom 10 in.^{3} sleeve air gun (synthetic polymer, polyoxymethylene) was used for conditions C1–C4, and a BOLT 2800 LLX air gun (Teledyne Bolt, Houston, TX) with a 5 in.^{3} custom chamber was used to generate higher received levels for condition C5. In both cases, the air gun was suspended (with air supply and electrical lines secured) from a stainless-steel cable connected to a davit arm above the test pool. A portable air supply system was used to deliver an operational line pressure of 30–120 psi to the sleeve gun and 500 psi to the BOLT gun. The air gun was always pressurized before being submerged to a depth of 1 m. The horizontal distance relative to the exposure station was 1 m for the sleeve gun and 1.5 m for the BOLT air gun. The exact, fixed position of each source was determined through spatial characterization of received noise prior to the experiment; noise stimuli generated by either source were evaluated in terms of received level and acoustic characteristics to ensure the integrity and repeatability of received pulses at the exposure station in the pool. Reichmuth *et al.* (2016) provide additional details regarding sound source selection and consideration of these impulse stimuli relative to those generated by operational air gun arrays.

Single pulses from either air gun were triggered from a custom LabVIEW virtual instrument. The impulsive sounds were received by the Reson TC4013 hydrophone mounted at the exposure station, passed through a Reson VP2000 voltage preamplifier (with EC6069 battery module) and the NI 6259 data acquisition module, and measured in the LabVIEW software. Each noise exposure was quantified in terms of SEL, PCW-weighted SEL, peak-to-peak sound pressure, and peak sound pressure level.[2] Prior to each exposure session and without the subject present in the test pool, calibrated levels were determined and the operating pressure was adjusted to generate received levels that would fall within the target range established for the testing condition (see Table I). Every subject exposure during testing was also directly measured.

3. Hearing threshold measurements

Hearing was evaluated using a multiple-response go/no-go procedure to enable rapid assessment of hearing threshold. The subject was cued by a trainer to dive to the listening station and complete a series of signal detection trials before returning to the surface. During each trial, the trial light was illuminated to indicate the 4-s window within which a signal could occur. Correct responses—reporting a signal detection on a signal-present trial or remaining still on the station during a signal-absent trial—were marked by a conditioned acoustic reinforcer, after which the subject proceeded to the next trial. Incorrect responses—failure to report the signal on a signal-present trial (*miss*) or reporting a detection on a signal-absent trial (*false alarm*)—were not marked and the subject continued to the next trial. Each dive sequence consisted of 2–5 correct trials. An acoustic buzzer cued the subject to return to the surface following a correct response on the last trial of the dive, where a fish reward was delivered

https://doi.org/10.1121/10.0002649

by the trainer in proportion to the number of correct responses during the preceding block of trials. The percentage of signal-present trials within a session was predetermined and varied between 50% and 65%.

An adaptive staircase method (Cornsweet, 1962) was used to estimate hearing threshold. Testing began with salient signals 15–20 dB above the expected threshold. During the warm-up period of each session, signal level was decreased by 3 dB after each correct detection until the first miss. Subsequently, signal SPL was increased by 3 dB following each miss and decreased by 3 dB following each correct detection until a total of five hit-to-miss transitions were completed. If initial misses were elevated—indicating a potential shift—testing was continued until performance stabilized. However, hearing threshold was always calculated from the trials between the first descending miss and the fifth descending miss (inclusive) of the session. Each session concluded with several trials at suprathreshold levels, which served to maintain subject motivation and behavioral control on the task.

Hearing threshold for a given session was determined from signal-present trials following the method of Dixon and Mood (1948). Threshold was defined as the SPL resulting in a 50% correct detection rate. Signal-absent trials were used to quantify response bias; false alarm rate was defined as the proportion of signal-absent trials on which the seal reported the detection of a signal (pre-stimulus responses on signal-present trials were also classified as false alarms).

4. Noise exposure training and testing

The subject was gradually conditioned to tolerate low-level impulsive sounds prior to participation in air gun exposure sessions. Details of the training process can be found in Reichmuth *et al.* (2016).

Once testing began, each exposure condition (including both actual and mock exposures) was completed prior to advancing to the next, higher level. The subject began with a pre-exposure threshold session at 100 Hz. He could advance to exposure testing if the pre-exposure threshold was within 3 dB of the reference threshold, the session false alarm rate was <30%, and the ambient noise level in the 1/3-octave band including 100 Hz was within 6 dB of the pre-exposure measurement. Provided these criteria were met, the subject moved on to either (1) exposure to impulsive noise at the exposure station (*exposure session*) or (2) an equivalent period on the exposure station with no air gun pulses (*control session*). The exposure was initiated 1–4 s after the seal positioned at the exposure station and no warning stimulus preceded the impulsive sound. Following the exposure event, the subject was cued to swim to the listening station and a post-exposure threshold session began immediately. The first failed detection (miss) typically occurred within 3 min of the air gun exposure, while the fifth descending miss was within 8–9 min of exposure. Threshold shift (TS) was calculated as the difference between the pre-exposure and the post-exposure thresholds. The ratio of control to exposure sessions was 1:4 throughout testing.

5. Behavioral response scoring

The subject's behavioral responses were recorded to video during all exposure and control events. These video recordings were later processed into individual clips that included the subject's behavior on the exposure station just prior to, during, and after the exposure/control event. Audio was stripped from each clip and a red circle was added as a visual marker to delineate the response window, which lasted from the start of the exposure/control event until the subject was prompted to the surface for reinforcement (fish). Additionally, a yellow "warning" circle appeared 0.5 s prior to the start of the response window. The video clip contained no visual indication of whether an event was an exposure or a control.

Videos were reviewed and scored by three experimentally blind observers at the end of the study. The observers rated the subject's reaction during the response window on a scale from 0 to 5. A score of "0" indicated no detectable change in stationing behavior, "1" indicated a just-detectable change (slight movement or flinch without breaking contact with the station), "2" indicated a momentary change (brief movement of the subject's head from the station), "3" indicated that the subject moved less than one-half of a body-length from the station and returned within the response window, "4" indicated that the subject moved greater than one-half of a body-length from the station and returned within the response window, and "5" indicated that the subject's stationing behavior was disrupted and did not recover within the response window.

Scores from the three observers were averaged for each exposure/control event. Exposure series scores were then grouped according to condition (C1–C5), while control session scores were pooled across all testing conditions.

C. Experiment 2: The effect of single-shot exposures on hearing at the frequency of maximum sensation level

To ensure that hearing loss was not occurring at frequencies above 100 Hz, experiment 2 evaluated TTS at 400 Hz—the frequency of greatest sensation level for the test subject (see Fig. 1). Experiment 2 replicated the two highest-amplitude exposure conditions (C4 and C5) from experiment 1 with 400 Hz as the hearing test frequency (see Table I). Experimental methods were identical to those applied in experiment 1 except where noted below.

As the subject's baseline threshold at 100 Hz was so similar to his previously measured audiogram threshold, his pretest thresholds at 400 Hz were referenced to his 400 Hz audiogram threshold (67 dB re 1 μPa) when determining whether to proceed to exposure testing.

Response time data from correct detections on signal-present trials were compared for pretest sessions relative to posttest sessions with paired *t*-tests. For this statistical

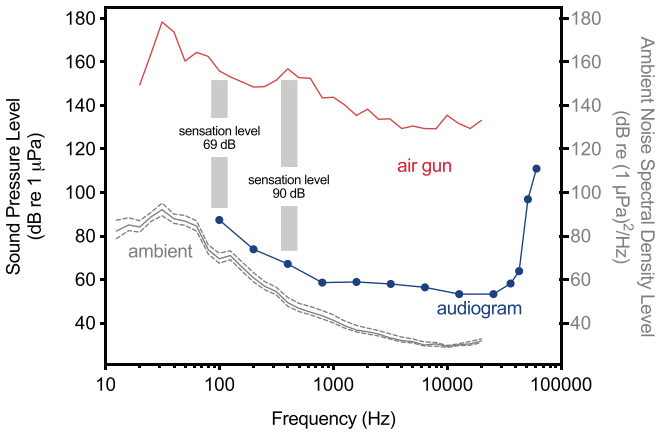

FIG. 1. (Color online) Average 1/3-octave band levels measured at the exposure station during condition C5 air gun testing are shown relative to the absolute underwater audiogram of the bearded seal subject (Sills *et al.*, 2020; left *y* axis). The air gun spectrum is an exemplar of the impulsive stimulus used (see Fig. 2, upper and lower panels); this stimulus was highly repeatable throughout testing (see Table III). The offset between the received air gun stimulus and the auditory threshold (i.e., the sensation level) is shown for both 100 and 400 Hz. Ambient noise spectral density levels were calculated from the median of measured 1/3-octave band levels ($n = 150$; see text and Fig. 2 lower panel), and are reported on the right *y* axis as the 50th percentile level of the noise distribution (L50, solid line). The 10th (L10, dashed line, above) and 90th (L90, dashed line, below) percentile levels are also given to characterize variability in background noise during the experiment.

comparison, data from experiments 1 (at 100 Hz) and 2 (at 400 Hz) were pooled to increase sample size and evaluated in terms of sensation level (i.e., SPL relative to threshold). While combining data for two frequencies may obscure absolute reaction times, this approach should have been sufficient to detect a change in latency from pre- to posttest sessions.

D. Experiment 3: The effects of multiple-shot exposures on hearing

Experiment 3 involved auditory testing with the bearded seal before and after exposure to multiple consecutive pulses from the BOLT air gun operated at the highest exposure condition (C5). Hearing was evaluated following two-, four-, and ten-shot exposure sequences. The inter-shot-interval was 10 s, which is representative of operational air gun arrays (International Association of Oil and Gas Producers, 2011; Gisiner, 2016).

Threshold testing was initially conducted at both 100 and 400 Hz. After a potential auditory effect was observed at 400 Hz during two- and four-shot testing, sessions were continued only at this frequency. As in experiment 2, the audiogram threshold served as the reference threshold for pretest sessions. However, testing proceeded more conservatively with a higher ratio of control sessions (~1:2). In order to evaluate fine-scale patterns of auditory recovery, TTS was calculated both in terms of full session thresholds (based on five hit-to-miss transitions) and based on just the first miss of the pre- and posttest sessions.

As another precautionary measure, supplemental data were collected at a nearby frequency during four- and ten-shot testing. After 400 Hz, 800 Hz had the highest sensation level from the air gun exposure. Preliminary testing was conducted at 800 Hz in a second post-exposure session, immediately following the first post-exposure session. While these threshold data at 800 Hz were typically collected 11–15 min following the noise exposure, screening at this nearby frequency was conducted to ensure that any substantial shifts (which would not likely recover within this time frame) would be detected. Similarly, during four- and ten-shot testing, additional sessions following the primary post-exposure session were sometimes run at the two main test frequencies (100 and 400 Hz) to screen for large shifts.

III. RESULTS

A. Ambient noise during air gun exposure testing

Ambient noise measurements from 75 days of testing yielded 150 1-min samples. Median 1/3-octave band 50th percentile levels are shown in the lower panel of Fig. 2; corresponding noise spectral density levels are reported in Fig. 1 as the 10th, 50th, and 90th percentile levels of the noise distribution. Median L50 ambient noise spectral density levels within the 100 Hz 1/3-octave band for pre-exposure sessions were similar to those measured for post-exposure sessions on the same day (two-tailed paired *t*-test; $t_{1.2,74}$, $p > 0.05$, $n = 75$). Median L50 ambient noise spectral density levels within the 400 Hz 1/3-octave band for pre-exposure sessions were also similar to those measured for post-exposure sessions (two-tailed paired *t*-test; $t_{0.7,74}$, $p > 0.05$, $n = 75$).

Comparison of hearing thresholds to ambient noise spectral density levels demonstrated average threshold-to-noise offsets of 17 dB at 100 Hz (14–23 dB) and 17 dB at 400 Hz (10–22 dB). These offsets are similar to the previously measured critical ratios for the bearded seal at the same frequencies (Sills *et al.*, 2020). However, while noise in the 100 and 400 Hz 1/3-octave bands did fluctuate somewhat from day to day, threshold measurements were relatively stable (standard deviation 1.8 dB at 100 Hz and 2.0 dB at 400 Hz), suggesting that ambient noise did not substantively influence measured hearing thresholds. Furthermore, the lack of systematic differences in noise from pre- to post-exposure sessions indicated that measured TSs could not be explained by increasing noise.

B. Experiment 1: The effect of single-shot exposures on hearing near the frequency of maximum exposure level

The mean baseline threshold ($n = 12$) measured for the bearded seal subject at 100 Hz prior to the start of exposure testing was 86 dB re 1 µPa. This threshold, obtained using the multiple-response method, was within 1 dB of the threshold measured previously for the same subject using single-response audiometry (Sills *et al.*, 2020). Response bias was stable during testing with a mean session false alarm rate of 16%.

https://doi.org/10.1121/10.0002649

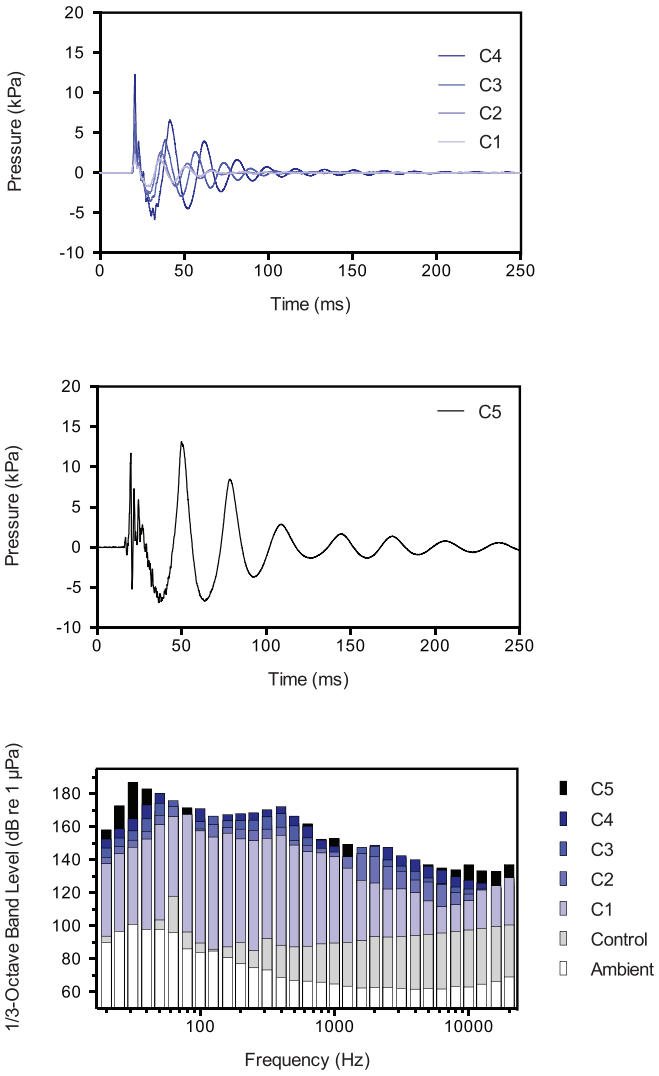

FIG. 2. (Color online) Air gun pulses received at the exposure station during testing. The upper panel shows examples of received waveforms from the four exposure conditions with the 10 in.^{3} sleeve gun (C1–C4) superimposed to align the primary pulse onsets. The center panel shows an exemplar received waveform for the highest exposure condition (C5) using the BOLT 2800 LLX air gun. The lower panel shows the frequency spectrum (0.01–20 kHz) of received 1/3-octave band levels from impulsive noise exemplars for each condition (C1–C5). These are the maximum, fast (125 ms time constant), unweighted noise levels for a 1-s period beginning at the onset of the pulse. Control bars show comparable levels measured with the same hydrophone during mock exposure conditions (note elevation over ambient levels due to the electrical noise of the measurement system). Ambient bars show the true background noise levels measured with a high-sensitivity hydrophone; these are median 1/3-octave band 50th percentile levels measured just prior to each pre-exposure and post-exposure session during the study period (1-min, unweighted noise samples, $n = 150$).

1. Received air gun exposures

Received exposure levels are reported as SEL, peak-to-peak sound pressure, and peak sound pressure level in Table II.[3] Representative waveforms for received noise stimuli are provided in Fig. 2. Data from conditions C1–C4 are combined in the upper panel of Fig. 2, while a representative condition C5 waveform is plotted in the middle panel. Noise exposures were reliable both within and across testing days within an experimental condition. Received stimuli from the sleeve air gun in conditions C1–C4 demonstrated the expected sharp-onset high-pressure peak followed by a negative pressure peak and subsequent bubble oscillations; this pattern is similar to that described in more detail in Reichmuth *et al.* (2016). Although received stimuli from the BOLT air gun used in condition C5 showed the same general patterns, there were some differences. The second positive peak (relative to hydrostatic pressure) was the highest, and there was comparatively greater energy in oscillations later in the time series. Another difference between the two seismic sources was the frequency distribution of received stimuli, which can be viewed in terms of maximum received 1/3-octave band levels in the lower panel of Fig. 2. Overall, there was more energy in lower frequency bands for the BOLT air gun used during condition C5 testing. For all exposures (C1–C5), measured peak-to-peak values were 3–5 dB higher than peak values.

2. Auditory responses

The bearded seal completed 32 exposures and 8 control sequences at 100 Hz, with median TSs from conditions C1–C5 provided in Table II. Individual and median TSs in each exposure and control condition are also depicted in the upper left panel of Fig. 3. All TSs were below the specified 6-dB criterion defining TTS onset, including at the highest exposure level of 185 dB re 1 μPa^2 s in condition C5. Median TS values of -1.5, $+0.3$, -0.4, $+0.6$, and $+0.8$ dB were observed for exposure sequences in conditions C1, C2, C3, C4, and C5, respectively, compared to a median TS of $+0.8$ dB in control sequences.

Also shown in Table II is a statistical measure of differences in false alarm rates for pre- and post-exposure threshold sessions. There were no significant differences in false alarm probability that could have affected TS measurements. There were no systematic trends in post-exposure audiometric data (as evaluated by linear regression) that would indicate possible recovery of hearing during these sessions.

3. Behavioral responses

Mean (rounded) behavioral scores for the bearded seal are shown for each testing condition in the upper right panel of Fig. 3. Mild but detectable behavioral responses were observed for the majority of exposure events, with no responses observed for the controls. Consistent avoidance responses were not observed. Mean responses did not exceed a behavioral score of *2* (with possible maximum of *5*); no individual response was scored higher than a *3*.

C. Experiment 2: The effect of single-shot exposures on hearing at the frequency of maximum sensation level

1. Received air gun exposures

The received noise stimuli in experiment 2 were similar to those in conditions C4 and C5 of experiment 1, shown in the upper two panels of Fig. 2. Received exposure levels for

TABLE II. Summary of received noise exposures for each single-shot condition (experiments 1 and 2), shown with corresponding TSs between pre- and post-exposure sessions. Received unweighted SEL (dB re 1 μPa^2 s), peak-to-peak sound pressure (pk-pk, dB re 1 μPa), and peak sound pressure level (pk, dB re 1 μPa) are shown as median values for each condition. TS is shown in dB as the median difference in absolute thresholds for each experimental (pre- to post-exposure) sequence, and ΔFA indicates the statistical difference in response bias from pre- to post-exposure sessions [two-tailed Fisher's exact test (0.05 α level); nonsignificant difference, ns; SD, standard deviation]. Control conditions conducted during 100 and 400 Hz testing are pooled.

Exposure condition	Test frequency (Hz)	Replicate exposure series n	Received SEL (SD)	Received pk-pk (SD)	Received pk (SD)	TS (SD)	ΔFA
C1	100	4	166 (0.5)	192 (0.5)	187 (0.9)	−1.5 (3.0)	ns
C2	100	8	171 (0.9)	196 (0.5)	191 (0.6)	+0.3 (1.3)	ns
C3	100	8	175 (0.8)	200 (1.5)	196 (2.0)	−0.4 (1.7)	ns
C4	100	8	179 (0.6)	206 (0.6)	202 (0.7)	+0.6 (2.7)	ns
C4	400	8	179 (0.5)	206 (0.5)	203 (0.6)	+0.4 (1.6)	ns
C5	100	4	184 (0.3)	206 (0.4)	203 (0.1)	+0.8 (1.6)	ns
C5	400	4	185 (0.4)	207 (0.4)	203 (0.5)	+0.5 (1.1)	ns
Control		11	—	—	—	+0.8 (1.6)	ns

experiment 2 are reported as SEL, peak-to-peak sound pressure, and peak sound pressure level in Table II.

2. Auditory responses

The bearded seal completed 12 exposures and 3 control sequences at 400 Hz, with median TSs from conditions C4 and C5 provided in Table II. Individual and median TSs for each exposure and control condition are also depicted in the lower left panel of Fig. 3. All TSs were below the 6-dB criterion defining TTS onset, including at the highest exposure level of 185 dB re 1 μPa^2 s in C5. Median TS values of +0.4 and +0.5 dB were observed at 400 Hz for exposure sequences in conditions C4 and C5, respectively, compared to a median TS of +0.8 dB in control sequences.[4]

A statistical measure of differences in false alarm rates for pre- and post-exposure threshold sessions is shown in Table II. As in experiment 1, there were no significant

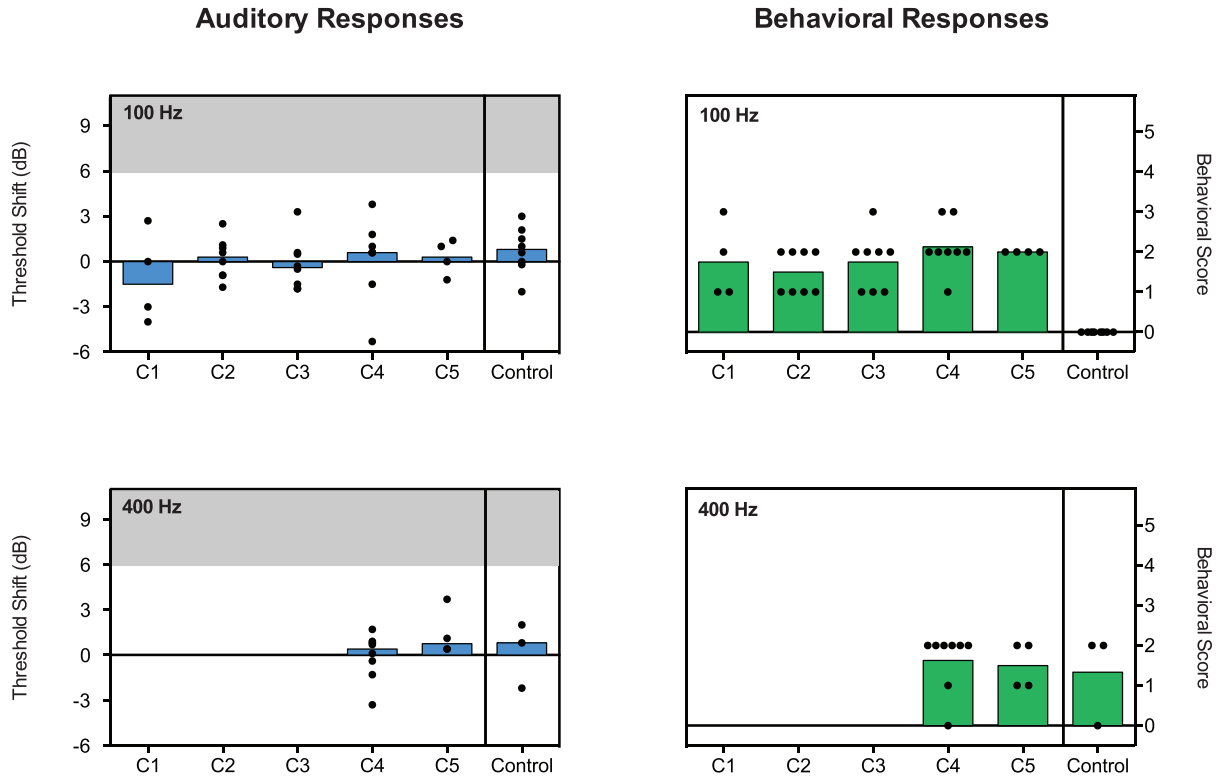

FIG. 3. (Color online) Auditory and behavioral responses of the seal are shown for each of the single-shot exposure conditions (C1–C5) and the control (no-exposure) condition. The upper panels depict testing at 100 Hz, while the lower panels provide results for testing at 400 Hz. Auditory responses (left panels) are shown as individual (points) and median (colored bars) TSs (dB). Median TSs did not exceed 1.0 dB, and no individual TS exceeded the 6-dB TTS onset criterion denoted by the shaded portion of the plot. Behavioral responses (right panels) are shown as individual (points) and mean (colored bars) behavioral scores obtained for the same exposure and control conditions. Score definitions for the 0–5 scale are provided in the text. During air gun exposure testing, the seal showed mean behavioral scores ≤2 in all exposure conditions, indicating relatively mild behavioral responses following training with lower amplitude impulsive sounds.

https://doi.org/10.1121/10.0002649

differences in false alarm probability that could have affected TS measurements, and there were no systematic trends in post-exposure audiometric data (as evaluated by linear regression) that would indicate possible recovery of hearing during these sessions.

Auditory reaction time data collected during threshold testing at 100 and 400 Hz (pooled for experiments 1 and 2) confirmed the lack of any effect in the highest testing condition (C5) as compared to control sessions. Auditory reaction times for sensation levels from 1 to 23 dB showed no systematic increase following noise exposure, suggesting that stimulus salience was similar before and after noise exposure. There was no significant difference in auditory reaction time in 18/19 paired pre- to post-exposure comparisons (T-test, $p > 0.05$); in one case, there was a detectable decrease in response time.

3. Behavioral responses

Behavioral scores for the bearded seal are shown in the bottom right panel of Fig. 3. Mild but detectable behavioral responses were observed for the majority of exposure events, with some (but fewer) responses for controls. None of the mean responses exceeded a behavioral score of *2* (with possible maximum of *5*); no individual response was scored higher than a *2*. As in experiment 1, consistent avoidance responses were not observed.

D. Experiment 3: The effects of multiple-shot exposures on hearing

1. Received air gun exposures

The individual pulses in experiment 3 were similar to those received in condition C5 of experiments 1 and 2, with single-shot SEL of approximately 185 dB re 1 μPa^2 s, peak-to-peak sound pressure of approximately 207 dB re 1 μPa, and a peak sound pressure level of approximately 203 dB re 1 μPa (see Table II, C5). Within a multiple-shot exposure series, the pulses were repeatable and well described by the middle plot in Fig. 2. Received levels for experiment 3 are reported for each exposure series in Table III, both as an unweighted cSEL value and with PCW-weighting applied. The separation between emitted shots in these sequences was 10 s except in the cases noted below.

2. Auditory responses

The bearded seal completed ten multiple-shot exposure sequences at 400 Hz (the primary test frequency), four exposure sequences at 100 Hz, and six control sequences. Of the exposures, four were two-shot exposure sequences, six were four-shot sequences, and four were ten-shot sequences. Table III provides the testing order, received noise exposure levels, and median TSs observed in each testing sequence in experiment 3. TS is reported both in terms of the full session (first five descending misses following noise exposure) and

TABLE III. Summary of multiple-shot noise exposure sequences during experiment 3. Received cumulative sound exposure level (cSEL, dB re 1 μPa^2 s) is provided for each exposure series both as an unweighted value and with PCW weighting applied (Southall *et al.*, 2019). For reference, the received unweighted SEL, peak-to-peak sound pressure, and peak sound pressure level values for the single pulses in each multiple-shot exposure were ~185 dB re 1 μPa^2 s, ~207 dB re 1 μPa, and ~203 dB re 1 μPa, respectively (see Table II, C5). TSs are reported in dB as the difference in absolute thresholds between pre- and post-exposure sessions, both for the full session (first five descending misses) and for the first miss only, which occurred 68–309 s (median 184 s) after the offset of the fatiguing noise (see Fig. 4). Behavioral responses are provided for each exposure series as the mean score across pulses; score definitions for the 0–5 scale are provided in the text. ΔFA indicates statistical difference in response bias from pre- to post-exposure sessions [two-tailed Fisher's exact test (0.05 α level); nonsignificant difference, ns; significant difference ($p < 0.05$), higher or lower].

Number of shots	Exposure series number	Test frequency (Hz)	Received cSEL (SD)	Received PCW-weighted cSEL (SD)	TS, session (SD)	TS, first miss (SD)	Behavioral score (SD)	ΔFA
2	1	100	188	163	−1.1	0.0	1.8 (0.2)	—
	2	100	187	163	−0.7	−6.0	2.0 (0.0)	—
	3	400	188	164	+5.4	+3.0	1.0 (1.4)	—
	4	400	188	164	+2.3	+3.0	1.8 (0.2)	—
	Summary ($n = 2$)	100	188 (0.3)	163 (0.1)	−0.9 (0.3)	−3.0 (4.2)	1.9 (0.1)	ns
	Summary ($n = 2$)	400	188 (0.2)	164 (0.1)	+3.9 (2.2)	+3.0 (0.0)	1.4 (0.6)	(higher)
4	1	400	191	167	+9.4	+15.0	1.8 (0.3)	—
	2	400	191	166	+5.6	+3.0	1.1 (0.7)	—
	3	100	191	166	+2.4	0.0	2.2 (0.4)	—
	4	400	191	167	+6.4	+3.0	1.6 (0.7)	—
	5	100	191	166	−0.9	−6.0	1.7 (0.3)	—
	6	400	191	167	−1.8	0.0	1.7 (0.6)	—
	Summary ($n = 2$)	100	191 (0.1)	166 (0.2)	+0.8 (2.3)	−3.0 (4.2)	1.9 (0.4)	ns
	Summary ($n = 4$)	400	191 (0.3)	167 (0.4)	+6.0 (4.8)	+5.3 (6.7)	1.5 (0.3)	ns
10	1	400	195	170	+4.1	+15.0	1.8 (1.2)	—
	2	400	194	171	+3.9	+12.0	2.0 (0.7)	—
	3	400	194	171	+0.5	+3.0	1.5 (0.4)	—
	4	400	194	171	−0.5	0.0	1.5 (0.7)	—
	Summary ($n = 4$)	400	194 (0.3)	171 (0.4)	+2.2 (2.4)	+7.5 (7.1)	1.7 (0.3)	ns
	Control (pooled, $n = 6$)	—	—	—	−0.2 (1.8)	−1.0 (3.1)	1.6 (0.4)	ns

in terms of the first miss only (post-exposure SPL referenced to pre-exposure SPL). Also provided in Table III is a statistical measure of differences in false alarm rates for pre- and post-exposure threshold sessions. As in the earlier experiments, there were no significant differences in false alarm probability that could have affected TS measurements.

At 400 Hz, TSs following two-shot exposures were below the 6-dB criterion defining TTS onset. However, testing did reveal shifts of +2.3 to +5.4 dB, which were higher than in earlier experiments. Subsequent four-shot exposure testing revealed a median shift of +6.0 dB at 400 Hz, with more variability in shifts measured in terms of the first miss (range 0.0 to +15.0 dB). Finally, ten-shot exposure testing resulted in a median shift of +2.2 dB, and a median shift of +7.5 dB when considering just the first miss.

Hearing at 400 Hz was also evaluated three times in secondary post-exposure sessions following primary four-shot testing at 100 Hz: twice after air gun exposures and once after a control sequence. In the two sessions following exposures, shifts of +7.8 and +3.7 dB were measured at 400 Hz relative to the audiogram threshold; initial TS was estimated at +13.0 and +7.0 dB for these sessions, respectively, based on just the first miss in each case. In the secondary post-exposure session following the control sequence, the measured TS was 0.0 dB. While these supplementary data are not summarized in Table III, they are included in Fig. 4, which depicts patterns in auditory performance at 400 Hz during four- and ten-shot exposure testing. Individual misses are plotted in Fig. 4 with respect to timing and signal SPL so that they can be evaluated in relation to the 6-dB TTS onset criterion. Threshold for these secondary post-exposure sessions was typically measured between 11 and 16 min following noise exposure.

At 100 Hz, all individual and median TSs during two- and four-shot exposure testing were below the 6-dB criterion defining TTS onset. Based on these results and because there were indications of a change in hearing sensitivity at 400 Hz at these levels, no further testing was conducted with 100 Hz as the primary test frequency. Hearing at 100 Hz was evaluated four times in secondary post-exposure sessions following primary testing at 400 Hz: three times after air gun exposure sequences and once following a control sequence. There was no indication of TS in any of these sessions.

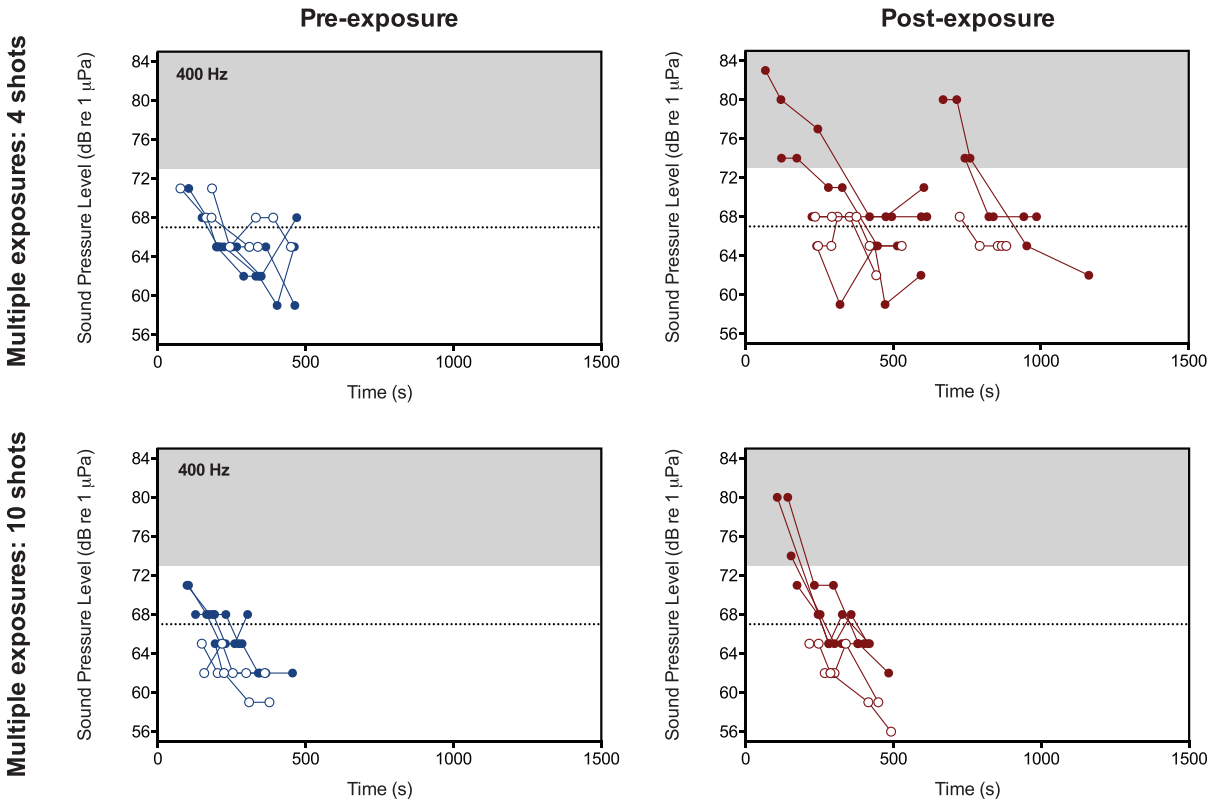

FIG. 4. (Color online) Patterns of performance during auditory testing at 400 Hz before and after exposure to multiple air gun pulses at condition C5 levels (experiment 3). Only failures to detect the audiometric signal (misses) are shown, with sequential misses from each individual session connected by a line. Misses are plotted in terms of timing and SPL of the audiometric signal. Sessions conducted before and after exposure to the air gun stimulus are shown with closed circles, while sessions conducted before and after control (mock) exposures are shown with open circles. Pre- and post-exposure sessions are shown in the left and right panels, respectively, for each four-shot (upper panels) and ten-shot (lower panels) testing series. Note that pre-exposure timing is referenced to the first trial of the session while post-exposure timing is referenced to the offset of the fatiguing (air gun) stimulus (shown at 0 s). The shaded portion of each plot denotes the 6-dB TTS onset criterion relative to the audiogram threshold at 400 Hz (67 dB re 1 μPa, dotted line). While the open circles (control data) show the typical patterns of performance during pre- and post-exposure sessions, elevated misses following air gun exposures (the closed circles in the shaded regions of the plots) demonstrate rapidly recovering shifts in auditory sensitivity at the test frequency.

https://doi.org/10.1121/10.0002649

Supplementary testing at 800 Hz was conducted four times during secondary post-exposure sessions: once following a four-shot exposure sequence, twice following ten-shot exposure sequences, and once following a ten-shot control sequence. In all cases, the post-exposure threshold showed no elevation relative to the audiogram threshold measured previously at the same frequency.

In a few cases, the timing of the interval between pulses varied somewhat from the nominal 10-s duration. If the subject's head was not positioned suitably at the exposure station, the experimenter would manually override the exposure. Once the subject re-stationed sufficiently, the experimenter would allow the sequence to continue. In three instances, this resulted in an interval of 12–20 s between two shots in an exposure sequence. For one session during four-shot testing, there was a delay of approximately 4 min between the first and second pulses in the series; the +6.4 dB TS measured in this case may, therefore, be a conservative estimate of TS.

No systematic differences in response times to 100 and 400 Hz audiometric stimuli were observed in experiment 3. Small sample sizes precluded reaction time comparisons within a single testing series, which may have revealed changes in response times following noise exposure events that produced TTS.

3. Behavioral responses

Behavioral scores for each exposure sequence and the control sequences are provided in Table III. Mild but detectable behavioral responses were observed for the majority of exposure events and controls during multiple-shot testing. As in prior experiments, consistent avoidance responses were not observed.

IV. DISCUSSION

There was no evidence of TS at 100 or 400 Hz in a bearded seal following exposure to single-shot air gun pulses with received SEL up to 185 dB re 1 μPa^2 s, peak-to-peak sound pressure up to 207 dB re 1 μPa, and peak sound pressure level up to 203 dB re 1 μPa. Similarly, multiple-shot exposures at this level, with cumulative SEL up to 191 dB re 1 μPa^2 s (PCW-weighted cSEL 167 dB re 1 μPa^2 s), caused no apparent change in auditory sensitivity at 100 Hz. However, the bearded seal's performance at 400 Hz—while somewhat variable—showed evidence of transient shifts in auditory sensitivity following exposure to four or more pulses with received cSEL of 191–195 dB re 1 μPa^2 s (PCW-weighted cSEL 167–171 dB re 1 μPa^2 s). The largest shift measured following exposure was +9.4 dB, whereas the largest shift based on the first miss following noise exposure was +15.0 dB. Hearing recovered quickly, and always returned to baseline levels during post-exposure testing ($\leq$16 min).

The rapid recovery of and variation in TSs measured at 400 Hz following four- and ten-shot exposure sequences make it difficult to precisely describe the onset of TTS. However, following seven of ten exposures (five with 400 Hz as the primary test frequency and two with 400 Hz as the secondary test frequency), initial misses were 6 dB or more above this subject's audiogram threshold. While recovery of hearing during these post-exposure sessions resulted in lower shifts when measured over the threshold session, there was clearly an auditory effect at this level of noise exposure.

These findings underscore the importance of timing in any study of TTS. Here, the timing of threshold measurement was generally similar to the TTS_5 metric used previously for pinnipeds (Finneran *et al.*, 2003; Reichmuth *et al.*, 2016; Reichmuth *et al.*, 2019). However, it is likely that some recovery of hearing has already occurred after five minutes (see, e.g., Reichmuth *et al.*, 2019). Despite generating a more variable result, direct comparison between the first miss of the pre-exposure session and the first miss of the post-exposure session may provide a more accurate assessment of the maximum, initial TS after noise exposure. For example, in this study the largest TTS measured in this way was +15.0 dB—at the frequency of maximum sensation level for the bearded seal subject—while the shift measured based on the full session threshold was +4.1 dB for the same exposure series. However, this approach requires many exposures to provide robust measures.

In addition to the auditory data directly evaluating TTS, reaction times were used as a secondary metric to confirm the absence of an effect on hearing when auditory TSs were not observed. No changes in reaction time were observed during experiments 1 and 2. Due to small sample sizes, we were not able to directly compare reaction times in experiment 3 for pre- and post-exposure threshold sessions in cases when a shift did occur. In these cases, a difference in response latency at a particular signal level would have been expected. In future studies, it would be useful to further explore the relationship between TSs and changes in response time. However, such an effort would also require a greater number of high exposure-level sessions than were conducted here (with a corresponding increase in response time measurements at each signal level), or else much higher TSs than induced in this study.

Similarly, the behavioral data complement the primary measurements of auditory sensitivity. The observed responses of the bearded seal were not suggestive of self-mitigation, which (if present) could have confounded measurements of TTS (see, e.g., Finneran *et al.*, 2015; Nachtigall *et al.*, 2016; Kastelein *et al.*, 2020). The seal was gradually trained to tolerate successively louder pulses before the start of exposure testing and, thus, had a unique exposure history relative to wild or naive individuals. The relatively mild behavioral responses of the bearded seal to these air gun stimuli should not be taken as an indication of how wild seals might react to an operational array. However, this seal's willingness to participate in exposure sequences that temporarily harmed hearing indicates that free-ranging seals may experience TTS (or permanent threshold shift, see Reichmuth *et al.*, 2019) in the absence of overt behavioral indicators.

A significant challenge for TTS studies is determining how to measure the fatiguing exposure in terms of the most biologically relevant metric. For impulsive noise, peak sound pressure level and SEL have been proposed as dual metrics to describe noise stimuli and predict TTS onset (Southall *et al.*, 2007; Finneran, 2016; National Marine Fisheries Service, 2018; Southall *et al.*, 2019), with the intent of addressing both intense instantaneous events and sustained or repeated exposures. The aim in the present study was to identify TTS onset conditions following impulsive noise exposure, with target exposure levels set primarily based on SEL. The experimental design was developed to reach predicted TTS onset levels for one exposure metric (SEL) while not overshooting the other (peak sound pressure level). If target levels had instead been set based on peak sound pressure level, the corresponding cSELs for multiple-shot exposures would have been considerably higher—well above predicted TTS onset levels and likely exceeding the behavioral tolerance of the subject. This SEL-based approach was sufficient to induce TTS, despite noise exposures with peak sound pressure levels reaching only 203 dB re 1 μPa, well below the predicted TTS-onset level of 212 dB re 1 μPa. While peak sound pressure level is certainly relevant for single high-amplitude exposures, SEL may be the more effective metric for most exposure scenarios with multiple, repeated impulses (Southall *et al.*, 2007; Southall *et al.*, 2019). Additional research is needed to confirm how best to characterize impulsive noise exposures with respect to hearing in marine mammals.

Another issue for TTS studies using impulsive, broadband noise is knowing where to look for auditory effects that may be distributed across frequencies. Auditory effects are suspected to occur at lower frequencies, in the region of greatest noise exposure; however, it is also in this frequency range that more time-consuming behavioral, rather than neurophysiological, methods are required. Behavioral studies conducted with spotted, ringed, and bearded seals exposed to impulsive noise (Reichmuth *et al.*, 2016; this study, experiment 1) considered auditory effects at frequencies just higher than the maximum energy in the broadband exposure (100 Hz). Evaluating hearing 1/2-octave above the exposure frequency is common in marine mammal studies (see Finneran, 2015). For example, recent work using tonal exposures has shown that—while the frequency of maximum TTS may vary with exposure level—auditory effects typically manifest at the center frequency of the exposure or 1/2-octave higher (Kastelein *et al.*, 2014; Kastelein *et al.*, 2019). Conversely, experiment 3 of the present study revealed the primary auditory effect following broadband, impulsive exposures at the frequency of greatest sensation level. Of two primary frequencies tested, the larger effect was observed at the frequency with the greater exposure level relative to the subject's auditory sensitivity. While we cannot rule out the possibility that more substantial TTS occurred at a higher frequency, preliminary screening at 800 Hz suggests this was not the case. Thus, when evaluating the effects of impulsive noise on hearing, it appears that expected patterns with respect to the frequency spread of TTS may not hold, and that considering the sensation level of the exposure may better predict the frequency (or frequencies) of maximum shift. The question of how broadband noise exposures manifest with respect to frequency-specific hearing effects is an important one, which should be evaluated through additional research. An improved understanding of the frequency of maximum TTS following impulsive exposures would both inform future empirical studies of noise-induced hearing loss and enable more accurate predictions of the auditory and ecological effects of impulsive noise on free-ranging seals.

This study highlights some of the difficulties involved in acquiring information about auditory responses in marine mammals, where sample size and exposure conditions are both constrained by time-consuming methods and significant expense. Experiment 1 of this study with one bearded seal extends the results of earlier work with spotted and ringed seals (Reichmuth *et al.*, 2016), demonstrating comparable responses to single-shot exposures. This expands available data from two to three species and from four to five individuals, which substantially increases the generality of these results. In addition to these data close to the frequency of maximum exposure, experiment 2 captures auditory effects at the frequency of maximum sensation level for one bearded seal—with opportunistic testing for one ringed seal[2]—lending additional confidence to the finding of no effect following single-shot exposures with SEL up to 185 dB re 1 μPa^2 s. Experiment 3 builds upon this research and hones in on the multiple-shot exposure conditions that produce auditory damage in seals. Although the results presented in experiment 3 are for a moderate number of multiple-shot exposures with a single individual, and are not conclusive with respect to the growth of TTS, the onset data provided are important and strengthened by the foundational data at lower received levels and with multiple species.

Considered together with the findings from Reichmuth *et al.* (2016), these results for five individuals significantly advance understanding of how impulsive noise affects the hearing of seals. With respect to current regulatory guidelines, this body of work suggests that the PCW-weighted TTS-onset level of 170 dB re 1 μPa^2 s SEL (predicted by Finneran, 2016; National Marine Fisheries Service, 2018; Southall *et al.*, 2019) is likely appropriate for seals in water. However, future work documenting larger TSs and patterns of auditory recovery following exposure to impulsive noise will be required to precisely define the exposure conditions resulting in TTS onset.

ACKNOWLEDGMENTS

Research was supported by the Joint Industry Programme on Sound and Marine Life through Contract No. JIP 22 07-23. In particular, we are grateful to L. Brzuzy, J. Campbell, R. Gentry, G. Wolinsky, and P. Van Der Sman for their support at various stages of the project. We thank the Native Village of Kotzebue (especially A. Whiting and

J. Goodwin), the Alaska SeaLife Center (especially B. Long, Dr. C. Goertz, and Dr. K. Woodie), and UC Santa Cruz veterinarian Dr. D. Casper for invaluable help with animal acquisition and care. TNO (F. P. Lam and E. Jansen) and Teledyne Marine (B. Kawejsza and J. Norton) provided technical assistance with sound source selection, fabrication, calibration, maintenance, and safety protocols for the sleeve gun and BOLT LX 2800 air gun, respectively. J. Finneran of the U.S. Navy Marine Mammal Program provided access to the custom LabVIEW software used to measure noise exposures and auditory thresholds. We thank J. Mulsow and one anonymous reviewer for helpful feedback that improved this manuscript. This work was made possible by our dedicated husbandry and research team at Long Marine Laboratory; in particular, we thank J. Sullivan and C. Casey for animal training support; C. Lew for assistance with experimental sessions; A. Rouse for technical support; and J. Ahrens, S. Fullmer, E. Jones, and M. Meranda for assistance with behavioral analysis.

[1]The frequency content of the exposure is weighted relative to auditory parameters for the functional hearing group. Frequencies within the range of best hearing are minimally weighted, whereas frequencies above and below this range are weighted according to the exposure function. See Houser *et al*. (2017) for details about the use of auditory weighting functions to predict the effects of noise on marine mammal hearing.

[2]The desired noise levels for these experiments were determined with a focus on SEL as the primary metric, with peak-to-peak sound pressure (which captured the asymmetrical nature of the received waveform) considered secondarily. For comparison to predicted TTS onset thresholds, PCW-weighted SEL and peak sound pressure level are also provided in Sec. III (Results).

[3]To supplement the primary acoustic pressure measurements, maximum broadband (0.01–1 kHz) particle velocity measurements (dB re 1 nm/s) were obtained along the main axis of transmission for typical received air gun exposures in conditions C4 and C5. A calibrated, negatively buoyant M20 velocity sensor (GeoSpectrum Technologies, Inc., Dartmouth, Nova Scotia, Canada) was suspended in a stable orientation from a polyurethane mounting rope affixed to a steel pipe spanning (but decoupled from) the pool. Three measurements per condition were obtained at the position of the exposure station with the sensor oriented to maximize directional sensitivity. As with the measured pressure values, maximum particle velocities were consistent between shots. The median of maximum particle velocity measurements for representative exposures was 162 dB re 1 nm/s in condition C4 and 163 dB re 1 nm/s in condition C5.

[4]A second subject, a 7-year-old female ringed seal identified as *Nayak* (NOA0006783), participated in a portion of experiment 2 in addition to the bearded seal. *Nayak* had previously completed single-shot air gun TTS testing at 100 Hz, up to condition C4 received levels (Reichmuth *et al*., 2016). Here, she repeated condition C4 testing at 400 Hz. *Nayak* completed four exposures and one control sequence at 400 Hz. This ringed seal had a median TS value of +1.2 dB at 400 Hz for exposure sequences in condition C4, compared to a TS of −0.3 dB in the control sequence. There were no systematic trends in her post-exposure audiometric data that would indicate possible recovery of hearing during these sessions. These supplemental data confirmed the absence of an auditory effect at 400 Hz following single-shot noise exposures with levels up to 180 dB re 1 μPa^2 s.

Cornsweet, T. N. (**1962**). "The staircase method in psychophysics," Am. J. Psychol. **75**, 485–491.

Dixon, W. J., and Mood, A. M. (**1948**). "A method for obtaining and analyzing sensitivity data," J. Am. Stat. Assoc. **43**, 109–126.

Erbe, C., Reichmuth, C., Cunningham, K., Lucke, K., and Dooling, R. (**2016**). "Communication masking in marine mammals: A review and research strategy," Mar. Pollut. Bull. **103**, 15–38.

Finneran, J. J. (**2003**). "An integrated computer-controlled system for marine mammal auditory testing," Technical Document No. 3159, SSC Pacific, San Diego, CA.

Finneran, J. J. (**2015**). "Noise-induced hearing loss in marine mammals: A review of temporary threshold shift studies from 1996 to 2015," J. Acoust. Soc. Am. **138**, 1702–1726.

Finneran, J. J. (**2016**). "Auditory weighting functions and TTS/PTS exposure functions for marine mammals exposed to underwater noise," Technical Report No. 3026, San Diego, CA.

Finneran, J. J., Dear, R., Carder, D. A., and Ridgway, S. H. (**2003**). "Auditory and behavioral responses of California sea lions (*Zalophus californianus*) to single underwater impulses from an arc-gap transducer," J. Acoust. Soc. Am. **114**, 1667–1677.

Finneran, J. J., Schlundt, C. E., Branstetter, B. K., Trickey, J., Bowman, V., and Jenkins, K. (**2015**). "Effects of multiple impulses from a seismic air gun on bottlenose dolphin hearing and behavior," J. Acoust. Soc. Am. **137**, 1634–1646.

Gedamke, J., and McCauley, R. D. (**2010**). "Initial quantification of low frequency masking potential of a seismic survey," in *Rep. Mtg Int. Whal. Commn.* SC/2062/E Vol. 12, p. 7.

Gisiner, R. (**2016**). "Sound and marine seismic surveys," Acoust. Today **12**(4), 10–18.

Hildebrand, J. A. (**2009**). "Anthropogenic and natural sources of ambient noise in the ocean," Mar. Ecol. Prog. Ser. **395**, 5–20.

Houser, D., Yost, W., Burkard, R., Finneran, J. J., Reichmuth, C., and Mulsow, J. (**2017**). "A review of the history, development and application of auditory weighting functions in humans and marine mammals," J. Acoust. Soc. Am. **141**(3), 1371–1413.

International Association of Oil and Gas Producers (**2011**). "An overview of marine seismic operations," Report No. 448, April.

Kastak, D., Reichmuth, C., Holt, M. M., Mulsow, J., Southall, B. L., and Schusterman, R. J. (**2007**). "Onset, growth, and recovery of in-air temporary threshold shift in a California sea lion (*Zalophus californianus*)," J. Acoust. Soc. Am. **122**, 2916–2924.

Kastak, D., Schusterman, R. J., Southall, B. L., and Reichmuth, C. (**1999**). "Underwater temporary threshold shift induced by octave-band noise in three species of pinniped," J. Acoust. Soc. Am. **106**, 1142–1148.

Kastak, D., Southall, B. L., Schusterman, R. J., and Reichmuth Kastak, C. (**2005**). "Underwater temporary threshold shift in pinnipeds: Effects of noise level and duration," J. Acoust. Soc. Am. **118**, 3154–3163.

Kastelein, R. A., Gransier, R., Marijt, M. A. T., and Hoek, L. (**2015**). "Hearing frequency thresholds of harbor porpoises (*Phocoena phocoena*) temporarily affected by played back offshore pile driving sounds," J. Acoust. Soc. Am. **137**, 556–564.

Kastelein, R. A., Helder-Hoek, L., Cornelisse, S. A., von Benda-Beckmann, A. M., Lam, F. P. A., de Jong, C. A., and Ketten, D. R. (**2020**). "Lack of reproducibility of temporary hearing threshold shifts in a harbor porpoise after exposure to repeated airgun sounds," J. Acoust. Soc. Am. **148**(2), 556–565.

Kastelein, R. A., Helder-Hoek, L., and Gransier, R. (**2019**). "Frequency of greatest temporary hearing threshold shift in harbor seals (*Phoca vitulina*) depends on fatiguing sound level," J. Acoust. Soc. Am. **145**, 1353–1362.

Kastelein, R. A., Helder-Hoek, L., Kommeren, A., Covi, J., and Gransier, R. (**2018**). "Effect of pile-driving sounds on harbor seal (*Phoca vitulina*) hearing," J. Acoust. Soc. Am. **143**(6), 3583–3594.

Kastelein, R. A., Helder-Hoek, L., Van de Voorde, S., von Benda-Beckmann, A. M., Lam, F. P. A., Jansen, E., de Jong, C. A. F., and Ainslie, M. A. (**2017**). "Temporary hearing threshold shift in a harbor porpoise (*Phocoena phocoena*) after exposure to multiple airgun sounds," J. Acoust. Soc. Am. **142**(4), 2430–2442.

Kastelein, R. A., Schop, J., Gransier, R., and Hoek, L. (**2014**). "Frequency of greatest temporary hearing threshold shift in harbor porpoises (*Phocoena phocoena*) depends on the noise level," J. Acoust. Soc. Am. **136**(3), 1410–1418.

Lucke, K., Siebert, U., Lepper, P. A., and Blanchet, M-A. (**2009**). "Temporary shift in masked hearing thresholds in a harbor porpoise (*Phocoena phocoena*) after exposure to seismic airgun stimuli," J. Acoust. Soc. Am. **125**(6), 4060–4070.

McDonald, M. A., Hildebrand, J. A., and Wiggins, S. M. (**2006**). "Increases in deep ocean ambient noise in the Northeast Pacific west of San Nicolas Island, California," J. Acoust. Soc. Am. **120**, 711–718.

Nachtigall, P. E., Supin, A. Ya., Smith, A. B., and Pacini, A. F. (**2016**). "Expectancy and conditioned hearing levels in the bottlenose dolphin (*Tursiops truncatus*)," J. Exp. Biol. **219**, 844–850.

National Marine Fisheries Service (**2018**). "2018 revisions to: Technical guidance for assessing the effects of anthropogenic sound on marine mammal hearing (version 2.0): Underwater acoustic thresholds of permanent and temporary threshold shifts," NOAA Technical Memorandum NMFS-OPR-59, U.S. Dept. of Commerce, NOAA.

Nieukirk, S. L., Mellinger, D. K., Moore, S. E., Klinck, K., Dziak, R. P., and Goslin, J. (**2012**). "Sounds from airguns and fin whales recorded in the mid-Atlantic Ocean, 1999–2009," J. Acoust. Soc. Am. **131**(2), 1102–1112.

Reichmuth, C., Ghoul, A., Sills, J. M., Rouse, A., and Southall, B. L. (**2016**). "Low-frequency temporary threshold shift not observed in spotted or ringed seals exposed to single air gun impulses," J. Acoust. Soc. Am. **140**, 2646–2658.

Reichmuth, C., Holt, M. M., Mulsow, J., Sills, J. M., and Southall, B. L. (**2013**). "Comparative assessment of amphibious hearing in pinnipeds," J. Comp. Physiol. A.: Neuroethol. Sens. Neural. Behav. Physiol. **199**, 491–507.

Reichmuth, C., Sills, J. M., Mulsow, J., and Ghoul, A. (**2019**). "Long-term evidence of noise-induced permanent threshold shift in a harbor seal (*Phoca vitulina*)," J. Acoust. Soc. Am. **146**(4), 2552–2561.

Richardson, W. J., Greene, C. R., Malme, C. I., and Thomson, D. H. (**1995**). *Marine Mammals and Noise* (Academic, San Diego, CA).

Sills, J. M., Reichmuth, C., Southall, B. L., Whiting, A., and Goodwin, J. (**2020**). "Auditory biology of bearded seals (*Erignathus barbatus*)," Polar Biol. **43**, 1681–1691.

Sills, J. M., Southall, B. L., and Reichmuth, C. (**2014**)."Amphibious hearing in spotted seals (*Phoca largha*): Underwater audiograms, aerial audiograms and critical ratio measurements," J. Exp. Biol. **217**, 726–734.

Sills, J. M., Southall, B. L., and Reichmuth, C. (**2015**). "Amphibious hearing in ringed seals (*Pusa hispida*): Underwater audiograms, aerial audiograms and critical ratio measurements," J. Exp. Biol. **218**, 2250–2259.

Southall, B. L., Bowles, A. E., Ellison, W. T., Finneran, J. J., Gentry, R. L., Greene, C. R. J., Kastak, D., Ketten, D. R., Miller, J. H., Nachtigall, P. E., Richardson, J. W., Thomas, J. A., and Tyack, P. L. (**2007**). "Marine mammal noise exposure criteria: Initial scientific recommendations," Aquat. Mamm. **33**, 411–521.

Southall, B. L., Finneran, J. J., Reichmuth, C., Nachtigall, P. E., Ketten, D. R., Bowles, A. E., Ellison, W. T., Nowacek, D. P., and Tyack, P. L. (**2019**). "Marine mammal noise exposure criteria: Updated scientific recommendations for residual hearing effects," Aquat. Mamm. **45**, 125–232.

Conservation Physiology

Volume 9 • 2021 10.1093/conphys/coaa112

SEB SOCIETY FOR EXPERIMENTAL BIOLOGY

Research article

Molting strategies of Arctic seals drive annual patterns in metabolism

Nicole M. Thometz[1,2,*], Holly Hermann-Sorensen[2], Brandon Russell[3], David A. S. Rosen[4] and Colleen Reichmuth[2,3]

[1]Department of Biology, University of San Francisco, 2130 Fulton St, San Francisco, 94117 CA, USA
[2] Institute of Marine Sciences, University of California Santa Cruz, Long Marine Laboratory, 115 McAllister Way, Santa Cruz, 95060 CA, USA
[3] Alaska SeaLife Center, 301 Railway Ave, Seward, 99664 AK, USA
[4] Marine Mammal Research Unit, Institute for the Oceans and Fisheries, The University of British Columbia, 2202 Main Mall, Vancouver, BC V6T 1Z4, Canada.

***Corresponding author:** Department of Biology, University of San Francisco, 2130 Fulton St, San Francisco, 94117 CA, USA.
Email: nthometz@usfca.edu

Arctic seals, including spotted (*Phoca largha*), ringed (*Pusa hispida*) and bearded (*Erignathus barbatus*) seals, are directly affected by sea ice loss. These species use sea ice as a haul-out substrate for various critical functions, including their annual molt. Continued environmental warming will inevitably alter the routine behavior and overall energy budgets of Arctic seals, but it is difficult to quantify these impacts as their metabolic requirements are not well known—due in part to the difficulty of studying wild individuals. Thus, data pertaining to species-specific energy demands are urgently needed to better understand the physiological consequences of rapid environmental change. We used open-flow respirometry over a four-year period to track fine-scale, longitudinal changes in the resting metabolic rate (RMR) of four spotted seals, three ringed seals and one bearded seal trained to participate in research. Simultaneously, we collected complementary physiological and environmental data. Species-specific metabolic demands followed expected patterns based on body size, with the largest species, the bearded seal, exhibiting the highest absolute RMR (0.48 ± 0.04 L O_2 min^{-1}) and the lowest mass-specific RMR (4.10 ± 0.47 ml O_2 min^{-1} kg^{-1}), followed by spotted (absolute: 0.33 ± 0.07 L O_2 min^{-1}; mass-specific: 6.13 ± 0.73 ml O_2 min^{-1} kg^{-1}) and ringed (absolute: 0.20 ± 0.04 L O_2 min^{-1}; mass-specific: 7.01 ± 1.38 ml O_2 min^{-1} kg^{-1}) seals. Further, we observed clear and consistent annual patterns in RMR that related to the distinct molting strategies of each species. For species that molted over relatively short intervals—spotted (33 ± 4 days) and ringed (28 ± 6 days) seals—metabolic demands increased markedly in association with molt. In contrast, the bearded seal exhibited a prolonged molting strategy (119 ± 2 days), which appeared to limit the overall cost of molting as indicated by a relatively stable annual RMR. These findings highlight energetic trade-offs associated with different molting strategies and provide quantitative data that can be used to assess species-specific vulnerabilities to changing conditions.

Key words: Bearded seals, climate change, resting metabolic rate, ringed seals, sea ice loss, spotted seals

Editor: Steven Cooke

Received 26 June 2020; Revised 30 September 2020; Editorial Decision 8 November 2020; Accepted 9 November 2020

Cite as: Thometz NM, Hermann-Sorensen H, Russell B, Rosen DAS, Reichmuth C (2021) Molting strategies of Arctic seals drive annual patterns in metabolism. *Conserv Physiol* 9(1): coaa112; doi:10.1093/conphys/coaa112.

Introduction

Rapid human-induced climate change is having disproportionate effects in the Arctic, where intense shifts in environmental conditions threaten the overall health and stability of Arctic and sub-Arctic ecosystems (Hinzman *et al.*, 2005; Post *et al.*, 2009; Serreze and Barry, 2011; Comiso and Hall, 2014). The present rate of change may be too rapid for long-lived and slowly reproducing species, such as marine mammals, to effectively adjust routine behavior or alter timing of life-history events. Associated threats to Arctic marine mammals include significant loss of sea ice habitats, changes in prey distribution and abundance, climate-induced stressors to body condition and health, and increased disturbance (Laidre *et al.*, 2008; Moore and Huntington, 2008). Rapid warming and dramatic declines in sea ice are of particular concern for ice-dependent Arctic seals, as loss of haul-out substrate could prevent individuals from successfully completing key life-history events and/or alter individual energy budgets. For many of these species, we lack appropriate data to make robust and meaningful predictions about the physiological impacts of environmental change. Specifically, directed studies examining energetic requirements and physiological constraints are urgently needed.

Resting metabolic rate (RMR) is a standard measure of individual energy expenditure, devoid of the influences of digestion, thermoregulation and reproduction. RMR is commonly used to compare energy needs across taxa (Kleiber, 1947; Thompson and Nicoll, 1986; Williams and Maresh, 2016), has been shown to scale to other measures of energy expenditure in marine mammals (Kooyman, 1989; Castellini *et al.*, 1992; Costa and Williams, 1999; Richmond *et al.*, 2006) and is a key component of many predictive modeling efforts (Winship *et al.*, 2002; Ophir *et al.*, 2010; Rechsteiner *et al.*, 2013; Villegas-Amtmann *et al.*, 2015; Costa *et al.*, 2016; Beltran *et al.*, 2017). Among phocids (i.e. true seals), RMR and overall energy budgets fluctuate annually in concert with environmental cues and internal biological cycles (Renouf and Noseworthy, 1990; Boily and Lavigne, 1997; Rosen and Renouf, 1998; Beck *et al.*, 2003; Sparling *et al.*, 2006). As a result, species-specific metabolic data—encompassing time-periods both inside and outside critical life-history events—are essential to more accurately forecast the consequences of sea ice loss for Arctic seals.

Although there are some studies of metabolism in Arctic seals (Gallivan and Ronald, 1981; Ashwell-Erickson *et al.*, 1986; Renouf and Gales, 1994; Ochoa-Acuña *et al.*, 2009), the majority of physiological data comes from field sampling of harvested animals that is often conducted in cooperation with native subsistence communities (Lenfant *et al.*, 1970; Ryg *et al.*, 1990a, 1990b; Lydersen *et al.*, 1992; Andersen *et al.*, 1999; Chabot and Stenson, 2002; Tryland *et al.*, 2006; Burns *et al.*, 2007; Quakenbush and Citta, 2008; Quakenbush *et al.*, 2009, 2011a, 2011b; Lestyk *et al.*, 2009; Ferreira *et al.*, 2011; Harwood *et al.*, 2012; Routti *et al.*, 2013). These sampling events generally take place in spring during annual breeding and molting periods when seals are most visible and accessible. Such efforts are useful for inter-annual comparisons of specific demographic groups but, due to the terminal nature of data collection, cannot provide fine-scale longitudinal data for individuals. Similarly, physiological data obtained during tagging expeditions are typically acquired once for each individual, as free-ranging Arctic seals are difficult to recapture for repeated measurements. Instrumentation secured to the pelage can be useful in collecting longitudinal behavioral data; however, the efficacy of such tags is reduced during the spring molt, as the probability of tag loss increases with molt progression. The overrepresentation of point-sampled data from individuals and data obtained from one period each year may bias our understanding of reference ranges for key parameters and limit our ability to understand the impact of specific life-history events on annual energetic profiles.

The molt is a significant physiological event that occurs following the breeding season each spring. During this time seals shed and re-grow their fur as well as several layers of epidermis. To facilitate this annual process, seals haul out for extended periods, increase blood flow to the skin and maintain elevated skin temperatures (Chang, 1926; Feltz and Fay, 1966; Boily, 1995). Hence, it has been proposed that the molt period should be characterized by increased metabolic rates; however, the cost of molt has been measured in a number of phocids with mixed results. Grey seals (*Halichoerus grypus*) (Boily, 1996; Boily and Lavigne, 1997), harp seals (*Pagophilus groenlandicus*) (Renouf and Gales, 1994; Hedd *et al.*, 1997; Chabot and Stenson, 2002), Hawaiian monk seals (*Neomonachus schauinslandi*) (Williams *et al.*, 2011) and southern elephant seals (*Mirounga leonia*) exhibit the predicted increase in metabolism coincident with molt. Northern elephant seals (*Mirounga angustirostris*) have been suggested to experience little to no energetic cost associated with molt (Worthy *et al.*, 1992). Alternatively, studies of spotted (*Phoca largha*) and harbor (*Phoca vitulina*) seals have documented decreases in metabolism during the molt (Ashwell-Erickson *et al.*, 1986; Rosen and Renouf, 1998). These conflicting findings suggest that the physiological consequences of molt are not fully resolved in phocids.

Given that the timing of molt is typically entrained to specific environmental cues like photoperiod (Ling, 1984; Mo *et al.*, 2000), and has evolved to coincide with particular sea ice conditions for Arctic seals, the ongoing and rapid loss of adequate haul-out substrate may have significant energetic implications for ice seals during this time. If seals must increase time in cold polar water during the molt, lowered skin temperatures could inhibit hair growth, resulting in prolonged, disrupted, or failed molt cycles (Boily, 1995). More time in water during molt may also lead to increased heat loss and an overall increase in the metabolic cost of molting. Alternately, seals may modify their behavior if suitable sea ice becomes unavailable in preferred areas, choosing instead

Table 1: Subject information for study animals, with age, mass and data collection dates presented as ranges across the sampling period. Location of study animals include the ASLC in Seward, AK, and the LML in Santa Cruz, CA

Species	Individual	Location	Sex	Age (yrs)	Mass (kg)	Data collection
Phoca largha	Amak	ASLC	M	5.8–9.2	49.2–85.0	Feb 2016—Jun 2019
	Tunu	ASLC	M	5.8–9.2	59.5–85.5	Feb 2016—Jun 2019
	Sura	ASLC	F	2.8–5.2	36.0–59.0	Feb 2017—Jun 2019
	Kunik	ASLC	M	1.8–4.1	37.0–59.0	Feb 2017—Jun 2019
Pusa hispida	Nayak	LML	F	5.5–8.1	24.9–32.5	Nov 2016—Jun 2019
	Pimniq	ASLC	M	3.5–5.2	25.3–31.7	Oct 2017—Jun 2019
	Dutch	ASLC	F	2.8–3.2	27.3–28.6	Jan 2019—May 2019
Erignathus barbatus	Noatak	LML	M	2.0–4.3	102.4–144.6	Mar 2017—Jun 2019

to molt on substrate farther away from foraging grounds (Von Duyke *et al.*, 2020) and/or molt on land, which could raise both daily energy budgets (Hamilton *et al.*, 2015) and predation risk (Smith, 1980). Such behavioral changes will likely influence the degree to which Arctic seals can maintain energy balance.

In this study we use a comparative framework to examine annual patterns in metabolic requirements for three Arctic phocids that differ greatly in their use of and dependence on sea ice. Spotted seals are an ice-associated species found in both sub-Arctic and Arctic regions that utilize seasonal pack ice edges for pupping and molting, but may also use coastal haul-outs during the summer and fall in some locations (Burns, 1970; Lowry *et al.*, 1998). Ringed (*Pusa hispida*) and bearded (*Erignathus barbatus*) seals have circumpolar Arctic distributions and are strongly ice-dependent. Ringed seals maintain breathing holes and excavate subnivean lairs in order to remain in areas of extensive fast ice for much of the year, only hauling out on exposed sea ice for extended periods during the spring molt (Burns, 1970; Smith and Stirling, 1975). In contrast, bearded seals use broken and moving pack ice, particularly in regions over shallow foraging grounds, as a platform for pupping and molting (Burns, 1970; Breed *et al.*, 2018; Cameron *et al.*, 2018). Sea ice loss will impact the ability of all three species to successfully carry out important life-history events and alter individual energy budgets (Laidre *et al.*, 2015; Hamilton *et al.*, 2016); however, the extent and severity of effects will depend on the physiology, life-history characteristics and behavioral flexibility of each species.

Due to the remote habitats and cryptic behavior of these species, the only way to obtain year-round metabolic data is through the study of captive individuals. This approach enables the examination of fine-scale changes in parameters over time, under controlled conditions. Working with four spotted seals, three ringed seals and one bearded seal trained to participate in physiological sampling, we document fine-scale changes in the RMR of individuals over a four year-period, with particular focus on using within-subject repeated measures to determine the metabolic implications of molt. Here, we provide measures of RMR for each species, describe seasonal changes, examine potential drivers of observed patterns and discuss the relevance of our findings for each species in light of rapid sea ice loss and ongoing climate change.

Methods

Animals

Eight ice seals participated in this multi-year study at two facilities (Table 1). The spotted and ringed seals stranded at young ages in the wild and were brought to the Alaska SeaLife Center (ASLC) for rehabilitation. Individual seals spent an average of two to three months in rehabilitation and were deemed healthy by veterinary staff prior to entry into this study. The bearded seal was collected in the wild, brought to ASLC for one and a half months and then moved to Long Marine Laboratory (LML) at six months of age for participation in research. One ringed seal and one bearded seal were housed at LML, Santa Cruz, CA (36.9497° N, 122.0656° W). Four spotted seals and two ringed seals were housed at ASLC, Seward, AK (60.0999° N, 149.4410° W). Study animals included both males and females, as well as sub-adult and adult individuals. The seals were trained to voluntarily participate in data collection and routine husbandry care using positive reinforcement methods. Seals at both facilities were housed in natural seawater pools with water temperatures that ranged seasonally with local environmental conditions (LML T_w = 8.6 °C—19.3 °C; ASLC T_w = 4.0 °C—11.5 °C) and had access to haul-out areas at all times of day and during all seasons. TidBit v2 temperature data loggers (Onset Computer Corporation, Bourne, MA, USA) were used to measure and record ambient air and water temperatures at each facility at one-hour intervals. Mean daily air and water temperatures were determined by averaging hourly measurements for each 24-hour period. Seals were kept outdoors under local photoperiod at each facility.

Seals were fed a daily diet composed of several prey types that included relatively high-fat clupeid fish (e.g. herring—*Clupea* spp.) and relatively high-protein osmerid fish (e.g. capelin—*Mallotus villosus*), supplemented with cephalopod or bivalve mollusks. Vita-Zu marine mammal tablets (Mazuri, PMI Nutrition International LLC) were included in the diet to ensure proper nutrition. Metrics of food motivation and appetite were scored daily by experienced staff and used to determine optimal diet each day, which allowed caloric intake and body mass to vary seasonally in a natural manner. A subsample of each prey batch was analyzed for proximate and energetic analyses (Michelson Labs Inc., Commerce, CA) and daily food consumption was recorded in both mass (kg) and energy (kcal). Animals were weighed weekly to the nearest tenth of a kilogram using a calibrated platform scale.

Research was conducted under United States National Marine Fisheries Permit 18 902 issued to C. Reichmuth with authorization from the Ice Seal Committee. Institutional Animal Care and Use Committees at the University of California Santa Cruz and Alaska SeaLife Center approved research protocols and provided oversight of animal welfare.

Metabolic measurements

In-water, RMRs were determined for all ice seals using an open-flow respirometry system designed for marine mammals. Individuals were trained to remain stationary beneath a custom-built metabolic dome attached to a PVC piping frame that floated at the top of the water surface (101 cm long x 90 cm wide x 46 cm high). Animals were able to move into and out of the dome freely, but were trained to voluntarily station and rest beneath the dome for extended intervals. Sessions were conducted in the morning following an overnight fast to ensure that seals were postprandial. To establish consistent and relaxed cooperative behavior, seals rehearsed this routine for 4–8 min each morning and were rewarded with 30 to 40% of their scheduled diet. Data collection trials were attempted weekly with average duration ranging between 10–13 min depending on the pre- and during-trial behavior of each animal on a given day. RMR measurements were considered useable only when animals were at continuous rest beneath the dome for a minimum of 5 min, and the metabolic trace contained an interval of resting equilibrium that exceeded 4 min.

Rate of oxygen consumption ($\dot{V}O_2$) during metabolic trials was determined by pulling ambient air through a metabolic dome at known rates between 150–200 L/min by a mass flow controller (Sable Systems International, North Las Vegas, NV, USA). Exact flow rates were dependent on individual mass and set to ensure that the oxygen content within the dome was maintained above 20.10% at all times. Subsamples of dome exhaust were dried (Drierite, W. A. Hammond Drierite, Xenia, OH, USA), scrubbed of carbon dioxide (Sodasorb, Smiths Medical Inc., Minneapolis, MN) and dried again, before entering an oxygen analyzer (Sable Systems International, North Las Vegas, NV, USA). Oxygen content of dome exhaust was recorded every 1.0 s on a laptop computer using EXPEDATA software (Sable Systems International, North Las Vegas, NV, USA). Ambient air baselines were collected before and after animals were under the dome to account for system drift and for use in $\dot{V}O_2$ calculations. Temperature and relative humidity of chamber air was determined during trials using a handheld temperature and humidity sensor (Vaisala HM40, Vantaa, Finland). Flow rates were corrected to standard temperature and pressure dry (STPD) and $\dot{V}O_2$ determined using EXPEDATA software (Sable Systems International, North Las Vegas, NV, USA) and standard equations (Withers, 1977). Before each trial the oxygen analysis system was calibrated with dry, ambient air. Metabolic systems at both facilities were routinely checked for leaks and accuracy using 100% nitrogen gas (Fedak et al 1981; Davis *et al.* 1985).

Molt status

We documented the timing, progression and overall duration of the visible molt for each animal annually. Data on molt were compiled from detailed photographic records, molt monitoring data sheets and husbandry records. The start date of each molt was defined as the first documentation of loose hair and/or active hair loss. The end of each molt was defined by the complete loss of the old coat and complete re-growth of a new coat. The 50% molt date was the day at which half of the new coat was determined to have grown in. For statistical analyses the molt status of an individual for a given metabolic data collection session was categorized in one of four ways: not molting, 1 month pre-molt, actively molting or 1 month post-molt.

Statistical analyses

We did not assume each species would respond similarly to changes in fixed parameters and therefore, evaluated each species independently.

To examine potential drivers of metabolism in ringed and spotted seals we used linear mixed-effects (LME) models. We included individual as a random effect within each LME model for each species, which allowed us to account for repeated measures and avoid issues associated with pseudoreplication (Harrison *et al.*, 2018). Absolute $\dot{V}O_2$ data (rather than mass-specific) were used in statistical analyses to avoid any *a priori* bias based on scaling (Nagy, 1987; Glazier, 2005). We assessed potential fixed effects for each model—mass, age, sex, molt status, air temperature and water temperature—for collinearity using scatterplot matrices. Animal location (ASLC, LML) was not included as a fixed effect, as the inclusion of air and water temperature accounted for regional differences. Although photoperiod is known to affect the timing of molt in seals (Mo *et al.*, 2000), we did not include it in our models as photoperiod is strongly correlated with molt status, and our aim was to determine the effect of molt status, not photoperiod, on metabolism.

Prior to model building we assessed dependent variables for normality. Spotted seal absolute $\dot{V}O_2$ data were log transformed to improve normality. Ringed seal absolute $\dot{V}O_2$ data were normally distributed and no transformation was needed. For spotted seals and ringed seals, age and mass were highly collinear and age was subsequently dropped. In addition, we examined data for homogeneity of variance. Sex violated the homogeneity of variance assumption using Bartlett's test for both spotted seals and ringed seals. Given the inclusion of only one female and one male in the study for spotted and ringed seals, respectively, we dropped sex as a fixed factor in both models. We used backwards elimination and corrected Akaike's Information Criteria (AICc) for model selection. Finally, residuals of the final models were plotted to confirm homoscedasticity and normality, and thus proper model selection.

For bearded seal data analysis we began by using multiple linear regressions. Absolute $\dot{V}O_2$ data were log transformed to improve normality. We assessed potential fixed effects (age, mass, molt status, air temperature and water temperature) for collinearity using scatterplot matrices. Age and mass, as well as air and water temperature were highly correlated. Age and air temperature were subsequently dropped. Using backwards elimination and corrected Akaike's Information Criteria (AICc) in model selection, we found there was no appropriate regression model to describe the bearded seal data. Therefore, we directly tested the effect of molt status on absolute $\dot{V}O_2$ using a one-way ANOVA with Tukey's *post hoc* comparisons. Homogeneity of variance was confirmed using Bartlett's test.

All statistical analyses were completed using JMP14 statistical software program (SAS Institute, Cary, NC). Metabolic data are presented as mean values ±SD. Results were considered significant if $P < 0.05$.

Results

Over a four-year period, we collected 812 metabolic data points from eight individuals across three species. Specifically, we collected 542 RMR measurements from four spotted seals, 175 measurements from three ringed seals and 95 measurements from one bearded seal (Table 1). On average, four data points were collected for each individual per month. To account for differences in sample sizes between individuals when determining species-average RMR values we calculated a grand species mean from individual seal means. Although there were intraspecific differences in metabolism, interspecific demands for these individuals followed expected metabolic relationships based on body size (Table 2). Ringed seals had the lowest absolute energy demands (0.20 ± 0.04 L O_2 min^{-1}), but the highest mass-specific demands (7.01 ± 1.38 ml O_2 min^{-1} kg^{-1}). Spotted seals exhibited a mean absolute RMR of 0.33 ± 0.07 L O_2 min^{-1}, with a mean mass-specific RMR of 6.13 ± 0.73 ml O_2

Table 2: Summary of molt and metabolic data for all study animals. Data are presented as means ± standard deviations with sample sizes displayed in parentheses. Molt cycle sample sizes refer to the number of documented molt cycles, while metabolic sample sizes refer to number of data points

Species	Individual	Typical molt timing	Molt duration (d)	Absolute RMR (L O_2 min^{-1})			Mass-specific RMR (ml O_2 min^{-1} kg^{-1})		
				Annual mean	Non-molting	Molting	Annual mean	Non-molting	Molting
Phoca largha	Amak	May–Jun	38±13 (4)	0.43±0.08 (154)	0.42±0.06 (131)	0.51±0.13 (23)	6.98±1.54 (154)	6.68±1.34 (131)	8.69±1.48 (23)
	Tunu	May–Jun	31±6 (4)	0.36±0.06 (172)	0.35±0.06 (150)	0.42±0.06 (22)	5.47±1.00 (172)	5.34±0.96 (150)	6.41±0.75 (22)
	Sura	Apr–May	36±21 (3)	0.28±0.06 (106)	0.27±0.04 (84)	0.33±0.08 (22)	6.49±1.07 (106)	6.22±1.04 (84)	7.53±1.08 (22)
	Kunik	Apr–May	27±2 (3)	0.25±0.07 (110)	0.24±0.05 (92)	0.31±0.11 (18)	5.58±1.03 (110)	5.35±0.78 (92)	6.79±1.31 (18)
Pusa hispida	Nayak	Mar–Apr	36±8 (3)	0.25±0.03 (122)	0.24±0.03 (110)	0.30±0.03 (12)	8.93±1.29 (122)	8.78±1.21 (110)	10.31±1.21 (12)
	Pimniq	May–Jun	21±1 (2)	0.18±0.05 (42)	0.17±0.04 (35)	0.25±0.06 (7)	6.37±1.66 (42)	5.90±1.29 (35)	8.72±1.33 (7)
	Dutch	May	26 (1)	0.16±0.05 (11)	0.13±0.03 (7)	0.21±0.03 (4)	5.73±1.73 (11)	4.68±0.95 (7)	7.57±1.04 (4)
Erignathus barbatus	Noatak	Dec–Apr	119±2 (3*)	0.48±0.04 (95)	0.47±0.04 (60)	0.50±0.05 (35)	4.10±0.47 (95)	3.96±0.33 (60)	4.34±0.56 (35)

** Actual start date of molt could not be determined for this seal during its first year; thus, average molt duration for this animal was determined using two of three molt cycles during the study.*

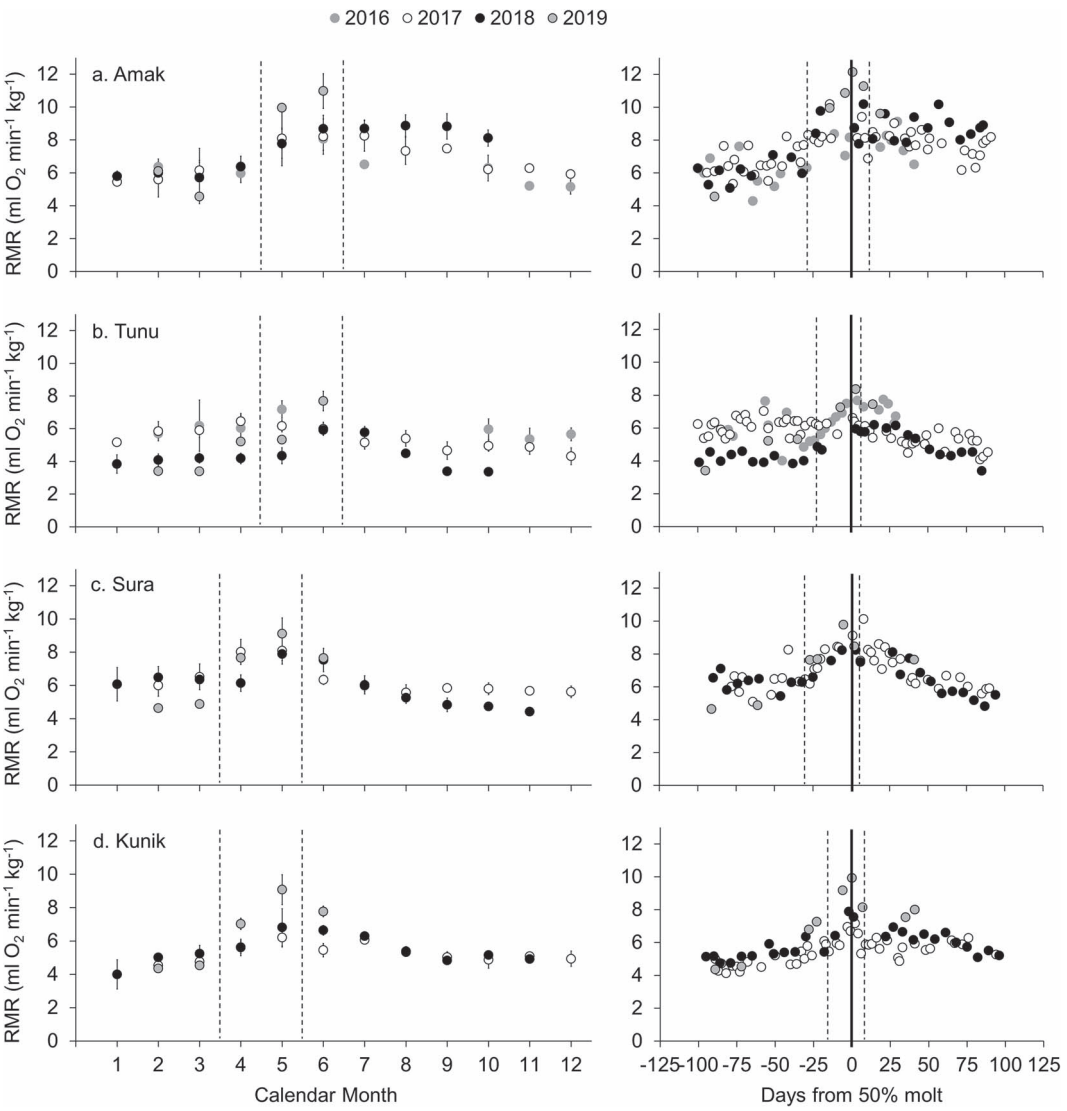

Figure 1: Longitudinal RMR data collected for four spotted seals (a–d) over a 4-year period. Data from each individual in successive years are stacked and displayed in two adjacent panels. Left panels display monthly mean mass-specific RMR (±SD) for each animal. On average, four data points (range: 1–11) were collected each month. Dashed vertical lines denote the typical molting period. Source data for the left panels, along with corresponding absolute RMR values and subject metadata, are provided as Supplementary Data. Right panels display individual metabolic data points collected during the 100 days preceding and 100 days following the 50% molt date each year (solid vertical line). Dashed vertical lines denote the mean start and end dates of molt referenced to the 50% molt date.

min^{-1} kg^{-1}. The bearded seal had the highest absolute RMR (0.48 ± 0.04 L O_2 min^{-1}) and lowest mass-specific RMR (4.10 ± 0.47 ml O_2 min^{-1} kg^{-1}).

We documented apparent species-level differences in the timing and duration of the annual molt. Spotted and ringed seals molted over relatively short time frames, 33 ± 4 days and 28 ± 6 days, respectively. In contrast, the bearded seal exhibited prolonged molting intervals that lasted an average of 119 ± 2 days. Within individuals, the timing and duration of the annual molt was consistent across years (Table 2), but there was some variation between individuals. Spotted seals generally molted between April and June in Alaska, with the two immature spotted seals beginning their molt a month earlier than the two adults. Both ringed seals in Alaska molted over a similar time frame (May–June), while the ringed seal in California molted earlier; generally, between March and April. The bearded seal molt, which lasted approximately 4 months, consistently occurred between December and April in California.

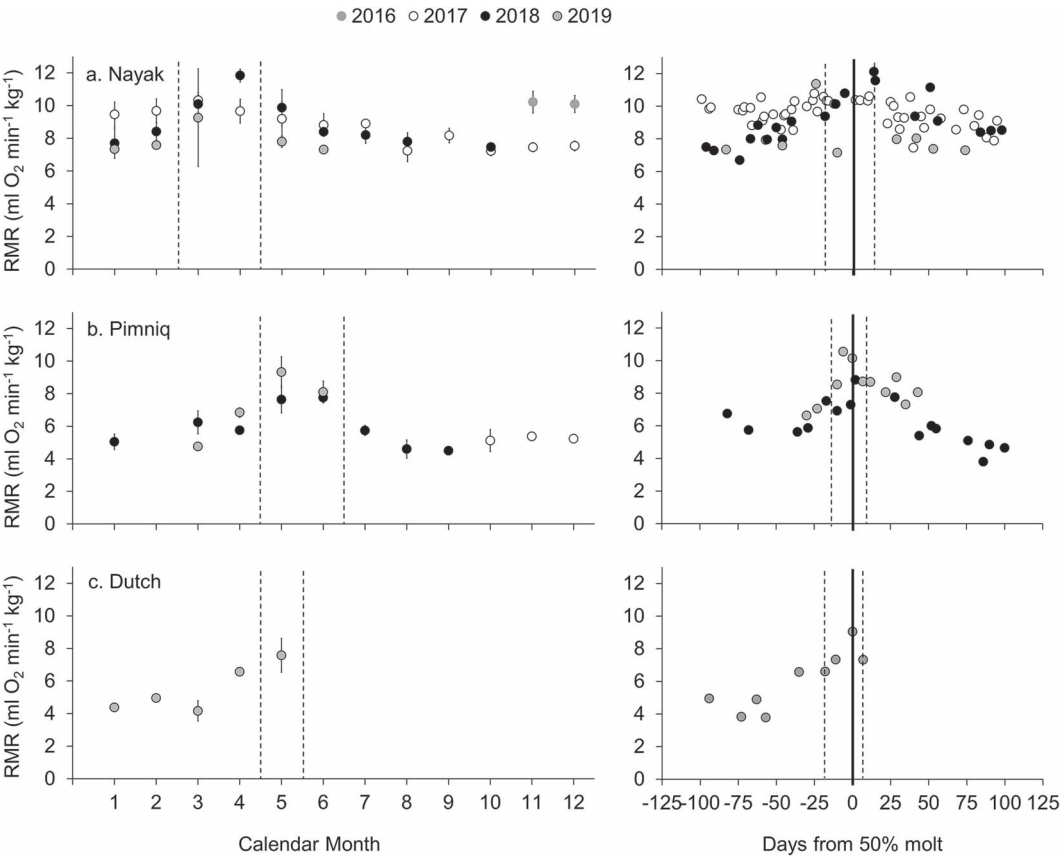

Figure 2: Longitudinal RMR data collected for three ringed seals (a-c) over a four-year period. Data from each individual are stacked and each individual's data are displayed in two adjacent panels. Left panels display monthly mean mass-specific RMR (±SD) for each animal. On average, three data points (range: 1–10) were collected each month. Dashed vertical lines denote the typical molting period. Source data for the left panels, along with corresponding absolute RMR values and subject metadata, are provided as Supplementary Data. Right panels display individual metabolic data points collected during the 100 days preceding and 100 days following the 50% molt date each year (solid vertical line). Dashed vertical lines denote the mean start and end dates of molt referenced to the 50% molt date.

We observed clear annual patterns in RMR for spotted (Fig. 1) and ringed (Fig. 2) seals that were highly consistent within individuals across years, with both absolute and mass-specific energy expenditure peaking coincident with the annual molt. The longitudinal metabolic patterns for spotted seals were strongly driven by molt status ($F_{3,534} = 67.79$, $P < 0.001$), air temperature ($F_{1,533} = 24.71$, $P < 0.001$) and body mass ($F_{1,482} = 101.26$, $P < 0.001$). RMR increased during molt, as well as with increasing body mass and air temperature (Table 3). Individual accounted for 46% of the observed variance in the spotted seal data. Annual patterns in RMR for ringed seals were driven most strongly by molt status ($F_{3,168.1} = 43.91$, $P < 0.001$) and water temperature ($F_{1,170} = 5.35$, $P = 0.022$). For ringed seals, RMR increased in association with the annual molt and decreased with increasing water temperature (Table 4). Individual accounted for 83% of the observed variance for ringed seals. For both species, molt status had a strong effect on metabolism. Mean molting RMR values—in both absolute and mass-specific terms—were consistently higher than non-molting values (Table 2; Supplementary Data), with maximum energetic costs occurring coincident with the 50% new coat date for both species (Figs 1, 2); for some individuals RMR more than doubled at this time relative to non-molting levels.

In contrast to spotted and ringed seals, the bearded seal did not exhibit notable seasonal patterns or discrete peaks in metabolism during the study period (Fig. 3). Despite comparably stable absolute and mass-specific RMR values (Table 2; Supplementary Data), we did discern an effect of molting on bearded seal metabolism (one-way ANOVA, $F_{3,91} = 4.51$, $P = 0.005$), with the only significant *post-hoc* comparison between molting and non-molting periods (Tukey's HSD, $P = 0.003$). However, the percentage difference in mean mass-specific RMR between molting and non-molting periods was much smaller for the bearded seal (9%) than for the spotted seals (18–26%) and ringed seals (16–47%).

Table 3: LME model best fit results for spotted seals with molt status ($F_{3,534} = 67.79$, $P < 0.001$), air temperature ($F_{1,533} = 24.71$, $P < 0.001$) and body mass ($F_{1,482} = 101.26$, $P < 0.001$) as fixed effects against absolute $\dot{V}O_2$. Individual was included as a random effect and accounted for 46% of the variance in the model

Parameters	β	S.E.	DF_{Den}	t-ratio	P
Intercept	−0.8161	0.044	11.08	−18.44	<0.001
Molt – during	0.0529	0.006	533	8.33	<0.001
Molt – no	−0.0566	0.005	534.1	−12.10	<0.001
Molt – 1 mo. post	0.0225	0.008	535	2.97	0.003
Air Temp	0.0043	0.001	533.3	4.97	<0.001
Mass	0.0053	0.001	481.8	10.06	<0.001

Table 4: LME model best fit results for ringed seals with molt status ($F_{3,168} = 43.91$, $P < 0.001$) and water temperature ($F_{1,170} = 5.35$, $P = 0.022$) as fixed effects against absolute $\dot{V}O_2$. Individual was included as a random effect and accounted for 83% of the variance in the model

Parameters	β	S.E.	DF_{Den}	t-ratio	P
Intercept	0.2399	0.039	2.42	6.18	0.016
Molt – during	0.0373	0.005	168.1	7.09	<0.001
Molt – no	−0.0349	0.004	168	−9.80	<0.001
Molt – 1 mo. post	0.0051	0.006	168	0.85	0.395
Water Temp	−0.0035	0.001	170	−2.31	0.022

Discussion

Baseline energy demands

Through the collection of fine-scale longitudinal data we were able to provide year-round, empirical RMR data for eight individuals comprising three Arctic seal species. Energy demands between species followed predicted trends based on body size with the bearded seal exhibiting the highest absolute and lowest mass-specific mean annual RMR, followed by the spotted seals and then the ringed seals. Most notably, our data revealed annual patterns in RMR that were strongly related to the distinct molting strategy of each species. Although we could not establish population-level values due to limited sample sizes for each species, by testing individual seals multiple times per month while in a consistent and calm state, we were able to establish high repeatability for our metabolic measurements both within individuals and across years. Thus, we are confident in the regularity of the annual patterns described here. Further, these types of fine-scale data are valuable for parameterizing predictive population and bioenergetics models.

Given that metabolic data are only available for a limited number of phocid seals, the values reported here improve our understanding of phocid energetics and provide species-specific information pertaining to the metabolic needs of ice-associated seals. Specifically, we contribute metabolic data for the smallest phocid species (i.e. ringed seal) as well as the largest Arctic phocid (i.e. bearded seal). Indeed, this is the first study to empirically measure metabolism in a bearded seal, which exhibited highly stable annual energy demands. The mean mass-specific RMR we determined for spotted seals was slightly lower than the value previously reported by Ashwell-Erickson et al. (1986); however, only immature individuals (≤2 yrs. old) were measured in that study, which would be expected to have elevated mass-specific demands relative to mature individuals (Kleiber, 1961). Further, as the seals in that study had not been conditioned to participate voluntarily in data collection, they may not have been in a true resting state during metabolic measurements. Thus, our slightly lower values likely reflect the increased age and larger body size of our spotted seals as well as our training protocol. For ringed seals, we found a higher mean RMR in-water than that reported by Ochoa-Acuña et al. (2009) in-air, who collected metabolic data for a single adult male in a haul-out chamber. Of note, the authors provided one in-water value for the same individual in that study, which was nearly twice that of his in-air RMR, but comparable to the mean in-water RMR values reported here.

As would be expected, there were some differences in mean RMR between individuals of the same species. Between-individual differences were minor in spotted seals and pronounced in ringed seals. Across our ringed seals, the greatest differences were observed between the ringed seal in California and those in Alaska. The female ringed seal in California had higher absolute and mass-specific energy demands than either ringed seal in Alaska, likely driven by differences in temperature regime and associated proportions of lean body mass and blubber. We do not believe the ringed seal in California was housed in conditions outside her thermoneutral zone (TNZ), as there was overlap between the ambient temperature ranges at both facilities; however, TNZ has not been established for this species and therefore this possibility cannot be ruled-out. Importantly, although RMR varied between individuals, we observed the same relative patterns across all three ringed seals with similar changes in RMR associated with molt.

Metabolic consequences of molt

We documented annual changes in RMR that were strongly related to species-specific molting phenology. Spotted and ringed seals molted over relatively short periods and exhibited markedly increased RMRs during this time, which peaked midway through the visible molt. This pattern was considerably different than that of the bearded seal, which took approximately four times longer to molt and exhibited a more subtle increase in RMR across the molting period. This prolonged molting strategy is unique among phocid seals. Although the bearded seal in this study molted earlier than

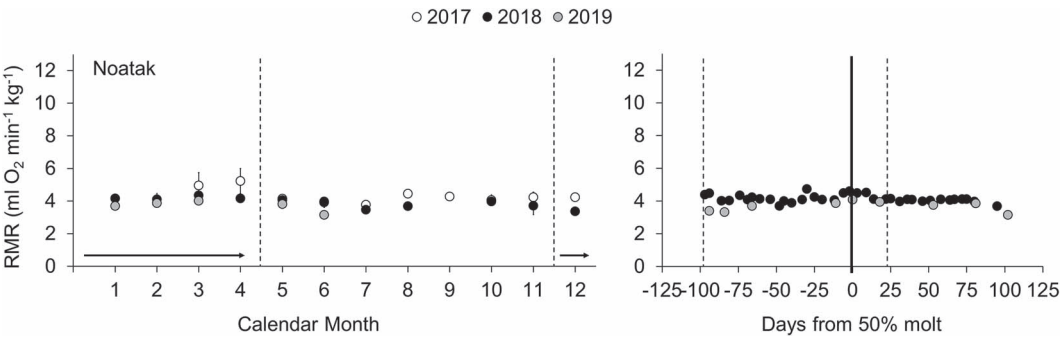

Figure 3: Longitudinal RMR data collected for one bearded seal over 3 years. Left panel displays monthly mean mass-specific RMR (±SD). On average, four data points (range: 1–6) were collected each month. Typical molt period denoted by a horizontal arrow between dashed vertical lines. Source data for the left panel, along with corresponding absolute RMR values and subject metadata, are provided as Supplementary Data. Right panel displays individual metabolic data points collected in the 100 days preceding and 100 days following the 50% molt date each year (solid vertical line). Dashed vertical lines denote the mean start and end dates of molt referenced to the 50% molt date.

free-ranging conspecifics, the duration and diffuse pattern of molt documented here agree with accounts of wild bearded seals (for review, see Cameron et al., 2010). Further, latitudinal gradients and ontogenetic differences in the timing of molt are common among Arctic seals; seals in lower latitudes tend to molt earlier than seals in higher latitudes likely driven by differences in photoperiod (Mo *et al.*, 2000), and younger seals tend to molt before mature seals (for review, see Boveng et al., 2008; Boveng et al., 2009; Cameron *et al.*, 2010; Kelly et al., 2010). Thus, given that our bearded seal was a young individual (1–3 years) housed in California under local photoperiod, his earlier molting period aligns with geographic and ontogenetic trends in molt timing observed for wild seals. Similarly, the ringed seal housed in California molted earlier than the two ringed seals housed in Alaska. All spotted seals housed in Alaska molted around the same time generally reported for their wild counterparts, with the two younger seals molting prior to the two sexually mature individuals.

The annual molt is generally considered an energetically expensive period for phocids (Boyd *et al.*, 1993; Renouf and Gales, 1994; Boily, 1995, 1996; Boily and Lavigne, 1997; Hedd *et al.*, 1997; Chabot and Stenson, 2002; Williams *et al.*, 2011; Walcott *et al.*, 2020); however, there are inconsistencies in the literature (Ashwell-Erickson *et al.*, 1986; Worthy *et al.*, 1992; Rosen and Renouf, 1998) that have led to the suggestion of a typical pattern of little to no cost of molt in phocids (Beltran *et al.*, 2018). In those species for which we have strong evidence of increased metabolic costs during molt, it is unclear whether the main drivers of those additional costs relate to energetic requirements of generating new hair or to thermal losses associated with sending blood to the periphery to maintain the elevated skin temperatures necessary for cellular growth (Boily, 1995). Our data reveal significant, short-term increases in RMR during the molt for ringed and spotted seals, but also suggest that these costs may be mitigated in some species (i.e. bearded seals) by molting over a longer time frame.

The majority of studies examining phocid molting energetics have used methods similar to those described here. Of those studies, significant molt-associated metabolic costs have been reported for grey seals (Boily, 1996; Boily and Lavigne, 1997), harp seals (Hedd *et al.*, 1997; Chabot and Stenson, 2002) and Hawaiian monk seals (Williams *et al.*, 2011); however, metabolic depression during molt has been reported for spotted and harbor seals (Ashwell-Erickson *et al.*, 1986; Rosen and Renouf, 1998). It is not apparent why there would be species-specific differences in the metabolic consequences of molt across phocids; however, resolution of this issue may be found through closer examination of the underlying data in the literature. For example, while Ashwell-Erickson *et al.* (1986) has long been cited as evidence of metabolic depression during molt, the authors actually documented increasing metabolic rates during the regenerative phase of molt. It appears that the interpretation of metabolic depression during molt was based on the early decline in metabolism observed during the 20–60 days preceding the visible molt. When considering only the visible molt, during which time hair is actively shed and regrown, their data largely agree with our findings—and those of other investigators—of additional costs associated with molting.

Increased levels of thyroid hormones have been linked with increased metabolism during the molt. In addition to their effect on metabolism, thyroid hormones stimulate the growth of new fur (Ramot *et al.*, 2009). Elevated thyroid hormones during the visible molt have been documented in grey (Boily, 1996) and harp (John *et al.*, 1987) seals, both species for which there are known metabolic costs associated with molt (Boily and Lavigne, 1997; Hedd *et al.*, 1997; Chabot and Stenson, 2002). Similarly, in penguins, increased thyroid hormone levels are associated with new feather synthesis and increased metabolism (Groscolas and Cherel, 2014). Routti *et al.* (2013) proposed an energetic cost of molt for ringed seals given a documented rise in thyroid hormones during this period, which was confirmed by the direct measures of RMR presented here. In spotted seals, thyroid hormones decline to

a minimum just before the molting period and then increase to their maximum values during the period of most rapid hair growth (Ashwell-Erickson *et al.*, 1986). This peak in spotted seal thyroid hormones during the period of most rapid hair growth support the increase in RMR documented in the present study, with peak RMR coinciding with the 50% molt date. Interestingly, in harbor seals—the only other species besides spotted seals for which a metabolic depression during molt has been proposed (Ashwell-Erickson *et al.*, 1986; Rosen and Renouf, 1998)—there are no documented changes in thyroid hormones in association with molting (Renouf and Brotea, 1991).

Although not well studied, it has long been believed that wild bearded seals undergo a protracted molt that differs from other phocids. Some have suggested that the diffuse molt of bearded seals involves year-round shedding of hair with a peak in molting activity during the spring when seals are regularly observed hauling out (for review, see Cameron *et al.*, 2010). Data from the bearded seal in this study supports this notion and a similar molting pattern was observed in two additional captive individuals (C. Reichmuth, unpublished data). Our bearded seal was housed under local photoperiod in California, rather than an Arctic photoperiod, but we do not believe this was the cause of its prolonged molt. Although photoperiod is known to affect timing of molt in seals (Mo *et al.*, 2000), its effect on duration is less clear. Indeed, the ringed seal housed in California consistently had an earlier onset of molt than the ringed seals in Alaska, but the progression and duration of molting was similar for all ringed seals. Thus, photoperiod was likely responsible for the early onset of the bearded seal's molt, but not a direct cause of its prolonged duration.

The pronounced elevation in RMR we observed in spotted and ringed seals during molt was noticeably absent in the bearded seal, with no observable increase associated with the 50% molt date. By having a diffuse molt over an extended period, bearded seals may limit the overall energetic cost of this annual event and/or spread out the costs to reduce the metabolic impact at any one point in time. This energy-saving strategy may be facilitated by the much larger body size of bearded seals relative to other ice seals. This strategy may be physiologically impractical for ringed and spotted seals due their smaller body sizes, higher surface area to volume ratios and potential rates of heat loss, which may necessitate more rapid molt cycles. However, there are likely other trade-offs associated with this protracted molting strategy that should be considered, such as the impact on haul-out behavior. Overall, our results support the notion of an extended molt in bearded seals, enhance our understanding of individual molt dynamics and reveal the potential benefits of this unique strategy.

One conflicting finding from our study was the species-specific effects of air and water temperature on metabolism. RMR increased with increasing temperature in spotted seals, but decreased with increasing temperature in ringed seals. Further, we found no effect of temperature on the bearded seal's RMR. While additional thermoregulatory costs can be accrued when animals are in environments outside their TNZ, this seems unlikely here. Based on studies of harbor seals, ambient temperatures experienced by our spotted seals were likely within their TNZ (Hansen, 1995; Hansen *et al.*, 1995). The pattern we observed for ringed seals might be explained if individuals were tested below their lower critical temperature at points during the study. However, the lowest water temperature experienced by our ringed seals was 4.0 °C, a temperature well within the normal range of their wild counterparts (Kelly *et al.*, 2010). Therefore, rather than temperature driving observed patterns in RMR, it is more likely that the timing of molt is associated with seasonal changes in temperature that do not themselves have independent effects on metabolism.

Conservation implications

Climate change is a pervasive threat to all ice-associated seals (Kovacs *et al.*, 2011; Laidre *et al.*, 2015), although the ability of these seals to adjust to changing conditions will depend on the unique characteristics of each species. Here, we provide some of the most comprehensive metabolic data for spotted, ringed and bearded seals with which to better predict the species-specific consequences of ongoing Arctic warming. These data fill important gaps in our understanding of the physiology of each species, and provide source data for predictive population and bioenergetic models that are important for conservation and management efforts. Further, this work highlights species-specific physiological attributes that are important when considering the impact of sea ice loss during key life-history events, such as molt.

In polar regions, the increased skin temperatures that are necessary to promote tissue regeneration during molt can only be achieved by ice seals when hauled out (Feltz and Fay, 1966; Boily, 1995; Walcott *et al.*, 2020). If seals were unable to do so, increased skin perfusion in polar water for prolonged periods would result in untenably high rates of heat loss (Watts *et al.*, 1993). Thus, adequate haul-out substrate is essential for polar seals during molt, raising specific concerns about the physiological consequences of declining sea ice. We found that spotted and ringed seals exhibit significant peaks in energy expenditure associated with their discrete molt and we observed them spending more time hauled out during this period than at any other time during the year. Despite the fact that our bearded seal exhibited minimal changes in metabolism associated with molt, we also observed his haul-out time to increase markedly during molt, particularly from around the 50% molt date through the end of molt. This suggests benefits of increased skin temperatures for molting bearded seals, despite their muted metabolic response.

Declining ice cover can also place energetic burdens on ice-dependent seals in other ways. To ensure adequate haul-out substrate during molt, there is evidence that ringed seals remain with preferred sea ice habitat as it retreats, even

into marginal foraging areas (Hamilton *et al.*, 2015; Von Duyke *et al.*, 2020). Our data suggest that this behavior reflects the bioenergetic priorities of seals during molt. The advantages of hauling out to promote tissue regeneration may outweigh the caloric benefits of remaining in preferred foraging areas. This behavioral change occurs despite the additional energetic investment that individuals must make to move with or travel to preferred sea ice regions. Bearded seals tend to select areas of broken, drifting pack ice over shallow foraging grounds (Burns, 1967; Smith and Stirling, 1975; Bengtson *et al.*, 2005). As this type of sea ice retreats from preferred foraging grounds, suitable haul-out substrate for bearded seals may become decoupled from important regions. This would force bearded seals to either move to areas of preferred ice cover, as has been observed for ringed seals, or to move coastal regions to haul out on land where risk of predation will be greater (Smith, 1980). Tagging data from juvenile bearded seals suggests they respond similarly to ringed seals, opting to move with preferred sea ice as it retreats (Breed *et al.*, 2018; Cameron *et al.*, 2018).

Although behavioral adjustments may currently allow seals to maintain contact with preferred sea ice habitat during molt, continued sea ice loss will likely require individuals to spend greater amounts of time in water. It remains unclear whether individuals can successfully molt without hauling out (Feltz and Fay, 1966; Boily, 1995). If seals curtail surface blood flow in response to spending more time in water, or cannot maintain elevated skin temperatures, this could slow, delay, or disrupt the overall process of tissue regeneration. Recent unusual mortality events (UMEs) for ice associated pinnipeds (2011–2016; 2018–present) may provide glimpses into the physiological consequences of reduced sea ice during molt (NOAA Fisheries, 2011a, 2011b, 2016, 2020). Although the cause of the 2011–2016 Alaska Pinniped UME is still unknown, seals and walruses presented with abnormal skin lesions and what appeared to be abnormal or disrupted molts (NOAA Fisheries, 2018). This UME coincided with many years of early sea ice breakup. A more recent UME, specific to ringed, bearded and spotted seals, began in 2018 and is ongoing (NOAA Fisheries, 2020). As part of this UME, seals are presenting with similar symptoms and appear in poor body condition, suggesting widespread energetic losses. These UMEs may be some of the first examples of the detrimental effects of the loss of sea ice for ice-associated seals.

The 2012 decision to list distinct population segments of bearded seals as threatened under the United States Endangered Species Act was driven by concern that sea ice loss would substantially reduce or eliminate adequate haul-out platforms for pupping and molting, leading to decreases in reproduction and survival (NMFS, 2012). Similar concerns exist for ringed seal populations, which are predicted to be at risk of major declines due to ongoing sea ice loss (Kelly *et al.*, 2010; Kovacs *et al.*, 2011; Reimer *et al.*, 2019). Spotted seals may be less impacted by reductions in sea ice as they are already known to successfully utilize coastal haul outs for pupping and molting in lower latitudes (Wang, 1986; Nesterenko and Katin, 2009); however, the cascading consequences of climate change will inevitably affect all three species. Ultimately, this work highlights potential energetic trade-offs associated with different molting strategies in these three species and more broadly, provides valuable quantitative data regarding annual patterns in energy demands that can be used to assess species-specific vulnerabilities of Arctic seals to changing conditions.

Funding

This work was supported by the National Oceanic and Atmospheric Administration's Alaska Pinnipeds Program [NA15NMF4390166, NA16NMF4390027, NA19NMF4390083].

Acknowledgements

We are grateful to the husbandry and veterinary teams at the Alaska SeaLife Center and Long Marine Laboratory for their dedicated work on this long-term project, especially Jenna Sullivan, Brandi Ruscher, Taylor Abraham, Mariah Tengler, Dave Casper, Jamie Mullins, Juliana Kim, Shelby Burman, Margaret Black, Brett Long, Derek Woodie, Kathy Woodie and Carrie Goertz. The authors thank John Goodwin, Alex Whiting, Andrew Rouse, Markus Horning, Lori Polasek, Lisa Hartman, Tara Reimer and Gary Griggs for their contributions. We also acknowledge the NOAA Polar Ecosystems Program and the Alaska Department of Fish and Game's Marine Mammals Program for thoughtful discussions about this work.

References

Andersen M, Hjelset AM, Gjertz I, Lydersen C, Gulliksen B (1999) Growth, age at sexual maturity and condition in bearded seals (*Erignathus barbatus*) from Svalbard, Norway. *Polar Biol* 21: 179–185.

Ashwell-Erickson S, Fay FH, Elsner R, Wartzok D (1986) Metabolic and hormonal correlates of molting and regeneration of pelage in Alaskan harbor and spotted seals (*Phoca vitulina* and *Phoca largha*). *Can J Zool* 64: 1086–1094.

Beck CA, Bowen DW, Iverson SJ (2003) Sex differences in the seasonal patterns of energy storage and expenditure in a phocid seal. *J Anima* 72: 280–291.

Beltran RS, Burns JM, Breed GA (2018) Convergence of biannual moulting strategies across birds and mammals. *Proc R Soc London B* 285: 20180318.

Beltran RS, Testa JW, Burns JM (2017) An agent-based bioenergetics model for predicting impacts of environmental change on a top marine predator, the Weddell seal. *Ecol Modell* 351: 36–50.

Bengtson JL, Hiruki-Raring LM, Simpkins MA, Boveng PL (2005) Ringed and bearded seal densities in the eastern Chukchi Sea, 1999–2000. *Polar Biol* 28: 833–845.

Boily P (1995) Theoretical heat flux in water and habitat selection of phocid seals and beluga whales during the annual molt. *J Theor Biol* 172: 235–244.

Boily P (1996) Metabolic an hormonal changes during the molt of captive gray seals (*Halichoerus grypus*). *Am J Physiol* 5: 1051–1058.

Boily P, Lavigne DM (1997) Developmental and seasonal changes in resting metabolic rates of captive female grey seals. *Can J Zool* 75: 1781–1789.

Boveng PL, Bengtson JL, Buckley TW, Cameron MF, Dahle SP, Kelly BP, Megrey BA, Overland JE, Williamson NJ (2009) Status review of the spotted seal (*Phoca largha*). *NOAA Tech Memo NMFS-AFSC* 200i–xiii: 1–153.

Boveng PL, Bengtson JL, Buckley TW, Cameron MF, Dahle SP, Megrey BA, Overland JE, Williamson NJ (2008) Status review of the ribbon seal (*Histriophoca fasciata*). *NOAA Tech Memo NMFS-AFSC* 191i–xiv: 1–115.

Boyd I, Arnbom T, Fedak M (1993) Water flux, body composition, and metabolic rate during molt in female southern elephant seals (*Mirounga leonina*). *Physiol Zool* 66: 43–60.

Breed GA, Cameron MF, Ver Hoef JM, Boveng PL, Whiting A, Frost KJ (2018) Seasonal sea ice dynamics drive movement and migration of juvenile bearded seals Erignathus barbatus. *Mar Ecol Prog Ser* 600: 223–237.

Burns JJ (1967) The Pacific bearded seal. Alaska Department of Fish and Game, Pittman-Robertson Project Report W-6-R and W-14-R. 66 p.

Burns JJ (1970) Remarks on the distribution and natural history of pagophilic pinnipeds in the Bering and Chukchi Seas. *J Mammal* 51: 445–454.

Burns JM, Lestyk KC, Folkow LP, Hammill MO, Blix AS (2007) Size and distribution of oxygen stores in harp and hooded seals from birth to maturity. *J Comp Physiol B* 177: 687–700.

Cameron MF *et al.* (2010) Status review of the bearded seal (*Erignathus barbatus*). *NOAA Tech Memo NMFS-AFSC* 211: i.

Cameron MF, Frost KJ, Ver Hoef JM, Breed GA, Whiting AV, Goodwin J, Boveng PL (2018) Habitat selection and seasonal movements of young bearded seals (*Erignathus barbatus*) in the Bering Sea. *PLoS One* 13: e0192743.

Castellini MA, Kooyman GL, Ponganis PJ (1992) Metabolic rates of freely diving Weddell seals: correlations with oxygen stores, swim velocity and diving duration. *J Exp Biol* 165: 181–194.

Chabot D, Stenson GB (2002) Growth and seasonal fluctuations in size and condition of male Northwest Atlantic harp seals *Phoca groenlandica*: an analysis using sequential growth curves. *Mar Ecol Prog Ser* 227: 25–42.

Chang HC (1926) Specific influence of the tyroid gland on hair growth. *Am J Physiol* 77: 562–567.

Comiso J, Hall D (2014) Climate trends in the Arctic as observed from space. *Wiley Interdiscip Rev Clim Chang* 5: 389–409.

Costa DP, Schwarz L, Robinson P, Schick RS, Morris PA, Condit R, Crocker DE, Kilpatrick AM (2016) A bioenergetics approach to understanding the population consequences of disturbance: elephant seals as a model system. In *The Effects of Noise on Aquatic Life II*. Springer, New York, pp. 161–169.

Costa DP, Williams TM (1999) Marine mammal energetics. In JE Reynolds, S Rommel, eds, *Biology of Marine Mammals*. Smithsonian Institution Press, Washington, DC, pp. 176–217.

Davis RW, Williams TM, Kooyman GL (1985) Swimming Metabolism of Yearling and Adult Harbor Seals *Phoca vitulina*. *Physiol Zool* 58: 590–596.

Fedak MA, Rome L, Seeherman HJ (1981) One-step N2-dilution technique for calibrating open-circuit VO2 measuring systems. *J Appl Physiol* 51: 772–776.

Feltz ET, Fay FH (1966) Thermal requirements in vitro of epidermal cells from seals. *Cryobiology* 3: 261–264.

Ferreira EO, Loseto LL, Ferguson SH (2011) Assessment of claw growth-layer groups from ringed seals (*Pusa hispida*) as biomonitors of inter-and intra-annual Hg, d15N, and d13C variation. *Can J Zool* 89: 774–784.

Gallivan GJ, Ronald K (1981) Apparent specific dynamic action in the harp seal (*Phoca groenlandica*). *Comp Biochem Physiol Part A Physiol* 69: 579–581.

Glazier DS (2005) Beyond the '3/4-power law': variation in the intra- and interspecific scaling of metabolic rate in animals. *Biol Rev* 80: 611–662.

Groscolas R, Cherel Y (2014) How to molt while fasting in the cold: the metabolic and hormonal adaptations of emperor and king penguins. *Ornis Scand* 23: 328–334.

Hamilton C, Lydersen C, Ims R, Kovacs K (2016) Coastal habitat use by ringed seals *Pusa hispida* following a regional sea-ice collapse: importance of glacial refugia in a changing Arctic. *Mar Ecol Prog Ser* 545: 261–277.

Hamilton CD, Lydersen C, Ims RA, Kovacs KM (2015) Predictions replaced by facts: a keystone species' behavioural responses to declining arctic sea-ice. *Biol Lett* 11: 1–6.

Hansen S (1995) *Temperature Effects on Metabolic Rate, and the Thermal Limits of Harbour (Phoca vitulina) and Grey Seals (Halichoerus grypus)*. University of Guelph, Guelph Ont.

Hansen S, Lavigne DM, Innes S (1995) Energy metabolism and thermoregulation in juvenile harbor seals (*Phoca vitulina*) in air. *Physiol Zool* 68: 290–315.

Harrison XA, Donaldson L, Correa-Cano ME, Evans J, Fisher DN, Goodwin CED, Robinson BS, Hodgson DJ, Inger R (2018) A brief introduction to mixed effects modelling and multi-model inference in ecology. *PeerJ* 6: e4794. doi: 10.7717/peerj.4794.

Harwood LA, Smith TG, Melling H, Alikamik J, Kingsley MCS (2012) Ringed seals and sea ice in Canada's Western Arctic: harvest-based monitoring 1992-2011. *Arctic* 65: 377–390.

Hedd A, Gales R, Renouf D (1997) Inter-annual consistency in the fuctuating energy requirements of captive harp seals *Phoca groenlandica*. *Polar Biol* 18: 311–318.

Hinzman LD *et al.* (2005) Evidence and implications of recent climate change in Northern Alaska and other Arctic regions. *Clim Change* 72: 251–298.

John TM, Ronald K, George JC (1987) Blood levels of thyroid hormones and certain metabolites in relation to moult in the harp seal (*Phoca groenlandica*). *Comp Biochem Physiol* 88A: 655–657.

Kelly BP *et al.* (2010) Status review of the ringed seal (*Phoca hispida*). *NOAA Tech Memo NMFS-AFSC* 212i–xiv: 1–250.

Kleiber M (1947) Body size and metabolic rate. *Physiol Rev* 27: 511–541.

Kleiber M (1961) *The Fire of Life: An Introduction to Animal Energetics*. John Wiley & Sons, New York.

Kooyman GL (1989) *Diverse Divers*. Springer, New York.

Kovacs KM, Lydersen C, Overland JE, Moore SE (2011) Impacts of changing sea-ice conditions on Arctic marine mammals. *Mar Biodivers* 41: 181–194.

Laidre KL *et al.* (2015) Arctic marine mammal population status, sea ice habitat loss, and conservation recommendations for the 21st century. *Conserv Biol* 29: 724–737.

Laidre KL, Stirling I, Lowry LF, Wiig Ø, Heide-Jørgensen MP (2008) Quantifying the sensitivity of Arctic marine mammals to climate-induced habitat change. *Ecol Appl* 18: S97–S125.

Lenfant C, Johansen K, Torrance JD (1970) Gas transport and oxygen storage capacity in some pinnipeds and the sea otter. *Respir Physiol* 9: 277–286.

Lestyk KC, Folkow LP, Blix AS, Hammill MO, Burns JM (2009) Development of myoglobin concentration and acid buffering capacity in harp (*Pagophilus groenlandicus*) and hooded (*Cystophora cristata*) seals from birth to maturity. *J Comp Physiol B* 179: 985–996.

Ling JK (1984) Epidermal cycles and moulting in marine mammals. *Acta Zool Fenn* 171: 23–26.

Lowry LF, Frost KJ, Davis R, DeMaster DP, Suydam RS (1998) Movements and behavior of satellite-tagged spotted seals (*Phoca largha*) in the Bering and Chukchi Seas. *Polar Biol* 19: 221–230.

Lydersen C, Ryg MS, Hammill MO, O'Brien PJ (1992) Oxygen stores and aerobic dive limit of ringed seals (*Phoca hispida*). *Can J Zool* 70: 458–461.

Mo G, Gili C, Ferrando P (2000) Do photoperiod and temperature influence the molt cycle of Phoca vitulina in captivity? *Mar Mammal Sci* 16: 570–577.

Moore SE, Huntington HP (2008) Arctic marine mammals and climate change: impacts and resilience. *Ecol Appl* 18: S157–S165.

Nagy K (1987) Field metabolic rate and food requirement scaling in mammals and birds. *Ecol Monogr* 57: 111–128.

Nesterenko VA, Katin IO (2009) Haulout: scope of the term and procedure for identification. *Russ J Ecol* 40: 48–54.

NMFS (2012) *Endangered and Threatened Species; Threatened Status for the Beringia and Okhotsk Distinct Population Segments of the Erignathus barbatus nauticus Subspecies of the Bearded Seal*. 77: 76740–76768.

NOAA Fisheries (2011a) *2011 Arctic Seal Disease Outbreak Fact Sheet*. U.S. Department of Commerce, National Oceanic and Atmospheric Administration, National Marine Fisheries Service, AK, USA.

NOAA Fisheries (2011b) *2011 Arctic Seal Disease Outbreak Update on Investigation and Findings*. U.S. Department of Commerce, National Oceanic and Atmospheric Administration, National Marine Fisheries Service, AK, USA.

NOAA Fisheries (2016) *2011 Arctic Pinniped Unusual Mortality Event (UME) Fact Sheet*. U.S. Department of Commerce, National Oceanic and Atmospheric Administration, National Marine Fisheries Service, AK, USA.

NOAA Fisheries (2018) Special Notice: The UME Involving Ice Seals with Hair Loss and Skin Lesions Is Now Closed. U.S. Department of Commerce, National Oceanic and Atmospheric Administration, National Marine Fisheries Service, AK, USA.

NOAA Fisheries (2020) *2018–2020 Ice Seal Unusual Mortality Event in Alaska*, https://www.fisheries.noaa.gov/alaska/marine-life-distress/2018-2020-ice-seal-unusual-mortality-event-alaska (last accessed 11 June 2020).

Ochoa-Acuña HG, Mcnab BK, Miller EH (2009) Seasonal energetics of northern phocid seals. *Comp Biochem Physiol Part A* 152: 341–350.

Ophir AG, Schrader SB, Gillooly JF (2010) Energetic cost of calling: general constraints and species-specific differences. *J Evol Biol* 23: 1564–1569.

Post E *et al.* (2009) Ecological dynamics across the Arctic associated with recent climate change. *Science* 325: 1355–1358.

Quakenbush L, Citta J (2008) *Biology of the Ribbon Seal in Alaska*, Final Rep to Natl Mar Fish Serv.

Quakenbush L, Citta J, Crawford J (2009) *Biology of the Spotted Seal (Phoca largha) in Alaska from 1962–2008*, Final Rep to Natl Mar Fish Serv.

Quakenbush L, Citta J, Crawford J (2011a) *Biology of the Ringed Seal (Phoca hispida) in Alaska, 1960–2010*, Final Rep to Natl Mar Fish Serv.

Quakenbush L, Citta J, Crawford J (2011b) *Biology of the Bearded Seal (Erignathus barbatus) in Alaska, 1961–2009*, Final Rep to Natl Mar Fish Serv.

Ramot Y, Paus R, Tiede S, Zlotogorski A (2009) Endocrine controls of keratin expression. *BioEssays* 31: 389–399.

Rechsteiner EU, Rosen DAS, Trites AW (2013) Energy requirements of Pacific white-sided dolphins (*Lagenorhynchus obliquidens*) as predicted by a bioenergetic model. *J Mammal* 94: 820–832.

Reimer JR, Caswell H, Derocher AE, Lewis MA (2019) Ringed seal demography in a changing climate. *Ecol Appl* 0: 1–18.

Renouf D, Brotea G (1991) Thyroid hormone concentrations in harbour seals (*Phoca vitulina*): No evidence of involvement in the moult. *Comp Biochem Physiol* 99A: 185–194.

Renouf D, Gales R (1994) Seasonal variation in the metabolic rate of harp seals: unexpected energetic economy in the cold ocean. *Can J Zool* 72: 1625–1632.

Renouf D, Noseworthy E (1990) Feeding cycles in captive harbour seals (*Phoca vitulina*): weight gain in spite of reduced food intake and increased thermal demands. *Mar Freshw Behav Physiol* 17: 203–212.

Richmond JP, Burns JM, Rea LD (2006) Ontogeny of total body oxygen stores and aerobic dive potential in Steller sea lions (*Eumetopias jubatus*). *J Comp Physiol B* 176: 535–545.

Rosen DAS, Renouf D (1998) Correlates of seasonal changes in metabolism in Atlantic harbour seals (*Phoca vitulina concolor*). *Can J Zool* 76: 1520–1528.

Routti H, Munro B, Lydersen C, Bäckman C, Arukwe A (2013) Hormone, vitamin and contaminant status during moulting and fasting period in ringed seals (*Phoca hispida*) from Svalbard. *Comp Biochem Physiol Part A* 155: 70–76.

Ryg M, Lydersen C, Markussen NH, Smith TG, Øritsland NA (1990a) Estimating the blubber content of phocid seals. *Can J Fish Aquat Sci* 47: 1223–1227.

Ryg M, Smith TG, Ortisland NA (1990b) Seasonal changes in body mass and body composition of ringed seals (*Phoca hispida*) on Svalbard. *Can J Zool* 68: 470–475.

Serreze MC, Barry RG (2011) Processes and impacts of Arctic amplification: a research synthesis. *Glob Planet Change* 77: 85–96.

Smith G (1980) Polar bear predation of ringed and bearded seals in the land-fast sea ice habitat. *Can J Zool* 58: 2201–2209.

Smith TG, Stirling I (1975) The breeding habitat of the ringed seal (*Phoca hispida*). The birth lair and associated structures. *Can J Zool* 53: 1297–1305.

Sparling CE, Speakman JR, Fedak MA (2006) Seasonal variation in the metabolic rate and body composition of female grey seals: fat conservation prior to high-cost reproduction in a capital breeder? *J Comp Physiol B* 176: 505–512.

Thompson SD, Nicoll ME (1986) Basal metabolic rate and energetics of reproduction in therian mammals. *Nature* 321: 690–693.

Tryland M, Krafft BA, Lydersen C, Kovacs KM, Thoresen SI (2006) Serum chemistry values for free-ranging ringed seals (*Pusa hispida*) in Svalbard. *Vet Clin Pathol* 35: 405–412.

Villegas-Amtmann S, Schwarz LK, Sumich JL, Costa DP (2015) A bioenergetics model to evaluate demographic consequences of disturbance in marine mammals applied to gray whales. *Ecosphere* 6: 1–19.

Von Duyke AL, Douglas DC, Herreman JK, Crawford JA (2020) Ringed seal (*Pusa hispida*) seasonal movements, diving, and haul-out behavior in the Beaufort, Chukchi, and Bering Seas (2011–2017). *Ecol Evol* 00: 1–22.

Walcott SM, Kirkham AL, Burns JM (2020) Thermoregulatory costs in molting Antarctic Weddell seals: impacts of physiological and environmental conditions. *Conserv Physiol* 8: 1–14.

Wang P (1986) Distribution, ecology, and resource conservation of the spotted seal in the Huanghai and Bohai Seas. *Acta Oceanol Sin* 5: 126–133.

Watts P, Hansen S, Lavigne DM (1993) Models of heat loss by marine mammals: thermoregulation below the zone of irrelevance. *J Theor Biol* 163: 505–525.

Williams TM, Maresh JL (2016) Exercise energetics. In MA Castellini, J Mellish, eds, *Marine Mammal Physiology: Requisites for Ocean Living*. CRC Press, Boca Raton, FL, pp. 47–68.

Williams TM, Richter B, Kendall T, Dunkin R (2011) Metabolic demands of a tropical marine carnivore, the Hawaiian monk seal (*Monachus schauinslandi*): implications for fisheries competition. *Aquat Mamm* 37: 372–376.

Winship AJ, Trites AW, Rosen DAS (2002) A bioenergetic model for estimating the food requirements of Steller sea lions *Eumetopias jubatus* in Alaska, USA. *Mar Ecol Prog Ser* 229: 291–312.

Withers PC (1977) Measurment of VO2, VCO2, and evaporative water loss with a flow-through mask. *J Appl Physiol* 42: 120–123.

Worthy GAJ, Morrie PA, Costa DP, Le Boeuf BJ (1992) Moult energetics of the northern elephant seal. *J Zool London* 227: 257–265.

© 2021. Published by The Company of Biologists Ltd | Journal of Experimental Biology (2021) 224, jeb235507. doi:10.1242/jeb.235507

SHORT COMMUNICATION

In vivo measurement of lung volume in ringed seals: insights from biomedical imaging

Holly Hermann-Sorensen[1], Nicole M. Thometz[2,3], Kathleen Woodie[4], Sophie Dennison-Gibby[5] and Colleen Reichmuth[3,4,*]

ABSTRACT

Marine mammals rely on oxygen stored in blood, muscle and lungs to support breath-hold diving and foraging at sea. Here, we used biomedical imaging to examine lung oxygen stores and other key respiratory parameters in living ringed seals (*Pusa hispida*). Three-dimensional models created from computed tomography (CT) images were used to quantify total lung capacity (TLC), respiratory dead space, minimum air volume and total body volume to improve assessment of lung oxygen storage capacity, scaling relationships and buoyant force estimates. The results suggest that lung oxygen stores determined *in vivo* are smaller than those derived from postmortem measurements. We also demonstrate that, whereas established allometric relationships hold well for most pinnipeds, these relationships consistently overestimate TLC for the smallest phocid seal. Finally, measures of total body volume reveal differences in body density and net vertical forces in the water column that influence costs associated with diving and foraging in free-ranging seals.

KEY WORDS: *Pusa hispida*, Buoyancy, Computed tomography, Diving physiology, Total lung capacity

INTRODUCTION

A key question in comparative physiology is how air-breathing vertebrates remain active under water for long periods on a single breath (Butler and Jones, 1997; Ponganis, 2015; Scholander, 1940). To support diving, marine mammals rely on oxygen reservoirs compartmentalized in blood, muscle and lungs. Blood and muscle oxygen stores are well studied in marine mammals relative to lungs. This can be attributed to reduced dependence on pulmonary oxygen stores in marine mammals relative to that in terrestrial species, as well as the difficulty of obtaining quantitative measurements from living, freely diving individuals (Ponganis and Williams, 2016).

Standard metrics of respiratory function include minimum air volume (MAV) and total lung capacity (TLC). MAV is the minimum volume of air in relaxed lungs (Fahlman et al., 2011; Kooyman, 1973), while TLC refers to lung volume at maximum inhalation or when manually inflated to a standard air pressure of 30 cm H_2O or 22 mmHg (Denison et al., 1971). TLC is not easily determined in living animals; for this reason, several techniques are employed to determine other respiratory parameters, which are then used to estimate TLC (Wanger et al., 2005). These methods include nitrogen washout (Sue, 2013), whole-body plethysmography (Kooyman et al., 1972; Lenfant et al., 1970) and various respirometry approaches (Scholander, 1940). In addition, allometric scaling relationships derived from empirical measurements enable estimation of TLC from body mass when species data are not available. For marine mammals, scaling relationships reported by Kooyman (1973, 1989) are used; however, these have not been updated recently, and source data for TLC often include pooled values of mixed age classes. Even so, this approach has been used ubiquitously with the assumption that estimates of TLC will hold across a wide range of body sizes and age classes.

TLC and MAV can be measured postmortem (Burns et al., 2007; Denison et al., 1971; Fahlman et al., 2011; Kooyman and Sinnett, 1979; Lydersen et al., 1992; Mitchell and Skinner, 2011) by excising the complete respiratory tract and measuring associated water displacement in both non-inflated (resting) conditions (i.e. MAV) and inflated conditions (i.e. TLC). The difference in displacement between each condition is related to the volume of the respiratory tract. Researchers interested in mammalian diving physiology rely on these postmortem estimates despite there being little information regarding the reproducibility of *ex situ* values in living animals (Fahlman et al., 2020b), with only a few studies directed at comparing pulmonary function and positioning both *in situ* and *ex situ* (Chevalier et al., 1978; Fahlman et al., 2014; Soutiere and Mitzner, 2004; Standaert et al., 1985).

Biomedical imaging has emerged as a valuable tool to examine comparative respiratory anatomy (Denk et al., 2020; Moore et al., 2011; Ponganis et al., 1992; Smodlaka et al., 2009), including the air reservoirs within living animals such as mice (Mitzner et al., 2001), dogs (Chevalier et al., 1978) and seabirds (Nevitt et al., 2014; Ponganis et al., 2015). Air spaces can be visualized and quantified using three-dimensional reconstructions of respiratory structures in both postmortem and living, anesthetized individuals. Importantly, this approach also allows for calculation of body volume (Ponganis et al., 2015), which can be used to evaluate body density and buoyancy.

We used computed tomography (CT) imaging data obtained during routine veterinary procedures to examine *in vivo* lung volume, lung capacity and whole-body buoyant force in living ringed seals (*Pusa hispida*). Their small body size and ease of handling enabled high-resolution volumetric quantification of discrete respiratory structures, including the anatomical dead space and individual lungs, as well as whole-body volume. We report respiratory parameters for the smallest phocid species, provide insight into the applicability of allometric scaling relationships, and discuss ecological implications of our findings for free-ranging seals.

[1]University of California Santa Cruz, Department of Ocean Sciences, 115 McAllister Way, Santa Cruz, CA 95060, USA. [2]University of San Francisco, Department of Biology, 2130 Fulton Street, San Francisco, CA 94117, USA. [3]University of California Santa Cruz, Institute of Marine Sciences, 115 McAllister Way, Santa Cruz, CA 95060, USA. [4]Alaska SeaLife Center, 301 Railway Ave, Seward, AK 99664, USA. [5]Televet Imaging Solutions, PLLC, Oakton, VA 22124, USA.

*Author for correspondence (coll@ucsc.edu)

H.H-S., 0000-0001-7345-2129; N.M.T., 0000-0002-5035-5219; K.W., 0000-0003-3270-4099; C.R., 0000-0003-0981-6842

Received 17 August 2020; Accepted 11 December 2020

Journal of Experimental Biology (2021) 224, jeb235507. doi:10.1242/jeb.235507

MATERIALS AND METHODS

Subjects and animal handling

One female and three male subadult ringed seals, *Pusa hispida* (Schreber 1775), were evaluated. Age was estimated from the length, mass and overall development of each individual at intake for rehabilitative care at the Alaska SeaLife Center (Seward, AK, USA). Length and mass were determined within 1 week of the CT procedure. Standard length (linear distance from nose to tail) was either directly measured on the day of the CT procedure or measured from full-body scans. Animal mass was obtained via a platform scale (W.C. Redmon Co., Peru, IN, USA; or Ohaus SD751, Ohaus Corp., Parsippany, NJ, USA). Two individuals (PH1701 and PH1804) presented with verminous pneumonia at intake and were treated with anti-helminthic drugs during rehabilitation, with resolution prior to imaging. Thus, the scans included in this study represent healthy individuals cleared of parasites, with no clinical evidence for lungworm infection present at the time of the scans.

Seals were briefly restrained at the Alaska SeaLife Center and given a pre-anesthetic intramuscular injection of midazolam (0.2–0.5 mg kg^{-1}) and butorphanol (0.24–0.7 mg kg^{-1}) (see Woodie et al., 2020). Following sedation, a single lumen central venous catheter (16–18 g, 13–15 cm) was placed in the epidural vertebral sinus flushed with heparinized saline and capped as in Goertz et al. (2008). Patency of the soft catheter was ensured prior to transport to the nearby imaging facility. Prior to the CT procedure, propofol (2–3 mg kg^{-1}) was administered intravenously via the catheter to allow for intubation and inflation of an endotracheal tube cuff. Seals were maintained on oxygen and isoflurane gas for the duration of the procedure. Full inflation of the cuff prevented air leakage around the tube. Supplemental intravenous propofol was titrated incrementally to facilitate intentional apneic intervals during scanning with manual, intermittent, positive-pressure ventilation prior to and following each imaging series. A non-steroidal anti-inflammatory medication (meloxicam, 0.2–0.5 mg kg^{-1}), and broad-spectrum antibiotic (cefazolin, 10–20 mg kg^{-1}) were administered intravenously via the catheter. Following the CT procedure, sedation was reversed with separate injections of intramuscular or intravenous naltrexone (2 mg naltrexone per 1 mg butorphanol) and intravenous flumazenil (1 mg flumazenil per 20 mg midazolam). The endotracheal tube was removed after regular spontaneous respirations resumed. Following extubation, seals were returned to the Alaska SeaLife Center where they resumed normal eating and activity within an hour. The duration of anesthesia was less than 1 h from propofol induction to recovery and extubation.

CT scans were performed with a GE 16 Light Speed Scanner, GE 16 Bright Speed Scanner (General Electric Healthcare, Chalfont St Giles, Bucks, UK), or a Siemens 32/64 Somatom GO-UP Scanner (Siemens, Munich, Germany). Modified thorax protocols (Table S1; S.D.-G., unpublished) were used to obtain optimized images of the full respiratory tract with slice thickness of 0.625–2.5 mm. An initial scan was obtained on two seals (PH1802 and PH1804) in sternal recumbency without lung inflation during apnea, with the pressure gauge of the anesthesia circuit at 0 mmHg. This condition was defined as the resting, relaxed position of the lungs when the seal was out of water. All seals were scanned in sternal recumbency with lungs hyperinflated to a pressure of 30 mmHg. To test for replicability of lung volume at a given pressure, variation in volume within inflation conditions, and the difference in volume as a result of patient position, one seal (PH1802) received additional scans in both dorsal and sternal recumbency at inflation pressures of both 30 and 37 mmHg.

Animal handling activities including rescue, rehabilitation and diagnostic CT procedures were authorized under NOAA's Marine Mammal Health and Stranding Response/Research Program 18786, Stranding Agreement SA-AKR-2019-01, and marine mammal research permit 18902. Research was approved by the Institutional Animal Care and Use Committees at the University of California Santa Cruz and the Alaska SeaLife Center.

Volumetry

To determine key respiratory parameters at known lung inflation conditions, DICOM images from CT series were imported to 3D Slicer (Fedorov et al., 2012; https://www.slicer.org/) and converted into closed-surface three-dimensional models. Anatomical structures were manually separated into volumetric segmentations of trachea, bronchi, and left and right lungs based on tissue attenuation (Fig. 1). Tracheal volume was defined from the image immediately caudal to the laryngeal cartilages extending to the image of the cranial margin of the carina. Bronchial volume was defined as the region from the carina to distal portions of the cranial and caudal lobar bronchi. Bronchioles were too diffuse to manually trace, so their volume is included in the volume of the lungs. TLC included both the tissue and air spaces of the left and right lungs, in addition to the bronchioles. The inclusion of the tissue and air spaces is in line with other studies (Lydersen et al., 1992) with which we compared our values. The volume of each segment was calculated in cubic centimeters and converted to milliliters.

Segments of the respiratory tract were considered with respect to whether surfaces were available for oxygen exchange. Anatomical dead space (the portion not in contact with gas exchange surfaces) was defined as the volume of the trachea plus the volume of the bronchi; this measure is not equivalent to respiratory dead space (Fowler, 1948; Rossier and Bühlmann, 1955) as the bronchioles could not be partitioned from the tissues of the lungs in this study. MAV was characterized here as the lung volume in the non-inflated (resting) condition, with inflation pressure of 0 mmHg. Because individuals were measured out of water, we presume this metric will differ somewhat from MAV values obtained from seals resting in water at the surface (Fahlman et al., 2020a). TLC was determined as the volume of the inflated lungs at 30 mmHg. This pressure is higher than the standard of 22 mmHg (30 cm H_2O) used to measure TLC in other mammalian studies (Denison and Kooyman, 1973; Denison et al., 1971; Kooyman and Sinnett, 1982; Loring et al., 2016; Moore et al., 2011; Weibel, 1973), but was necessary for the clinical diagnostic protocol. Specifically, the ringed seals' lungs were hyperinflated to ensure that no atelectasis (partial or full collapse) or scarring of lung tissue was present. To obtain the proportion of blubber that contributed to total body volume, blubber was segmented and quantified for the two animals for which we had

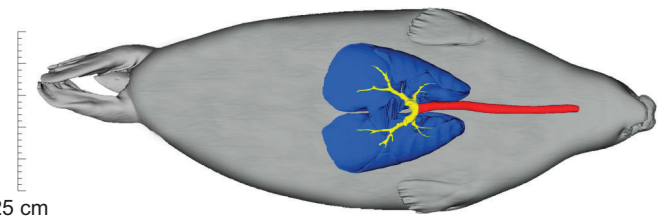

Fig. 1. 3D reconstruction of ringed seal PH1802 at a lung inflation pressure of 30 mmHg. Ventral side of animal shown with body contour in gray. The trachea is red, bronchi are yellow and lungs are blue. See Movie 1 for 3D reconstruction in both non-inflated and inflated conditions. (color online).

whole-body scans (PH1802 and PH1804). Further, surface area to volume ratio (SA:V) was directly measured for seal PH1802.

Allometry

To compare our results with those of other marine mammals, we considered the commonly used allometric scaling equation: $TLC=0.1M_b^{0.96}$ (Kooyman, 1989) (where M_b is body mass). We also determined another scaling equation specific to pinnipeds. The TLC data included in the pinniped-only allometric plot either were collected empirically or could be calculated from empirically reported mass-specific total lung oxygen stores. We evaluated our primary measure of mean TLC as a function of mean total body mass for the subadult ringed seals in our study. We then compared our results with expected values from these allometric relationships to determine whether total body mass is a reliable indicator of total lung capacity for ringed seals.

Body density and buoyant force

CT data were further used to estimate the whole-body buoyant force of two seals (PH1802 and PH1804) at specific lung inflation pressures, as in Ponganis et al. (2015). Body density was calculated by dividing body mass by total body volume and comparing this with the density of seawater. Total body volume (ml) was determined by segmentation of the CT data as described above. Whole-body buoyant force (N) was calculated for each seal at each lung inflation pressure:

$$\text{Buoyant force} = \boldsymbol{g} \times M_b \times (\rho_{\text{seawater}}/\rho_{\text{total body}}), \quad (1)$$

where $\boldsymbol{g}$ is the acceleration of gravity at 9.807 m s^{-2}, M_b is body mass in kg, ρ_{seawater} is the density of seawater at 10°C in g ml^{-1}, and $\rho_{\text{totalbody}}$ is the calculated density of the seal's body in g ml^{-1}. The corresponding downward (gravitational) force (N) was also determined:

$$\text{Downward force} = (\boldsymbol{g} \times M_b). \quad (2)$$

Net (total) force was determined by subtracting the downward force (Eqn 2) from the buoyant force (Eqn 1). Buoyant force was only calculated in the inflated condition for seal PH1804, as there was no full-body scan available in the non-inflated condition. Buoyant force was calculated in both inflated and non-inflated conditions for seal PH1802, and total body volume was compared at the level of the whole animal relative to changes in the respiratory tract volume.

RESULTS AND DISCUSSION

Volumetric measurements

Primary comparisons of respiratory structures and volumetric analyses were made at lung inflation pressures of 0 and 30 mmHg in sternal recumbency (Table 1). When inflated to 30 mmHg, TLC ranged from 870 to 2271 ml, resulting in mass-specific values between 52 and 92 ml kg^{-1}. The right lung was larger than the left in all individuals in the inflated condition, with an average size difference of 6.3%. For two individuals measured in the non-inflated condition, MAV was 564 and 886 ml, with mass-specific values of 22 and 32 ml kg^{-1}. Lung volume for these individuals increased by a factor of 2.5 when fully inflated.

Maximum respiratory tract volume was 904–2323 ml. This was equivalent to 11% and 18% of total body volume for the two seals with full-body scans (PH1804 and PH1802). The anatomical dead portion of the respiratory tract changed little with inflation for two individuals with comparable non-inflated and inflated scans (PH1503 and PH1802). These seals exhibited similar increases in tracheal volume (~15%) and negligible increases in bronchi volume (~1%) from non-inflated to inflated conditions. Thus, while the volume of the total respiratory tract changed by an average factor of 2.5 when the lungs were inflated, most of this difference was due to changes in lung volume.

Replicate scans in sternal recumbency at 37 mmHg for seal PH1802 showed that TLC varied by 5% (74 ml) between scans. Lung volume varied similarly between 30 and 37 mmHg, with an increase of 5% (75 ml) at the higher inflation pressure. When hyperinflated to 37 mmHg, lung volume was 13% (194 ml) greater in dorsal recumbency than in sternal recumbency.

Full-body scans for seal PH1802 were evaluated in both inflated and non-inflated conditions to determine changes in respiratory tract volume and total body volume. The increase in respiratory tract volume was 815 ml. In contrast, total body volume in the inflated condition increased by only 446 ml, equivalent to a 2% increase in body volume. The directly measured surface area of this seal was 58,193 cm^2 and its total body volume was 25,004 cm^3, resulting in a SA:V of 2.3:1. For the two seals for which total blubber volume could be measured from CT scans, blubber by total body volume was 33% (PH1804) and 49% (PH1802).

Allometric relationships

The scaling equation we determined for pinnipeds using previously published values ($TLC=0.1M_b^{0.98}$) is remarkably close to the classic relationship reported by Kooyman (1989) for marine mammals (Fig. 2). Indeed, the Kooyman (1989) equation falls within the 95% confidence interval of the pinniped-only equation, suggesting that this offset is not significant. Source data for the pinniped-only relationship are provided in Table S2 (Burns et al., 2007; Falke et al., 2008; Kooyman and Sinnett, 1982; Lenfant et al., 1970; Lydersen et al., 1992; Reed et al., 1994). The ringed seals in this study are the smallest pinnipeds for which TLC data are now available. When compared with the scaling relationships described above, our *in vivo* measurements obtained from ringed seals are about 27% lower than predicted.

Body density and net buoyant force

Body density and buoyant force were calculated from the measured total body volume of one individual (PH1804) in the inflated condition, and another individual (PH1802) in both non-inflated and inflated conditions. Taking body mass into account, both seals exhibited similar body density irrespective of inflation condition. Individual PH1802 was denser than seawater (1.027 g ml^{-1} at 10°C) at both 0 mmHg (1.052 g ml^{-1}) and 30 mmHg (1.033 g ml^{-1}) inflation conditions, whereas seal PH1804 was less dense than seawater (0.989 g ml^{-1}) in the inflated condition. Based on these measurements PH1802 had negative net vertical forces in both non-inflated (−6.0 N) and inflated (−1.3 N) conditions. In contrast, PH1804 had a positive net force of 7.8 N in the inflated condition.

Physiological and ecological considerations

The anatomical dead space of ringed seals comprised only 3% of total respiratory tract volume and changed little between non-inflated and inflated conditions. This negligible change can be attributed to the rigid hyaline cartilage reinforcement of the trachea (Smodlaka et al., 2009), which aids in lung collapse while diving by allowing compressed air from the lungs to be stored within this non-compliant compartment (Kooyman, 1973). The largest volume measured of the air-filled respiratory tract – including dead space and TLC – was 2.3 l. We found that TLC was three times smaller in

Journal of Experimental Biology (2021) 224, jeb235507. doi:10.1242/jeb.235507

Table 1. Respiratory volume for ringed seals, shown with measures of body volume and corresponding body density and vertical forces

Individual	PH1701[a]	PH1503[a]	PH1804[b]	PH1802[c]	Range
Sex	F	M	M	M	
Age (months)	15.6	43	16.7	25.8	
Mass (kg)	14.9	27.5	20.5	26.2	
ST length (cm)	–	90	81.5	86	
Non-inflated (0 mmHg)					
Trachea volume (ml)	–	39.9	–	26.2	26.2–39.9
Trachea volume (ml kg^{-1})	–	1.4	–	1.0	1.0–1.4
Bronchi volume (ml)	–	9.9	–	9.3	9.3–9.9
Bronchi volume (ml kg^{-1})	–	0.4	–	0.4	–
Left lung volume (ml)	–	465	–	262	262–465
Right lung volume (ml)	–	421	–	302	302–421
Total lung volume (ml)	–	886	–	564	564–886
Total lung volume (ml kg^{-1})	–	32.2	–	21.5	21.5–32.2
Total respiratory tract volume (ml)	–	936	–	599	599–936
Total body volume (ml)	–	–	–	24,913	–
Body density (g ml^{-1})	–	–	–	1.052	–
Buoyant force (N)	–	–	–	250.7	–
Downward force (N)	–	–	–	256.7	–
Net (total) force (N)	–	–	–	−6.0	–
Inflated (30 mmHg)					
Trachea volume (ml)	23.1	43.1	34.6	32.2	23.1–43.1
Trachea volume (ml kg^{-1})	1.6	1.6	1.7	1.2	1.2–1.7
Bronchi volume (ml)	11.2	9.1	13.7	10.3	9.1–13.7
Bronchi volume (ml kg^{-1})	0.8	0.3	0.7	0.4	0.3–0.8
Left lung volume (ml)	426	1108	912	650	426–912
Right lung volume (ml)	444	1163	977	723	444–1163
Total lung capacity (ml)	870	2271	1890	1372	870–2271
Total lung capacity (ml kg^{-1})	58.4	82.6	92.2	52.4	52.4–92.2
Diving lung volume (l)	0.4	1.1	0.9	0.7	0.4–1.1
Usable lung O_2 (l)	0.1	0.2	0.1	0.1	0.1–0.2
Diving lung O_2 store (ml kg^{-1})	4.4	6.2	6.9	3.9	3.9–6.9
Total respiratory tract volume (ml)	904	2323	1938	1415	904–2323
Total body volume (ml)	–	–	20,719	25,359	20,719–25,359
Body density (g ml^{-1})	–	–	0.989	1.033	0.989–1.033
Buoyant force (N)	–	–	208.7	255.4	–
Downward force (N)	–	–	200.9	256.7	–
Net (total) force (N)	–	–	7.8	−1.3	−1.3–7.8
Difference in respiratory tract (%)	–	148	–	136	–
Difference in total body volume (%)	–	–	–	2	–
Difference in total body volume (ml)	–	–	–	446.6	–

Diving lung volume is estimated as 50% of total lung capacity. Usable lung O_2 was calculated based on 15% oxygen extraction efficiency.
CT scanner model: [a]GE 16 Slice Light Speed, [b]GE 16 Slice Bright Speed, [c]Siemens 32/64 Somatom GO-UP.

our ringed seals measured *in vivo* than in ringed seal lungs assessed postmortem (Lydersen et al., 1992). This could be due in part to constraints of lung inflation within an enclosed body cavity versus when the respiratory tract is excised. While developmental differences may confound comparisons across age classes, our mass-specific estimates of TLC were also smaller than measures obtained from the excised lungs of adult seals (Lydersen et al., 1992), suggesting that postmortem measurements may overestimate lung capacity.

Given the hyperinflation applied during prescribed veterinary assessments, our measurements provide an upper bound of TLC. Notably, we found little difference in TLC at pressures of 30 and 37 mmHg, indicating that the lungs reached maximum expansion in both conditions. While normally measured at a standard pressure of 22 mmHg, the TLC values reported are likely biologically relevant as they capture full inflation of the lungs within the body cavity; however, they may not be physiologically accurate as a result of hyperinflation. We found that subject positioning had a greater influence on lung volume than inflation pressure, highlighting the differential effects of gravity and recumbency on TLC estimates obtained out of water. Measurements conducted in dorsal recumbency allowed for more complete expansion of the lungs and chest wall and more accurate assessment of TLC.

We measured MAV that was about 40% of TLC. This is much higher than values based on excised respiratory tracts in other marine mammals, which indicate MAV is 0–16% of TLC (Fahlman et al., 2011; Kooyman and Sinnett, 1979). Although it is a common metric, MAV can be difficult to compare across studies. Here, MAV was measured in living, apneic seals when lungs were relaxed in the non-inflated condition. Other studies have defined MAV as the volume of relaxed lungs when transpulmonary pressure is zero (Kooyman and Sinnett, 1979), a condition that can only be achieved postmortem. MAV has also been related to both functional residual capacity (FRC, the air volume remaining after a passive exhalation) and residual volume (RV, the air volume remaining after forceful exhalation) in living animals (Fahlman et al., 2011). Our definition of MAV most closely aligns with FRC; therefore, comparisons to

Journal of Experimental Biology (2021) 224, jeb235507. doi:10.1242/jeb.235507

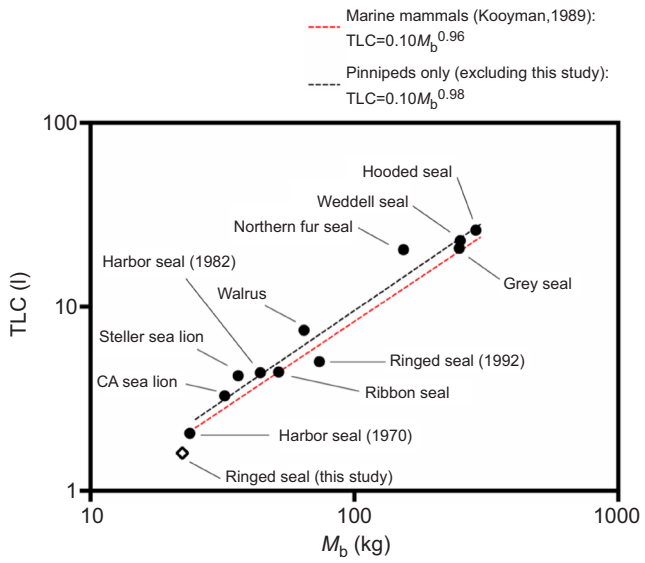

Fig. 2. Logarithmic plot of mean total lung capacity (TLC) as a function of total body mass (M_b). Kooyman's (1989) allometric scaling equation for marine mammals, TLC=0.1$M_b^{0.96}$ (red dashed line) is plotted with the pinniped-only relationship determined in this study, TLC=0.1$M_b^{0.98}$ (black dashed line). Source data for pinniped-only line are provided in Table S2. Ringed seals from this study are shown as a group mean (n=4).

postmortem studies of other marine mammals may not be appropriate.

Diving lung volume (DLV) is commonly estimated at 50% of TLC for pinnipeds, with an oxygen extraction efficiency of 15% (Kooyman, 1973; Kooyman and Sinnett, 1982; Kooyman et al., 1971). As direct measurements exist for only a few species (Kooyman et al., 1971; Ponganis, 2011), we often rely on these assumptions to quantify mass-specific DLV. For our ringed seals, the traditional assumptions yield a DLV ranging from 0.4 to 1.1 liters and corresponding mass-specific DLV from 3.9 to 6.9 ml kg^{-1}. Similar to TLC, these values for DLV in immature ringed seals are lower than previously reported for adult ringed seals (Lydersen et al., 1992), and more similar to values reported for harbor seal pups (Burns et al., 2005). Although the assumptions outlined above can be useful in estimating DLV when empirical data are lacking, much remains to be learned about how respiratory capacity including DLV may change across ontogeny.

Relative to predictions based on scaling relationships, the immature ringed seals in this study had lower than expected lung capacity. This was also the case for adult ringed seals measured postmortem (Lydersen et al., 1992), suggesting the relatively small TLC values obtained here are not explained by methodology or ontogeny. Rather, the deviation of ringed seal lungs from common scaling relationships may be explained by their compact body size and extensive blubber stores. One of the novel aspects of this work was our ability to directly measure SA:V in one individual. This metric is rarely empirically determined but is relevant to aspects of thermoregulation, hydrodynamics and energetics. To compensate for large SA:V and associated heat loss in polar waters, ringed seals have considerable blubber reserves that may comprise half their body volume. Although serving different primary functions, the relative volume of both lungs and blubber have important effects on buoyancy in the smallest phocid.

Seals must manage dynamic buoyant forces and associated energetic costs while diving (Watanabe et al., 2006; Williams et al., 2000). The imaging approach employed here enabled a variety of volumetric measurements relevant to evaluating constraints on diving. Despite high blubber content (48% of body volume), seal PH1802 had a net negative (sinking) force in both inflated and non-inflated lung conditions. In contrast, seal PH1804 had lower blubber volume (33% of body volume), but exhibited a net positive (buoyant) force in the inflated lung condition. These somewhat surprising results were driven by relatively small differences in overall body size (mass and volume) and body density, although in absolute terms, both seals were almost neutrally buoyant in seawater. For reference, some penguins have a net positive force of +15 to 50 N (Ponganis et al., 2015), while larger seal species exhibit net negative forces from −15 to −132 N (Beck et al., 2000; Webb et al., 1998). In comparison, the net vertical forces on the ringed seals were relatively small (−6 to +7 N) and could likely be adjusted by changes in lung volume at the start of a dive. These near-neutral values are physiologically advantageous as they should limit the overall cost of foraging, diving and moving through the marine environment (Adachi et al., 2014; Miller et al., 2012; Nousek-McGregor et al., 2014; Richard et al., 2014; Sato et al., 2013).

We conclude that *in vivo* measurements of lung capacity in ringed seals are smaller in both absolute and mass-specific terms relative to postmortem assessments. Further, total body mass consistently underestimates TLC in this species when considered in the context of established allometric relationships. This deviation likely results from their small, compact body size and exceptional blubber stores. Biomedical imaging can provide accurate quantification of specific regions of the respiratory tract, as well as additional measures of total body and blubber volume that have important ecological implications for free-ranging individuals.

Acknowledgements
We thank the stranding response and animal care teams at the Alaska SeaLife Center, as well as D. Rosen, C. Goertz, J. Belovarac, K. Strehlow, P. Martre, R. Cieri, J. Rasmussen, R. Nichols, R. Sills, T. Williams and A. Moore.

Competing interests
The authors declare no competing or financial interests.

Author contributions
Conceptualization: H.H.-S., N.M.T., C.R.; Methodology: H.H.-S., K.W., S.D.-G.; Formal analysis: H.H.-S.; Investigation: H.H.-S.; Resources: C.R.; Data curation: H.H.-S., K.W.; Writing - original draft: H.H.-S., N.M.T., C.R.; Writing - review & editing: H.H.-S., N.M.T., K.W., S.D.-G., C.R.; Visualization: H.H.-S.; Supervision: C.R.; Project administration: N.M.T., C.R.; Funding acquisition: N.M.T., C.R.

Funding
Funding was provided by the National Oceanic and Atmospheric Administration's Alaska Pinnipeds Program [NA15NMF4390166, NA16NMF4390027].

Data availability
Original DICOM data are available from the Dryad digital repository (Hermann-Sorensen et al., 2020): https://doi.org/10.7291/D1R68J

Supplementary information
Supplementary information available online at
https://jeb.biologists.org/lookup/doi/10.1242/jeb.235507.supplemental

References
Adachi, T., Maresh, J. L., Robinson, P. W., Peterson, S. H., Costa, D. P., Naito, Y., Watanabe, Y. Y. and Takahashi, A. (2014). The foraging benefits of being fat in a highly migratory marine mammal. *Proc. R. Soc. B Biol. Sci.* **281**, 20142120. doi:10.1098/rspb.2014.2120

Beck, C. A., Bowen, W. D. and Iverson, S. J. (2000). Seasonal changes in buoyancy and diving behaviour of adult grey seals. *J. Exp. Biol.* **203**, 2323-2330.

Burns, J. M., Costa, D. P., Frost, K. and Harvey, J. T. (2005). Development of body oxygen stores in harbor seals: effects of age, mass, and body composition. *Physiol. Biochem. Zool.* **78**, 1057-1068. doi:10.1086/432922

Burns, J. M., Lestyk, K. C., Folkow, L. P., Hammill, M. O. and Blix, A. S. (2007). Size and distribution of oxygen stores in harp and hooded seals from birth to maturity. *J. Comp. Physiol. B* **177**, 687-700. doi:10.1007/s00360-007-0167-2

Butler, P. J. and Jones, D. R. (1997). Physiology of diving of birds and mammals. *Physiol. Rev.* **77**, 837-899. doi:10.1152/physrev.1997.77.3.837

Chevalier, P. A., Rodarte, J. R. and Harris, L. D. (1978). Regional lung expansion at total lung capacity in intact vs. excised canine lungs. *J. Appl. Physiol.* **45**, 363-369. doi:10.1152/jappl.1978.45.3.363

Denison, D. M. and Kooyman, G. L. (1973). The structure and function of the small airways in pinniped and sea otter lungs. *Respir. Physiol.* **17**, 1-10. doi:10.1016/0034-5687(73)90105-9

Denison, D. M., Warrell, D. A. and West, J. B. (1971). Airway structure and alveolar emptying in the lungs of sea lions and dogs. *Respir. Physiol.* **13**, 253-260. doi:10.1016/0034-5687(71)90029-6

Denk, M., Fahlman, A., Dennison-Gibby, S., Song, Z. and Moore, M. (2020). Hyperbaric tracheobronchial compression in cetaceans and pinnipeds. *J. Exp. Biol.* **223**, jeb217885. doi:10.1242/jeb.217885

Fahlman, A., Loring, S. H., Ferrigno, M., Moore, C., Early, G., Niemeyer, M., Lentell, B., Wenzel, F., Joy, R. and Moore, M. J. (2011). Static inflation and deflation pressure-volume curves from excised lungs of marine mammals. *J. Exp. Biol.* **214**, 3822-3828. doi:10.1242/jeb.056366

Fahlman, A., Loring, S. H., Johnson, S. P., Haulena, M., Trites, A. W., Fravel, V. A. and Van Bonn, W. G. (2014). Inflation and deflation pressure-volume loops in anesthetized pinnipeds confirms compliant chest and lungs. *Front. Physiol.* **5**, 433. doi:10.3389/fphys.2014.00433

Fahlman, A., Meegan, J., Borque-Espinosa, A. and Jensen, E. D. (2020a). Pulmonary function and resting metabolic rates in California sea lions (*Zalophus californianus*) on land and in water. *Aquat. Mamm.* **46**, 67-79. doi:10.1578/AM.46.1.2020.67

Fahlman, A., Sato, K. and Miller, P. (2020b). Improving estimates of diving lung volume in air-breathing marine vertebrates. *J. Exp. Biol.* **223**, jeb216846. doi:10.1242/jeb.216846

Falke, K. J., Busch, T., Hoffmann, O., Liggins, G. C., Liggins, J., Mohnhaupt, R., Roberts, J. D., Stanek, K. and Zapol, W. M. (2008). Breathing pattern, CO_2 elimination and the absence of exhaled NO in freely diving Weddell seals. *Respir. Physiol. Neurobiol.* **162**, 85-92. doi:10.1016/j.resp.2008.04.007

Fedorov, A., Beichel, R., Kalpathy-Cramer, J., Finet, J., Fillion-Robin, J.-C., Pujol, S., Bauer, C., Jennings, D., Fennessy, F., Sonka, M. et al. (2012). 3D Slicer as an image computing platform for the quantitative imaging network. *Magn. Reson. Imaging* **30**, 1323-1341. doi:10.1016/j.mri.2012.05.001

Fowler, W. S. (1948). Lung function studies. II. The respiratory dead space. *Am. J. Physiol.* **154**, 405-416. doi:10.1152/ajplegacy.1948.154.3.405

Goertz, C. E. C., Gray, M. and Tuomi, P. (2008). Long-term catheters for phocids undergoing rehabilitation. In AAZV Annual Conference, Anchorage, Alaska.

Hermann-Sorensen, H., Thometz, N., Dennison-Gibby, S. and Reichmuth, C. (2020). CT DICOM studies from: In vivo measurements of lung volumes in ringed seals: insights from biomedical imaging. Dryad, Dataset. doi:10.7291/D1R68J

Kooyman, G. L. (1973). Respiratory adaptations in marine mammals. *Am. Zool.* **13**, 457-468. doi:10.1093/icb/13.2.457

Kooyman, G. L. (1989). *Diverse Divers: Physiology and Behavior*. Berlin, Heidelberg, New York: Springer-Verlag.

Kooyman, G. L. and Sinnett, E. E. (1979). Mechanical properties of the harbor porpoise lung, *Phocoena phocoena*. *Respir. Physiol.* **36**, 287-300. doi:10.1016/0034-5687(79)90042-2

Kooyman, G. L. and Sinnett, E. E. (1982). Pulmonary shunts in harbor seals and sea lions during simulated dives to depth. *Physiol. Zool.* **55**, 105-111. doi:10.1086/physzool.55.1.30158447

Kooyman, G. L., Kerem, D. H., Campbell, W. B. and Wright, J. J. (1971). Pulmonary function in freely diving Weddell seals, *Leptonychotes weddelli*. *Respir. Physiol.* **12**, 271-282. doi:10.1016/0034-5687(71)90069-7

Kooyman, G. L., Schroeder, J. P., Denison, D. M., Hammond, D. D., Wright, J. J. and Bergman, W. P. (1972). Blood nitrogen tensions of seals during simulated deep dives. *Am. J. Physiol.* **223**, 1016-1020. doi:10.1152/ajplegacy.1972.223.5.1016

Lenfant, C., Johansen, K. and Torrance, J. D. (1970). Gas transport and oxygen storage capacity in some pinnipeds and the sea otter. *Respir. Physiol.* **9**, 277-286. doi:10.1016/0034-5687(70)90076-9

Loring, S. H., Topulos, G. P. and Hubmayr, R. D. (2016). Transpulmonary pressure: the importance of precise definitions and limiting assumptions. *Am. J. Respir. Crit. Care Med.* **194**, 1452-1457. doi:10.1164/rccm.201512-2448CP

Lydersen, C., Ryg, M. S., Hammill, M. O. and O'Brien, P. J. (1992). Oxygen stores and aerobic dive limit of ringed seals (*Phoca hispida*). *Can. J. Zool.* **70**, 458-461. doi:10.1139/z92-069

Miller, P. J. O., Biuw, M., Watanabe, Y. Y., Thompson, D. and Fedak, M. A. (2012). Sink fast and swim harder! round-trip cost-of-transport for buoyant divers. *J. Exp. Biol.* **215**, 3622-3630. doi:10.1242/jeb.070128

Mitchell, G. and Skinner, J. D. (2011). Lung volumes in giraffes, *Giraffa camelopardalis*. *Comp. Biochem. Physiol. Part A Mol. Integr. Physiol.* **158**, 72-78. doi:10.1016/j.cbpa.2010.09.003

Mitzner, W., Brown, R. and Lee, W. (2001). In vivo measurement of lung volumes in mice. *Physiol. Genomics* **4**, 215-221. doi:10.1152/physiolgenomics.2001.4.3.215

Moore, M. J., Hammar, T., Arruda, J., Cramer, S., Dennison, S., Montie, E. and Fahlman, A. (2011). Hyperbaric computed tomographic measurement of lung compression in seals and dolphins. *J. Exp. Biol.* **214**, 2390-2397. doi:10.1242/jeb.055020

Nevitt, B. N., Langan, J. N., Adkesson, M. J., Mitchell, M. A., Henzler, M. and Drees, R. (2014). Comparison of air sac volume, lung volume, and lung densities determined by use of computed tomography in conscious and anesthetized Humboldt penguins (*Spheniscus humboldti*) positioned in ventral, dorsal, and right lateral recumbency. *Am. J. Vet. Res.* **75**, 739-745. doi:10.2460/ajvr.75.8.739

Nousek-McGregor, A. E., Miller, C. A., Moore, M. J. and Nowacek, D. P. (2014). Effects of body condition on buoyancy in endangered North Atlantic right whales. *Physiol. Biochem. Zool.* **87**, 160-171. doi:10.1086/671811

Ponganis, P. J. (2011). Diving mammals. *Compr. Physiol.* **1**, 447-465. doi:10.1002/cphy.c091003

Ponganis, P. (2015). *Diving Physiology of Marine Mammals and Seabirds*. Cambridge, UK: Cambridge University Press.

Ponganis, P. J. and Williams, C. L. (2016). Oxygen stores and diving. In *Marine Mammal Physiology: Requisites for Ocean Living* (ed. M. A. Castellini and J.-A. Mellish), pp. 29-43. CRC Press.

Ponganis, P. J., Kooyman, G. L., Sartoris, D. and Jobsis, P. (1992). Pinniped splenic volumes. *Am. J. Physiol.-Integr. Comp. Physiol.* **262**, R322-R325. doi:10.1152/ajpregu.1992.262.2.R322

Ponganis, P. J., St Leger, J. and Scadeng, M. (2015). Penguin lungs and air sacs: implications for baroprotection, oxygen stores and buoyancy. *J. Exp. Biol.* **218**, 720-730. doi:10.1242/jeb.113647

Reed, J. Z., Chambers, C., Fedak, M. A. and Butler, P. J. (1994). Gas exchange of captive freely diving grey seals (*Halichoerus grypus*). *J. Exp. Biol.* **191**, 1-18.

Richard, G., Vacquie-Garcia, J., Jouma'a, J., Picard, B., Genin, A., Arnould, J. P. Y., Bailleul, F. and Guinet, C. (2014). Variation in body condition during the post-moult foraging trip of southern elephant seals and its consequences on diving behaviour. *J. Exp. Biol.* **217**, 2609-2619. doi:10.1242/jeb.088542

Rossier, P. H. and Bühlmann, A. (1955). The respiratory dead space. *Physiol. Rev.* **35**, 860-876. doi:10.1152/physrev.1955.35.4.860

Sato, K., Aoki, K., Watanabe, Y. Y. and Miller, P. J. O. (2013). Neutral buoyancy is optimal to minimize the cost of transport in horizontally swimming seals. *Sci. Rep.* **3**, 2205. doi:10.1038/srep02205

Scholander, P. F. (1940). *Experimental Investigations on the Respiratory Function in Diving Mammals and Birds*, Vol. 22, pp. 1-131. Oslo: Hvalrådets Skrifter Norske Videnskaps-Akad.

Smodlaka, H., Henry, R. W. and Reed, R. B. (2009). Macroscopic anatomy of the ringed seal [*Pusa (Phoca) hispida*] lower respiratory system. *Anat. Histol. Embryol.* **38**, 177-183. doi:10.1111/j.1439-0264.2008.00904.x

Soutiere, S. E. and Mitzner, W. (2004). On defining total lung capacity in the mouse. *J. Appl. Physiol.* **96**, 1658-1664. doi:10.1152/japplphysiol.01098.2003

Standaert, T. A., LaFramboise, W. A., Tuck, R. E. and Woodrum, D. E. (1985). Serial determination of lung volume in small animals by nitrogen washout. *J. Appl. Physiol.* **59**, 205-210. doi:10.1152/jappl.1985.59.1.205

Sue, D. Y. (2013). Measurement of lung volumes in patients with obstructive lung disease. A matter of time (constants). *Ann. Am. Thorac. Soc.* **10**, 525-530. doi:10.1513/AnnalsATS.201307-236OC

Wanger, J., Clausen, J. L., Coates, A., Pedersen, O. F., Brusasco, V., Burgos, F., Casaburi, R., Crapo, R., Enright, P., van der Grinten, C. P. M. et al. (2005). Standardisation of the measurement of lung volumes. *Eur. Respir. J.* **26**, 511-522. doi:10.1183/09031936.05.00035005

Watanabe, Y., Baranov, E. A., Sato, K., Naito, Y. and Miyazaki, N. (2006). Body density affects stroke patterns in Baikal seals. *J. Exp. Biol.* **209**, 3269-3280. doi:10.1242/jeb.02402

Webb, P. M., Crocker, D. E., Blackwell, S. B., Costa, D. P. and Boeuf, B. J. (1998). Effects of buoyancy on the diving behavior of northern elephant seals. *J. Exp. Biol.* **201**, 2349-2358.

Weibel, E. R. (1973). Morphological basis of alveolar-capillary gas exchange. *Physiol. Rev.* **53**, 419-495. doi:10.1152/physrev.1973.53.2.419

Williams, T. M., Davis, R. W., Fuiman, L. A., Francis, J., Le Boeuf, B. J., Horning, M., Calambokidis, J. and Croll, D. A. (2000). Sink or swim: strategies for cost-efficient diving by marine mammals. *Science* **288**, 133-136. doi:10.1126/science.288.5463.133

Woodie, K., Reichmuth, C., Goertz, C., Belovarac, J. and McMillen, S. (2020). Clinical sedation of Alaskan phocid seals. In Alaska Marine Science Symposium, Anchorage, Alaska.

Table S1. Modified thoracic CT imaging protocols for ringed seal cases shown in Table 1.

	GE 16 Slice Light Speed	**GE 16 Slice Bright Speed**	**Siemens 32/64 Somatom GO-UP**
Scan type	Helical full	Helical full	Helical full
Rotation time (s)	0.5	0.5	1.5, 1.0 (opt 0.8)
Beam collimation (mm)	20	20	-
Thickness (mm)	0.6250 – 2.50	0.6250 – 2.50	2.0
Spiral pitch factor	1.35	1.35	0.8
Speed (mm/rotation)	27.5	27.5	17.89
Reconstruction interval	matched to slice thickness	matched to slice thickness	2.0
Gantry tilt	0	0	0
Gantry period	-	0.60	-
Scan FOV	Large	Large	Whole body
kVp	120	120	130
Xray tube current (mA)	100 – 440	100 – 440	40 – 42
Noise index	11.57	11.57	15
Dose reduction	260	260	On - 3
Algorithm	Standard, bone plus	Standard, bone plus	Br40, Br60
Reformats	Full	Full	Full

Table S2. Lung oxygen stores for marine carnivores, showing the ringed seals in this study with comparative data for other species. Species for which total lung capacity (TLC) is available are plotted in Figure 2. Diving lung volume (DLV) O_2 store calculated based on assumption that DLV is 50% of TLC for pinnipeds. Usable O_2 for gas exchange is estimated as 15% of DLV (Kooyman, 1989), and reported as mass-specific diving lung volume oxygen store (DLV O_2 store). Data are provided for individuals when possible (n=1), or as grouped mean values (n>1).

Species	Age	Mass (kg)	Sample (n)	TLC (L)	DLV (L)	DLV O_2 store (mL kg^{-1})	Method	Reference
Phocids								
Ringed seal *Pusa hispida*	subadult	26.2	1	1.37	0.69††[j]	3.9[j]	in vivo[f]	A
		20.5	1	1.89	0.94††[j]	6.9[j]	in vivo[f]	A
		27.5	1	2.27	1.14††[j]	6.2[j]	in vivo[f]	A
		14.9	1	0.87	0.44††[j]	4.4[j]	in vivo[f]	A
	adult	73.7†	50	5.04 ± 1.24†	2.52††[j]	6.8[j]	postmortem[a]	B
Harbor seal *Phoca vitulina*	mixed	23.8†	5	2.05†	1.03††[j]	6.5[j]	postmortem[a]	C
	neonatal	10.3 ± 0.4†	395			5.3[k]	postmortem[a]	D
	nursing pup	24.9 ± 1.5†				5.3[k]	postmortem[a]	D
	weaned pup	28.9 ± 0.5†				5.3[k]	postmortem[a]	D
	yearling	33.1 ± 0.5†				-	postmortem[a]	D
	adult	52.1 ± 1.6†				12.2[k]	postmortem[a]	D
	subadult	44	1	4.4			in vivo[c]	L
	subadult	40	1	4			in vivo[c]	L
	subadult	36	1	3.6			in vivo[c]	L
	subadult	52	1	5.1			in vivo[c]	L
	subadult	48	1	4.8			in vivo[c]	L
Grey seal *Halichoerus grypus*	pup	40.1 ± 1.3	10			4.1[k]	in vivo[c]	E
	yearling	51.6 ± 2.7†	10			4.1[k]	in vivo[c]	E
	adult female	191.5 ± 6.0†	10			4.1[k]	in vivo[c]	E
	adult	250†	4	20.81†	10.4††[j]	6.2[j]	in vivo[c]	F

Species	Age	Mass (kg)	Sample (n)	TLC (L)	DLV (L)	DLV O_2 store (mL kg^{-1})	Method	Reference
Ribbon seal *Histriophoca fasciata*	adult	51.7†	4	4.42†	2.2††	6.4 [j]	postmortem [a]	C
Harp seal *Pagophilus groenlandicus*	neonatal	10.3 ± 1.1†	40				postmortem[e]	G
	nursing pup	29.4 ± 1.1†					postmortem [e]	G
	weaned pup	36.6 ± 1.1†					postmortem [e]	G
	yearling	29.3 ± 1.6†					postmortem [e]	G
	adult	115.4 ± 4.7†					postmortem [e]	G
Hooded seal *Cistophora cristata*	adult female	252.1 ± 17.9†	6	(22.9)		6.8 [k]	postmortem [e]	G
	nursing pup	38.5 ± 12.5†	2	(1.4)		2.8 [k]	postmortem [e]	G
	weaned pup	48.1 ± 2†	6	(2.0)		3.1 [k]	postmortem [e]	G
Weddell seal *Leptonychotes weddellii*	pup	106	1			4.1†, [k]	in vivo [c]	H
		137	1			4.1†, [k]	in vivo [c]	H
		124	1			4.1†, [k]	in vivo [c]	H
		107	1			4.1†, [k]	in vivo [c]	H
	subadult	260	1	(22.2)	11.1	6.4 [j]	*in vivo* [b, h]	I
		345	1	(23.6)	11.8	5.1 [j]	*in vivo* [b, h]	I
		261	1	(32.6)	16.3	9.4 [j]	*in vivo* [b, h]	I
	adult	425†	4		14	4.1†, [j]	*in vivo* [b]	J
					14	4.1†, [j]	*in vivo* [b]	J
				Scruffy	11	4.1†, [j]	*in vivo* [b]	J
					20	4.1†, [j]	*in vivo* [b]	J
					7	4.1†, [j]	*in vivo* [b]	J
					20	4.1†, [j]	*in vivo* [b]	J
					13	4.1†, [j]	*in vivo* [b]	J
				Gentle Ben	7	4.1†, [j]	*in vivo* [b]	J
					13	4.1†, [j]	*in vivo* [b]	J

Species	Age	Mass (kg)	Sample (n)	TLC (L)	DLV (L)	DLV O_2 store (mL kg^{-1})	Method	Reference
					8	4.1[†,j]	*in vivo* [b]	J
				Ringo	5	4.1[†,j]	*in vivo* [b]	J
					13	4.1[†,j]	*in vivo* [b]	J
					6	4.1[†,j]	*in vivo* [b]	J
Otariids								
Northern fur seal *Callorhinus ursinus*	mixed	153.5[†]	4	20.45[†]	10.2[††]	10.0 [j]	postmortem [a]	C
Steller sea lion *Eumetopias jubatus*	mixed	36.3[†]	4	4.22[†]	2.1[††]	8.7 [j]	postmortem [a]	C
	neonatal	22[†]	1	1.96[†]	1.0[††]	6.7 [j]	postmortem [a]	C
Odobenids								
Walrus *Odobenus rosmarus*	mixed	64.5[†]	3	7.45[†]	3.7[††]	8.7 [j]	postmortem [a]	C
Mustelids								
Northern sea otter *Enhydra lutris lutris*	adult	27.6[†]	3	9[†]	5.7	31.0 [j]	postmortem [a]	C
Southern sea otter *Enhydra lutris nereis*	neonatal	2.6 ± 0.18[†]	5			42.7 ± 3.09 [k]	postmortem[i]	K
	small pup	4.4 ± 0.30[†]	2			48.7 ± 7.31 [k]	postmortem[i]	K
	large pup	8.5 ± 0.62[†]	4			41.6 ± 4.56 [k]	postmortem[i]	K
	juvenile	12.2 ± 0.99[†]	3			41.6 ± 1.60 [k]	postmortem[i]	K
	adult	19.9 ± 1.01[†]	6			31.1 ± 2.30 [k]	postmortem[i]	K

References: A: this study; B: Lydersen et al., 1992; C: Lenfant et al., 1970; D: Burns et al., 2005; E: Noren et al., 2005; F: Reed et al., 1994; G: Burns et al., 2007; H: Burns and Castellini, 1996; I: Falke et al., 2008; J: Kooyman et al., 1971; K: Thometz et al., 2015; L: Kooyman and Sinnett, 1982. Values represented within parentheses were back-calculated from diving lung volumes.

[a] Inflation of excised lungs via water displacement; [b] Nitrogen washout; [c] Author calculated or used values based on allometric equations established in other studies; [d] Author calculated based on allometric equations established from study itself; [e] Used combination of inflation of excised lungs and calculations from allometric equations established from study itself; [f] *In vivo* biomedical imaging; [g] Whole body plethysmography; [h] Pneumotachograph; [i] Used body size, lung mass, and empirical measures of lung volume to calculate TLC and DLV; [j] Value calculated here from usable O_2 and body mass. Mass-specific DLV O_2 store from southern sea otters used to calculate mass-specific DLV O_2 store for northern sea otters; [k] Value reported in original publication referenced; [†] Published value was either a mean with no individual value available or was given as a range with only one value for TLC calculated; in these cases, sample size is given; [††] Value calculated here based on assumption that DLV for pinnipeds is 50% of TLC, with 15% of DLV being usable O_2 for oxygen exchange (Kooyman, 1989). Usable O_2 (liters) for northern sea otters calculated from mass-specific DLV of southern sea otter adults measured in Thometz et al., 2015

Table S2 References

Burns, J. M. and Castellini, M. A. (1996). Physiological and behavioral determinants of the aerobic dive limit in Weddell seal (Leptonychotes weddellii) Pups. *J. Comp. Physiol. B* **166**, 473–483.

Burns, J. M., Costa, D. P., Frost, K. and Harvey, J. T. (2005). Development of Body Oxygen Stores in Harbor Seals: Effects of Age, Mass, and Body Composition. *Physiol. Biochem. Zool.* **78**, 1057–1068.

Burns, J. M., Lestyk, K. C., Folkow, L. P., Hammill, M. O. and Blix, A. S. (2007). Size and distribution of oxygen stores in harp and hooded seals from birth to maturity. *J. Comp. Physiol. B Biochem. Syst. Environ. Physiol.* **177**, 687–700.

Falke, K. J., Busch, T., Hoffmann, O., Liggins, G. C., Liggins, J., Mohnhaupt, R., Roberts, J. D., Stanek, K. and Zapol, W. M. (2008). Breathing pattern, CO2 elimination and the absence of exhaled NO in freely diving Weddell seals. *Respir. Physiol. Neurobiol.* **162**, 85–92.

Kooyman, G. L. (1989). *Diverse divers: physiology and behavior*. Berlin Heidelberg New York: Springer-Verlag.

Kooyman, G. L. and Sinnett, E. E. (1982). Pulmonary Shunts in Harbor Seals and Sea Lions during Simulated Dives to Depth. *Physiol. Zool.* **55**, 105–111.

Kooyman, G. L., Kerem, D. H., Campbell, W. B. and Wright, J. J. (1971). Pulmonary function in freely diving Weddell seals, Leptonychotes weddelli. *Respir. Physiol.* **12**, 271–282.

Lenfant, C., Johansen, K. and Torrance, J. D. (1970). Gas transport and oxygen storage capacity in some pinnipeds and the sea otter. *Respir. Physiol.* **9**, 277–286.

Lydersen, C., Ryg, M. S., Hammill, M. O. and O'Brien, P. J. (1992). Oxygen stores and aerobic dive limit of ringed seals (Phoca hispida). *Can. J. Zool.* **70**, 458–461.

Noren, S. R., Iverson, S. J. and Boness, D. J. (2005). Development of the blood and muscle oxygen stores in gray seals (Halichoerus grypus): Implications for juvenile diving capacity and the necessity of a terrestrial postweaning fast. *Physiol. Biochem. Zool.* **78**, 482–490.

Reed, J. Z., Chambers, C., Fedak, M. a and Butler, P. J. (1994). Gas exchange of captive freely diving grey seals (Halichoerus grypus). *J. Exp. Biol.* **191**, 1–18.

Thometz, N. M., Murray, M. J. and Williams, T. M. (2015). Ontogeny of Oxygen Storage Capacity and Diving Ability in the Southern Sea Otter (Enhydra lutris nereis): Costs and Benefits of Large Lungs. *Physiol. Biochem. Zool.* **88**, 311–27.

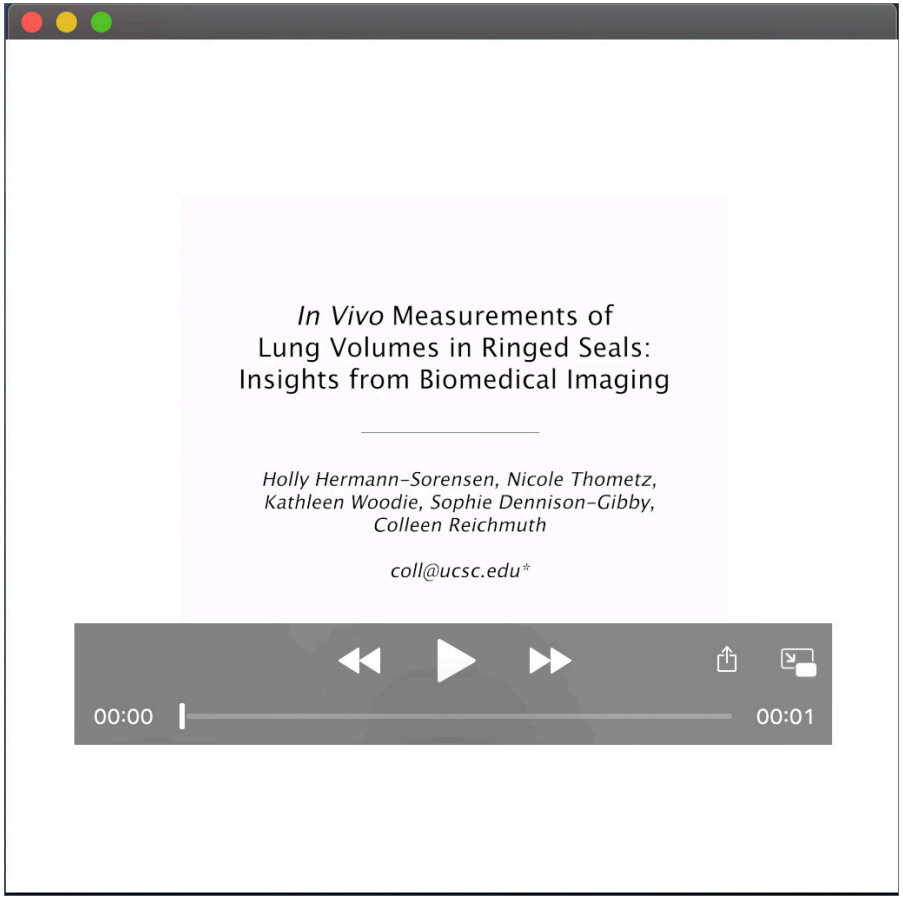

Movie 1. Three-dimensional reconstructions of ringed seal PH1802 at both inflated (0 mmHg) and inflated (30 mmHg) lung inflation pressures. The trachea is red, bronchi are yellow, and lungs are blue.

Hartwick M, Reichmuth C, Thometz NM (2021) Using physiological measures of captive seals to inform best practices of rapid body condition assessments of wild Arctic seals. Society for Integrative and Comparative Biology Annual Meeting, 3 January-28 February.

Using physiological measures of captive seals to inform best practices of rapid body condition assessments of wild Arctic seals

Michelle Hartwick[1], Colleen Reichmuth[2,3], Nicole Thometz[1,2]

[1]University of San Francisco
[2]UC Santa Cruz
[3]Alaska SeaLife Center

Predicting population-level responses to rapidly changing Arctic conditions requires empirical demographic and physiological data. Unfortunately, Arctic seals are particularly difficult to sample in the wild due to their remote, ice-covered habitats. Further, the ongoing Unusual Mortality Event (UME) of Alaskan ice seals—declared due to abnormally high numbers of seals stranding in poor body condition—highlights the urgent need to accurately monitor the health of wild populations. Body condition is commonly assessed in seals via blubber content and provides an important metric of individual health. As comprehensive assessments of body condition are generally not feasible to conduct during field research and subsistence activities, we evaluated the efficacy of simple metrics of body condition by comparing measurements obtained from captive seals. We used fine-scale morphometric data to calculate blubber content for one bearded (*Erignathus barbatus*), three ringed (*Pusa hispida*), and four spotted (*Phoca largha*) seals. We then ran regression analyses to evaluate how well seven different body condition metrics correlated with our comprehensive assessments of blubber content. Several simple metrics proved to be useful indicators of fat reserves. Metrics that utilized measures of blubber depth worked well across all species, while those relying on length-girth relationships were either species-specific or poor indicators. These results can refine and improve field sampling efforts and provide valuable information for conservation decision-making by management agencies as climate change continues to threaten Arctic seal populations.

Conference: Alaska Marine Science Symposium, 2021

Molting status differentially affects resting metabolism of Alaskan seals in air and water

Holly Hermann-Sorensen, Nicole Thometz, David Rosen, Colleen Reichmuth

Seals rely on thick blubber stores and regulation of peripheral blood flow to maintain thermal homeostasis and limit energetic costs. During the annual molt, seals rest out of water for extended periods to increase blood flow to the skin—providing essential nutrients and optimal temperatures for tissue regeneration—while limiting heat loss to the environment. It is unclear how Arctic seals will respond to ongoing sea ice loss and a reduction in available haul-out substrate. Seals may be forced to move with retreating sea ice, travel to terrestrial haul-outs, and/or spend increasing amounts of time in water. All of these scenarios will likely have negative energetic consequences, which may be exacerbated during the molting season. Here, we evaluate the energetic costs incurred by ice-dependent seals in air and in water, as a function of their molting status. If seals possess volitional control of heat loss via skin perfusion during molt, then metabolic costs of resting in water should be similar to costs incurred when resting in air. Alternatively, if seals have a reduced ability to regulate blood flow to the periphery during molt, then resting metabolism in water should be higher than in air. We used open-flow respirometry to measure the resting metabolic rate (RMR) of three spotted seals (*Phoca largha*) and one ringed seal (*Pusa hispida*) at the Alaska SeaLife Center. Measurements were obtained in air and in water prior to, during, and following the molting period. Resting metabolism was similar in the two mediums, with slightly higher RMR typically observed in water. However, during peak and late molting periods, RMR was notably higher in the haul-out condition compared to corresponding measurements in water. These data indicate that seals have some level of control over their peripheral blood supply and heat loss, irrespective of molting status. An improved understanding of thermoregulation in Alaskan seals as well as implications of increased time in water during molt will be required as preferred haul-out substrates continue to retreat.

The Effect of Molting Status on Resting Metabolism of Alaskan Seals In Water and During Haul Out

Holly Hermann-Sorensen [1], Nicole Thometz [1,2], David Rosen [3], and Colleen Reichmuth [1,4]

[1]University of California Santa Cruz, [2]University of San Francisco, [3]University of British Columbia, [4]Alaska SeaLife Center

ALASKA MARINE SCIENCE SYMPOSIUM

Alaskan ice seals are experiencing ongoing sea ice loss and associated reductions in available haul-out substrate. Seals will be forced to move with retreating sea ice, travel to terrestrial haul-outs, and/or spend increasing amounts of time in water. These scenarios pose potential negative energetic consequences, which may be exacerbated during the molting season. Here, we directly evaluate the energetic costs incurred by ice-associated seals in air and in water as a function of molting status.

H_0 If seals can control heat loss via skin perfusion during molt, then metabolic costs of resting in water will be similar to those costs incurred during haul out *(water ≈ air)*

H_1 If seals have a reduced ability to regulate blood flow to the periphery during molt, then metabolic costs of resting in water should be higher than in air *(water > air)*

Open-flow Respirometry

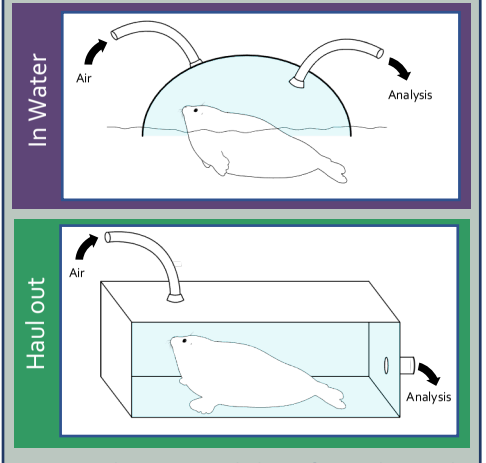

Measured resting metabolism of trained spotted and ringed seals at the Alaska SeaLife Center

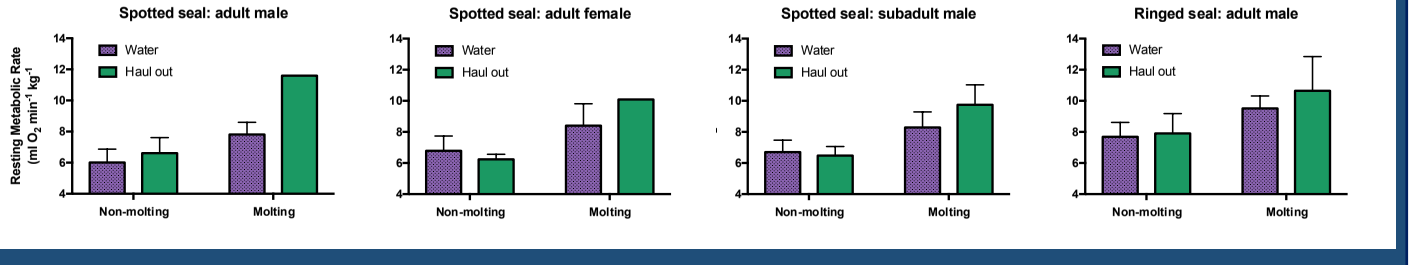

Direct measurements of Resting Metabolic Rate (RMR) are not higher when seals are in water. This supports H_0 indicating that spotted and ringed seals have control over their peripheral blood supply and heat loss, irrespective of molting status. An improved understanding of thermoregulation and the implications of increased time in water during molt will be required as preferred haul-out substrate for Alaskan seals continues to retreat.

Data collection was conducted without stress or harm to animals. This project was funded by NOAA's Alaska Pinniped Program and authorized by NMFS permit 18902, with approval from the Ice Seal Committee and IACUCs at UC Santa Cruz and the Alaska SeaLife Center. We thank our dedicated research and husbandry team, especially J. Kim, T. Abraham, J. Mullens, S. Burman, and M. Meranda. Sample sizes for non-molting RMR measurements ranged from 2 – 14 per seal; sample sizes for molting RMR measurements ranged from 1 – 7 per seal.

Alaska Marine Mammal Symposium

Cardiorespiratory patterns in resting Alaskan seals

Ryan A. Jones (Department of Ocean Sciences, University of California Santa Cruz), Madeline Meranda (ASLC and UCSC), Nicole M. Thometz (Department of Biology, University of San Francisco), Colleen Reichmuth (ASLC and UCSC)

When submerged, marine mammals enter a well-defined dive response characterized by apnea, bradycardia, and peripheral vasoconstriction. Further, phocid seals exhibit periods of apnea with accompanying physiological markers of the dive response while resting on land and ice. Given that most data have been obtained from a small number of well-studied species, relatively little is known about the cardiorespiratory patterns of seals from a comparative perspective. In the present study, paired respiratory and electrocardiogram data were obtained non-invasively from three species of Alaskan seals. Data were collected from nine healthy individuals conditioned to haul out and rest calmly on conductive electrode plates while breathing patterns were recorded. Preliminary analyses indicate that spotted seals (*Phoca largha*) show an expected bi-modal cardiorespiratory pattern during haul out with prolonged apnea (> 45 s) interrupted by extended eupnea (> 7 breaths). Heart rate in the spotted seals declined by ~ 60% during apnea. Ringed seals (*Pusa hispida*) showed similar alternating intervals of apnea and eupnea with some apparent differences, including shorter periods of apnea (> 25 s) and a higher heart rate during eupnea. Ringed seal heart rate declined by ~ 70% during apnea. The larger reduction in ringed seal heart rate when compared to spotted seals was primarily a consequence of higher heart rates during eupnea, as these species exhibited similar heart rates during apnea. In contrast to these smaller species, the bearded seal (*Erignathus barbatus*) showed an overall lower heart rate, increased and more regular breathing rate, and highly abbreviated apneustic intervals (< 10 s). Depth of bradycardia in the bearded seals was relatively shallow, with heart rate declining by only ~ 30% during apnea. These data suggest that bearded seals—the largest and most phylogenetically isolated Alaskan phocids—have a reduced innate dive response relative to that of more derived species. Ultimately, this initial description of cardiorespiratory patterns in spotted, ringed, and bearded seals contributes to our understanding of species-specific physiological adaptations to marine living.

Cardiorespiratory Patterns in Resting Alaskan Seals

Ryan A. Jones[1], Madeline Meranda[1,2], Nicole M. Thometz[3], and Colleen Reichmuth[1,2]

[1]University of California Santa Cruz, [2]Alaska Sealife Center, [3]University of San Francisco

OBJECTIVE

Most knowledge concerning the dive response in phocid seals comes from studies of a few representative species. To determine how well ice-dependent phocids fit expected patterns, we studied routine cardiorespiratory coupling in Alaskan seals with differing life histories and evolutionary adaptations for diving.

APPROACH

Electrocardiograms and respiratory behavior were recorded non-invasively from captive spotted, ringed, and bearded seals conditioned to rest calmly out of water. Instantaneous heart rate was determined from the interval between successive heart beats. Each breath was linked to the corresponding cardiac response.

FINDINGS

We observed a strongly bimodal pattern of heart rate that alternated between tachycardic (rapid heart rate) and bradycardic (slow heart rate) states in all seals. This pattern was linked to regular apneas that varied predictably in duration. While other true seals show similar adaptations for diving, these preliminary data suggest notable species differences.

Spotted Seal

Phoca largha

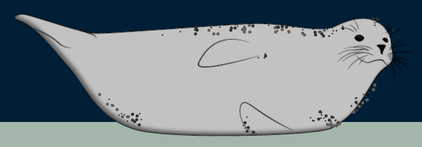

Spotted seals typically forage in the water column at depths < 100 m, with a usual duration from 3 – 4 min. These seals show evolutionarily derived features and are closely related to harbor seals.

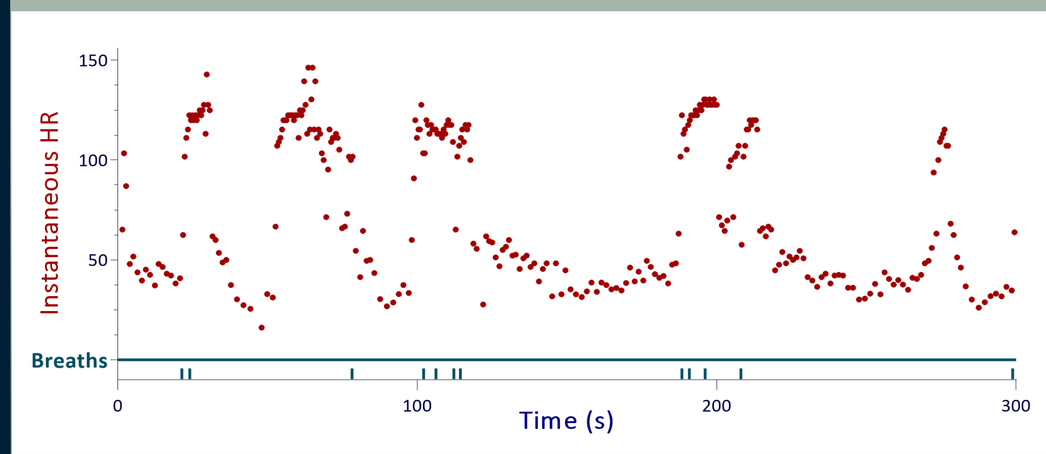

- Intermittent breathing pattern
- Clustered respirations: ~ 3 per minute
- Longer apnea duration > 45 s
- Bradycardia : Tachycardia = 40 : 120 beats per minute

Ringed Seal

Pusa hispida

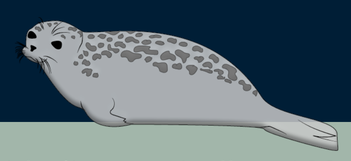

Ringed seals forage pelagically with dives typically < 100 m for 2 - 5 min. They are small phocids that rely on stable sea ice. More recently derived and closely related to other small, northern phocids.

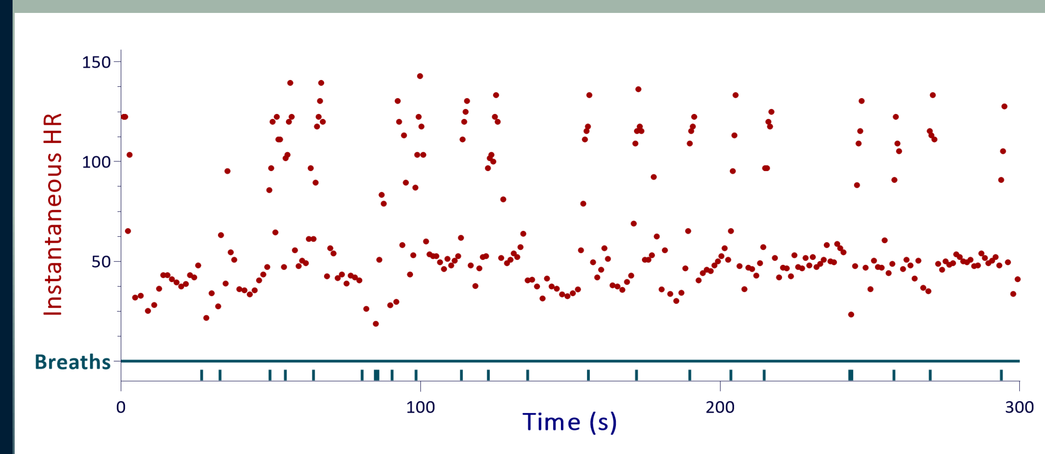

- Less intermittent breathing pattern
- Regular respirations: ~5 breaths per minute
- Moderate apnea duration < 25 s
- Bradycardia : Tachycardia = 50 : 120 beats per minute

Bearded Seal

Erignathus barbatus

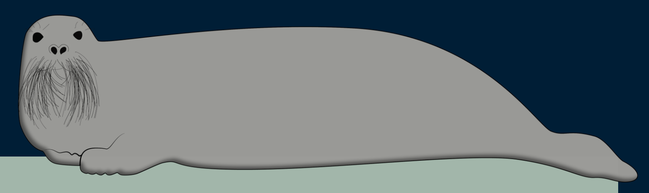

Bearded seals are an evolutionary outgroup isolated from other seals for about 14 million years. They are shallow divers (< 35 m) that forage benthically near pack ice. Dive durations are usually < 4 min.

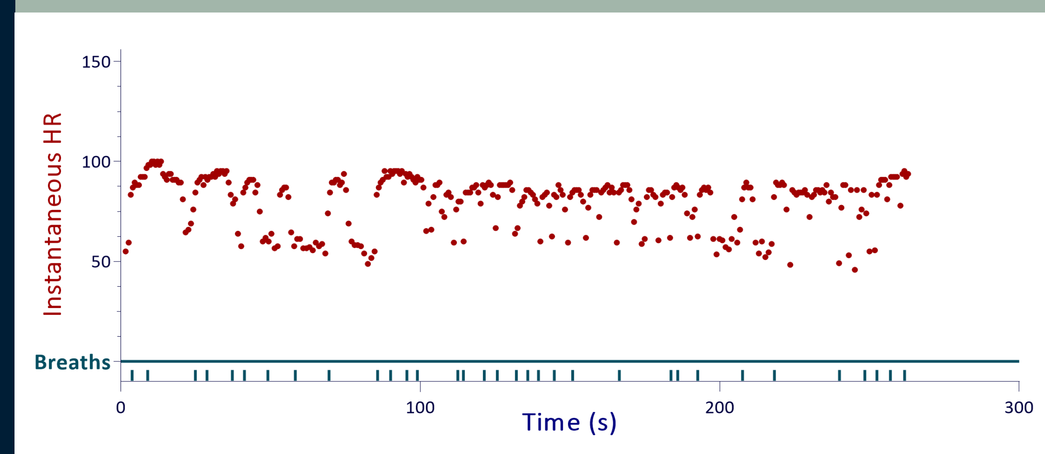

- More continuous breathing pattern
- Average Respiratory Rate: ~ 8 breaths per minute
- Brief apnea duration < 10 s
- Bradycardia : Tachycardia = 60 : 100 beats per minute

We thank our exceptional research and training teams in California and Alaska. Data were collected non-invasively and without harm to the animals. Sample size included 2-4 individuals per species. This project was supported by NOAA's Alaska Pinnipeds Program. Animal research was authorized by NMFS permit 18902 and approved by the Ice Seal Committee and IACUCs at UC Santa Cruz and the Alaska Sealife Center.

Society for Integrative and Comparative Biology

2020 Annual Meeting

Meeting Abstract

P3-116 Monday, Jan. 6 **Fiber-type profile of the *longissimus dorsi* muscle of the ringed seal**

MUKHTAR, V; DEAROLF, JL; THOMETZ, NM; BRYAN, A; REICHMUTH, C; Hendrix College, Conway, AR; Univ. of San Francisco, CA; Alaska Department of Fish and Game, Fairbanks; Univ. of California, Santa Cruz* mukhtarvv@hendrix.edu

The ringed seal (*Pusa hispida*) can dive into the ocean and forage in the water column for 8 min and dive 20 to 140 meters deep, which is greater than some other Arctic seal species. To better understand the ringed seal, we need to characterize the physiological profile of the ringed seal and determine how it could contribute to their swimming and diving behavior. The specific feature of the ringed seal that we focused on is the longissimus dorsi (LD) muscle, which is one of the muscles responsible for locomotion. We investigated the fiber-type profile of this muscle in order to ascertain how the structure of the muscle contributes to the diving behavior of the ringed seal. To determine the fiber-type profile of the ringed seal LD muscle, we froze the muscle samples from ten different specimens, cut sections from them using a cryostat, and placed the sections on microscope slides. Afterwards, we stained the sections for their myosin ATPase activity or their reaction to two myosin heavy chain antibodies, which would then be imaged. Imaging ATPase sections allowed us to count how many fast-twitch or slow-twitch fibers there were in the sections. The imaging also allowed us to measure the diameters of the fibers in ImageJ. All of these data will allow us to build a profile of the LD muscle and determine how it can contribute to the swimming and diving behavior of the ringed seal. We also will compare the fiber-type profile of the ringed seal LD with the profile of this muscle in other Arctic seal species, such as the bearded and spotted seal, to better understand the relationship between muscle characteristics and behavior.

Fiber-type Profile of the *Longissimus Dorsi* Muscle of the Ringed Seal (*Pusa hispida*)

MUKHTAR V.; DEAROLF, J.L.; THOMETZ, N.M.; BRYAN, A.; REICHMUTH, C.*
HENDRIX COLLEGE, CONWAY, AR; UNIV. OF SAN FRANCISCO, CA;
ALASKA DEPARTMENT OF FISH AND GAME, FAIRBANKS; UNIV. OF CALIFORNIA, SANTA CRUZ

Introduction

Due to global climate change, sea ice in the Arctic is diminishing (8). This sea ice is vital to many organisms that live in the Arctic, including the ringed seal (*Pusa hispida*) (**Fig. 1**). This seal is a pelagic forager, can dive 20 to 140 meters for 2 to 8 minutes (1), and uses the sea ice as a platform for its dives (4).

Figure 1. A picture of the ringed seal (*Pusa hispida*)

Because the loss of Arctic sea ice (8) will impact the continued survival of this seal, it necessitates an investigation of how these seals dive and swim, and these behaviors are made possible by their locomotor muscles.

Objective

The objective of our study was to determine the fiber-type profile of one of the ringed seal's locomotor muscles, the longissimus dorsi, as well as the sizes of the fibers that make it up. To achieve our goals, we used histo- and immunocytochemical methods.

Methods

- Ringed seal LD samples (**Table 1**) were collected by the Alaska Department of Fish and Wildlife, shipped to Hendrix College, and stored at -20°C until used for this study.
- Samples were prepared for histo- and immunocytochemistry (2, 10).
- The sections were stained for their myosin ATPase activity (6) and reaction to two myosin heavy chain antibodies (5).

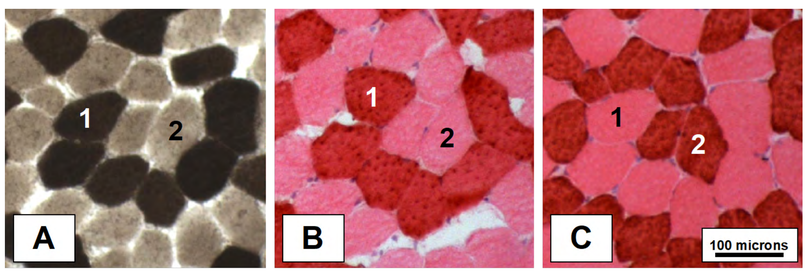

Figure 2. Representative cross-sections of ringed seal (*Pusa hispida*) longissimus dorsi muscle after histochemical and immunocytochemical staining. The LD was stained for its myosin ATPase activity (A) and for its reaction to and anti-fast IIA (SC-71) (B) and anti-slow (A4.951) (B) myosin antibodies (C). The labels 1 (type I, slow-twitch) and 2 (type IIA) indicate the same fibers on each of the images.

Methods Continued

- Digital images of the stained sections were captured (**Fig. 2**).
- Fiber-type profile and fiber diameter (Image J) data was collected from the images (10).
- Specimens were grouped into two age categories: pups (0+ years) and sub-adults and adults (> +4 years) (7).
- Average percentages and diameters (±1 S.D.) of fast- and slow-twitch fibers were calculated.

Table 1. Ringed seal (*Pusa hispida*) specimens analyzed

Specimen (I.D.)	Age Est (years)	Sex	Length (cm)
PH17GAM033	0+	Male	62.5
PH18SH013	9+	Male	138
PH18SH021	9+	Female	120
PH18SH022	0+	Male	92
PH18SH034	0+	Female	98
PH18SH035	0+	Male	90
PH18SH051	6+	Male	120
PH18SH052	0+	Male	95
PH18SH053	4+	Female	112

Results

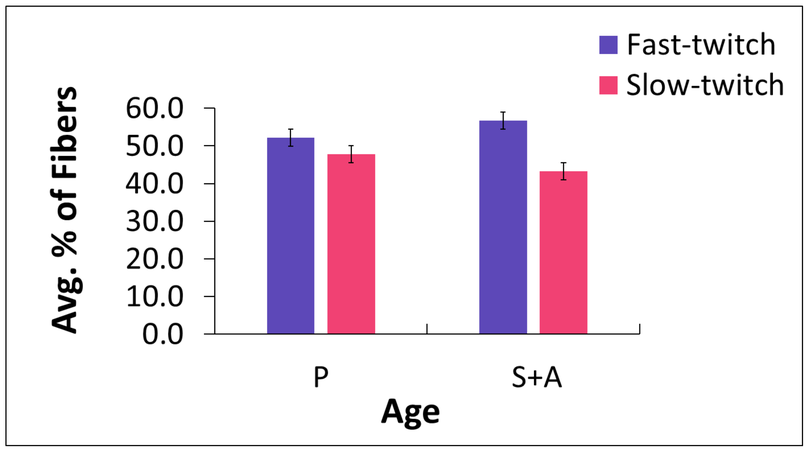

Figure 3. The average proportions of fast- and slow-twitch fibers found in the longissimus dorsi (LD) muscles of two age groups of ringed seals (*Pusa hispida*): pups (P) and sub-adults and adults (S + A). Error bars are ±1 S.D.

- The average proportions of fast-twitch IIA and slow-twitch fibers in the LD muscles of ringed seal pups were 52.2% (± S.D.) and 47.8% (± S.D.) respectively (**Fig. 3**).
- In comparison, the muscles of sub-adult and adult seals were 56.8% (± S.D.) fast-twitch IIA and 43.3% (± S.D.) slow-twitch (**Fig, 3**).
- The average diameter of fast-twitch IIA fibers in the LD muscles of ringed seal pups was 27.86 µm (± S.D.), which was slightly smaller than the slow-twitch fibers (28.68 ± S.D. µm) (**Fig. 4**).

Results Continued

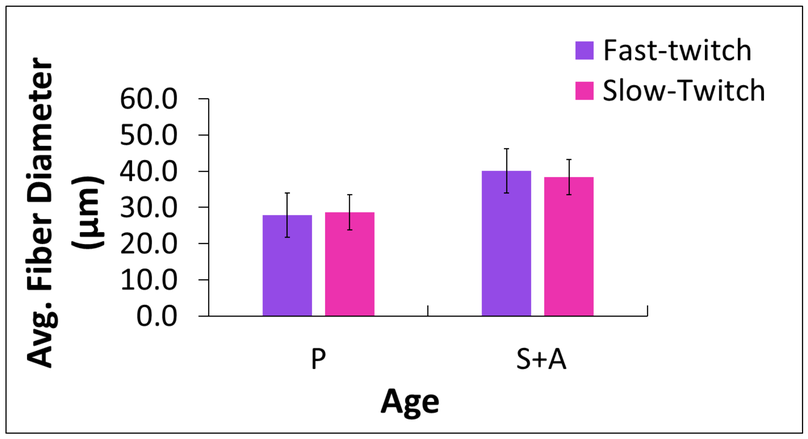

Figure 4. Average diameters (in microns) of fast- and slow-twitch fibers in the longissimus dorsi (LD) muscles of two different age classes of ringed seals (*Pusa hispida*): pups (P) and sub-adults and adults (S + A). Error bars are ±1 S.D.

- In comparison, the fast-twitch IIA fibers (40.09 ± S.D. µm) in the muscles of sub-adult and adult seals were slightly larger than the slow-twitch fibers (38.35 ± S.D. µm) (**Fig. 4**).

Discussion

The fiber-type profile of the ringed seal LD (**Fig. 3**) is similar to the profile of the harbor seal's epaxial muscle, which is 52.8% type IIA fast-twitch (11). The harbor seal can dive 5 to 100 meters for an average of 2 to 8.5 minutes, which is similar to the ringed seal's diving behavior (3,1). This muscle composition is indicative of mammals that are built for sustained, aerobic exercises, which is consistent with the diving of ringed seals (11).

Diameters of fibers in the ringed seal pup LD are smaller than those in the adult muscle (**Fig 4)**. This increase in fiber size with age is also seen in Northern elephant seals (9). It is hypothesized that larger fibers are an oxygen conserving mechanism (9), which could aid in the diving behavior of ringed seals.

Acknowledgements

The ringed seal LD muscle samples were obtained under NMFS Permit 15324, with a corresponding LOA from the NMFS West Coast Region. We thank the subsistence hunters of Point Hope, Alaska, Lori Quakenbush, the Alaska Department of Fish and Game's Arctic Marine Mammals Program, and the Ice Seal Committee for enabling this research. The authors would also like to thank Elijah Ballard, Lindsey Barrett, McKenzie Fletcher, and Sundus Nazar for their assistance in the lab. This project was funded in part by the Hendrix College Odyssey Program.

References

1. Crawford JA, et al. 2010. Polar Bio 42: 65-80.
2. Dearolf JL. 2003. J Morph 256: 79-88
3. Eguchi T, Harvey JT. 2005. Marine Mammal Science 21: 283-295
4. Gjertz I, et al. 2000. Polar Biol 23: 651-656.
5. Gurley CM. 2011. Pers. comm.
6. Hermanson JW, Hurley KJ. 1990. Acta Anat 137:146-156.
7. Jansen JK, et al. 2010. NOAA Tech Memo. NMFS-AFSC-212.
8. Mioduszewski JR, et al. 2019. Cryosphere 13: 113-124
9. Moore CD, et al. 2014. Front Physiol 5: 217
10. Thometz NM, et al. 2018. J Comp Physiol B 188:177-193.
11. Watson RR, et al. 2003. Journal of Exp Bio 206: 4105-4111.

Society for Integrative and Comparative Biology

2020 Annual Meeting

Meeting Abstract

P3-115 Monday, Jan. 6 **Fiber-type profile of the locomotor muscle of spotted seals** *NAZAR, S*; DEAROLF, JL; THOMETZ, NM; BRYAN, A; REICHMUTH, C; Hendrix College, Conway, AR; Univ. of San Francisco, CA; Alaska Department of Fish and Game, Fairbanks; Univ. of California, Santa Cruz* nazarss@hendrix.edu

Spotted seals (*Phoca largha*) can forage in the water column for 1 to 4 minutes and dive to a depth of 4 to 50 meters. Sea ice plays a significant role in the lives of spotted seals, as they depend heavily on it for reproduction and even molting. Climate change and global warming are two of the biggest environmental concerns for spotted seals, as they both directly affect the formation and melting of seasonal sea ice, the habitat for these seals. In order to develop new conservation strategies for spotted seals and to learn more about how climate change is affecting them, it is important to study their unique anatomy and physiology. In this study, we examine the fiber-type profile of a locomotor muscle of spotted seals, the longissimus dorsi (LD). We cut sections of ten spotted seal LD muscles in the cryostat and put them on microscopic slides. We then stained these sections of the LD muscles for their myosin ATPase activities, as well as their reaction to two myosin heavy chain antibodies (A4951-slow, type I myosin, SC71-fast, type IIa myosin). We also captured digital images of the stained slides, categorized fibers based on their dark and light staining, and counted them.. We also measured the diameters of the fibers using ImageJ. The fiber-type profile and fiber diameters of the LD muscle will be compared to those of two other Arctic seals to examine patterns in these features. Therefore, studying the fiber-type profile of the LD will enable us to learn more about the swimming and diving behavior of spotted seals.

Fiber-type profile of the locomotor muscle of spotted seals (*Phoca largha*)

NAZAR S.; DEAROLF, J.L.; THOMETZ, N.M.; BRYAN, A.; REICHMUTH, C.*
HENDRIX COLLEGE, CONWAY, AR; UNIV. OF SAN FRANCISCO, CA;
ALASKA DEPARTMENT OF FISH AND GAME, FAIRBANKS; UNIV. OF CALIFORNIA, SANTA CRUZ

Introduction

The spotted seal (*Phoca largha*) (**Fig. 1**)
- is an Arctic marine mammal
- uses sea ice seasonally as a diving platform
- dives to depths of 4 to 50 meters (1)
- forages for 1 to 4 minutes (1)

Figure 1. Photo of a spotted seal, the subject of this study.

The swimming and diving of these animals is:
- powered by locomotor muscles, including the *longissimus dorsi* (LD)
- of concern, because climate change is affecting the formation and melting of sea ice (2), their diving platform

Objective

The purpose of this study is to determine the fiber-type profile of the spotted seal LD using histo- and immunocytochemical methods to better understand the swimming and diving abilities of these marine mammals.

Methods

- Spotted seal LD samples (**Table 1**) were collected by the Alaska Department of Fish and Wildlife, shipped to Hendrix College, and maintained at -20°C until used for this study.
- Samples were prepared for histo- and immuno-cytochemistry (3).

Table 1. *Phoca largha* specimens utilized in this study

Specimen I.D.	Age (Years)	Sex	Standard Length (cm)
PL17GAM007	0+	F	65.5
PL18SHO49	2+	M	127
PL18SHO65	3+	M	147
PL18SHO19	4+	F	157
PL18SHO64	4+	F	149
PL18SHO23	4+	F	141
PL18SHO76	5+	M	155
PL18SHO32	5+	F	171

Methods Continued

- Sections were stained for their:
  - myosin ATPase activity (4)
  - reaction to anti-myosin antibodies [SC-71 (fast-twtich IIA) and A4.951 (slow-twitch)] (5)
- ATPase (**Fig. 2**) and antibody stained sections were imaged using a Zeiss AxioImager A1 microscope and Axiovision software (v. 4.7).
- Fiber-type profile and fiber diameter data (ImageJ) were collected from the images (3).
- Specimens were grouped into two age categories: 0+ years (pups) and > 2 years (sub-adults and adults) (1).
- Average percentages and diameters (±1 S.D.) of fast- and slow-twitch fibers were calculated.

Figure 2. Representative cross-section of spotted seal *longissimus dorsi* (LD) muscle after staining for its myosin ATPase activity after basic pre-incubation. Labels: IIA – fast-twitch IIA fiber; I – slow-twitch fiber

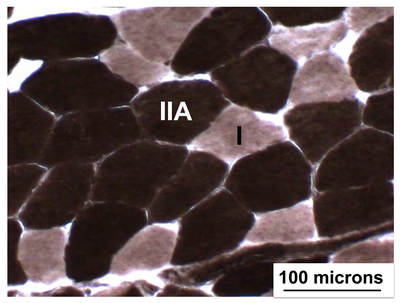

Results

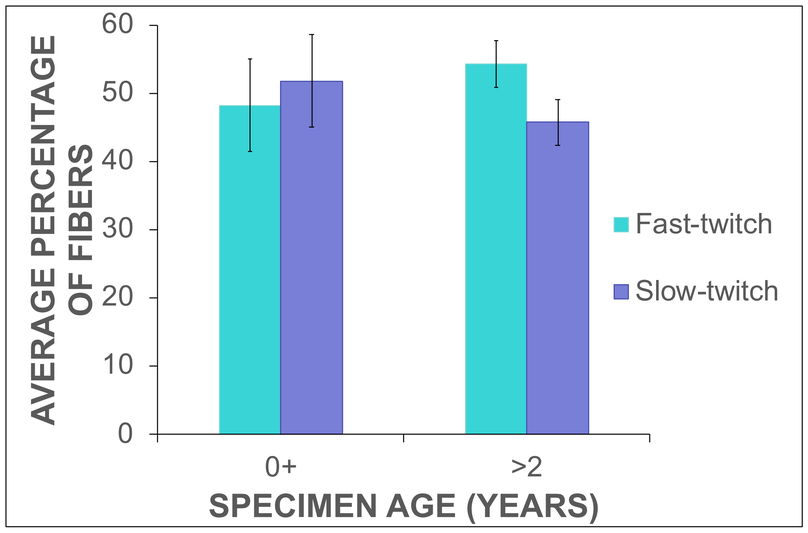

Figure 3. Average percentages of fast- and slow-twitch fibers in the *longissimus dorsi* muscle of spotted seals aged 0+ years and > 2 years. Error bars are ±1 S.D.

- The LD of spotted seals aged 0+ was 48.2 (± 6.8)% fast- (IIA) and 51.8 (± 6.8)% slow-twitch (**Fig. 3**).
- Similarly, the fiber-type profile of seals aged > 2 years was 54.3 (± 3.4)% fast- (IIA) and 45.7 (± 3.4) % slow-twitch (**Fig. 3**).
- Overall, the fiber-type profile of the spotted seal LD was 53.6 (± 3.8)% fast-twitch (IIA) (**Fig. 3**).
- The fast-twitch fibers (29.3 ± 5.8 μm) in the LD of spotted seals aged 0+ were smaller than the slow-twitch fibers (36.6 ± 5.7 μm) (**Fig. 4**).

Results Continued

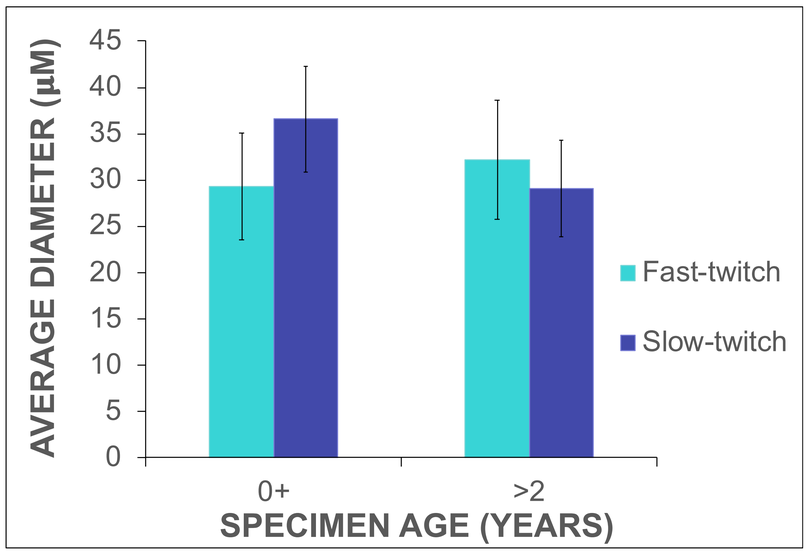

Figure 4. Average fiber diameters (in μm) of fast- and slow-twitch fibers in the *longissimus dorsi* muscle of spotted seals aged 0+ years and > 2 years. Error bars are ±1 S.D.

- In contrast, the fast-twitch fibers (32.2 ± 6.4 μm in the muscles of seals aged > 2 years were larger than the slow-twitch fibers (29.1 ± 5.2 μm) (**Fig. 4**).

Discussion

The average fiber-type profile of the spotted seal LD, regardless of age, was 53.6 (± 3.8)% fast-twitch (IIA) (**Fig. 3**). This profile is similar to the fiber-type profile of harbor seal epaxial muscle [52.8% IIA fibers (6)]. Thus, a locomotor muscle composed of approximately 50% fast IIA fibers seems to be necessary for seals that dive to intermediate depths [4-100 m (1,7)].

The diameters of the fibers in the LD of spotted seals increase as the seals become adults (**Fig.4**), a trend that has been noted in the muscles of other pinnipeds (8). A possible reason for this change in fiber size with age is that larger fibers are an oxygen conserving adaptation for diving in spotted seals (8).

Acknowledgements

The spotted seal LD muscle samples were obtained under NMFS Permit 15324, with a corresponding LOA from the NMFS West Coast Region. We thank the subsistence hunters of Point Hope, Alaska, Lori Quakenbush, the Alaska Department of Fish and Game's Arctic Marine Mammals Program, and the Ice Seal Committee for enabling this research. The authors would also like to thank Elijah Ballard, Lindsey Barrett, McKenzie Fletcher, and Vaneeza Mukhtar for their assistance in the lab. This project was funded in part by the Hendrix College Odyssey Program.

References

1. Boveng JL, et al. 2009. NOAA Technical Memorandum NMFS-AFSC-200. 155 p.
2. Mioduszewski JR, et al. 2019. Cryosphere 13:113-114.
3. Thometz NM, et al. 2018. J Comp Physiol B 188:177-193.
4. Hermanson JW, Hurley KJ. 1990. Acta Anat 137:146-156.
5. Gurley CM. 2011. Pers. comm.
6. Watson RR, et al. 2003. J Exp Biol 206:4105-4111.
7. Eguchi T, Harvey JT. 2005. Mar Mamm Sci 21:283-295.
8. Collby DM. et al. 2014. Front Physiol 5:217

Society for Integrative and Comparative Biology

2020 Annual Meeting

Meeting Abstract

P3-113 Monday, Jan. 6 **Fiber-type profile of bearded seal (*Erignathus barbatus*) longissimus dorsi muscle** *FLETCHER, ML*; BARRETT, LM; DEAROLF, JL; THOMETZ, NM; BRYAN, A; REICHMUTH, C; Hendrix College, Conway, AR; Univ. of San Francisco, CA; Alaska Department of Fish and Game, Fairbanks; Univ. of California, Santa Cruz* fletcherml@hendrix.edu

Bearded seals (*Erignathus barbatus*) are benthic-feeding, Arctic pinnipeds that typically do not dive past 100 meters. Knowing the physiology of their locomotor muscles could increase our understanding of how they dive, feed on the bottom, and swim between their feeding grounds and haul-out sites. Thus, the goal of this project was to quantify the percentages of slow- and fast-twitch fibers in the longissimus dorsi (LD) muscle of bearded seals. To achieve this goal, 9 and 11 µm thick sections of bearded seal LDs were cut with a cryostat and stained for their myosin ATPase activity after basic incubation. Additional sections were stained for two different myosin heavy chain antibodies: SC-71(anti-fast-twitch type 2A myosin) and A4951(anti-slow-twitch type 1 myosin). All of the stained sections were then imaged, and images of the three stains were taken from identical regions in each section. The images of the ATPase-stained tissue were used to identify and count darkly (fast-twitch) and lightly (slow twitch) staining fibers, as well as intermediately staining fibers. These data were used to determine the average percentages of these fibers in the LDs of bearded seals. We also used ImageJ software to measure the diameter of each type of fiber. The fiber-type profile of the bearded seal LDs, as well as the sizes of the fibers, will be compared to those of the LDs of two other Arctic seals, ringed and spotted. This comparison will allow us to identify any differences in these features between their locomotor muscles that may underlie the differences in swimming and diving abilities that exist between these three Arctic seal species.

Fiber-type profile of bearded seal (*Erignathus barbatus) longissimus dorsi muscle*

FLETCHER, M.F.; DEAROLF, J.L.; THOMETZ, N.M.; BRYAN, A.; REICHMUTH, C.*
HENDRIX COLLEGE, CONWAY, AR; UNIV. OF SAN FRANCISCO, CA;
ALASKA DEPARTMENT OF FISH AND GAME, FAIRBANKS; UNIV. OF CALIFORNIA, SANTA CRUZ

Introduction

Bearded seals (*Erignathus barbatus*) are benthic-feeding, Arctic pinnipeds (1) (**Figure 1**). They use sea ice to move between the ocean and ice caps in order to hunt and avoid predators, as well as for giving birth to their young and resting. Unfortunately, climate change has caused Arctic sea ice to decrease over 40% since 1979 (2), a change that may negatively impact bearded seals. Thus, the loss of Arctic sea ice (2), the diving platform of bearded seals (3), makes understanding how these marine mammals forage, dive, and travel between the ice and ocean critical.

Figure 1. Photo of a bearded seal, the subject of the study.

Objective

To investigate the swimming and diving of bearded seals, we are studying the fiber-type profile (percent fast- and slow-twitch fibers) and diameters of the fibers making up one of their locomotor muscles, the longissimus dorsi (LD). We will determine these characteristics by imaging sections of this muscle stained for their myosin ATPase activity and reaction to myosin heavy chain antibodies. These procedures will allow us to quantify the proportions of slow- and fast-twitch fibers in the muscle and measure their sizes.

Methods

Bearded seal LD samples were collected by the Alaska Department of Fish and Wildlife, shipped to Hendrix College, and maintained at -20°C until needed for this study. Samples were prepped for histo- and immuno-cytochemistry (4, 5).

For each specimen, we cut seven 9 μm and 11 μm thick sections and put each pair of sections on slides. These sections were stained for their myosin ATPase activity (5) and their reaction to anti-myosin antibodies [SC-71 (fast-twitch IIA) and A4.951 (slow-twitch)] (6).

The myosin ATPase stained sections, along with the antibody stained sections were imaged using a Zeiss AxioImager A1 microscope and Axiovision software (v. 4.7). Multiple sets of images were taken from identical regions of the tissue to compare the ATPase and antibody staining for each specimen.

Fiber-type profile (**Figure 2**) and fiber diameter data (ImageJ), were collected using images of identical sections stained for their myosin ATPase activity and their reaction to anti-myosin antibodies (4).

Methods Continued

Specimens were grouped into two age categories: sub-adult and adult (7). Twelve sub-adults and 10 adults were studied. Average percentages and diameters (±1 S.D.) of fast- and slow-twitch fibers were calculated.

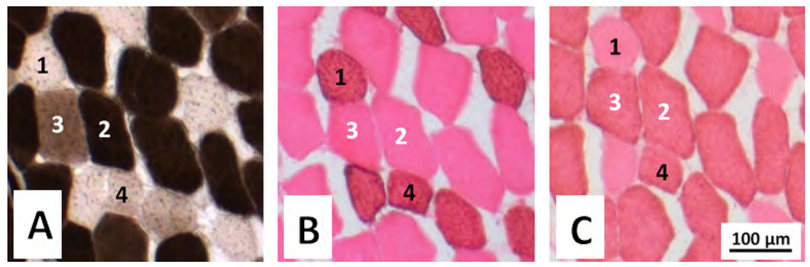

Figure 2. Representative cross-sections of bearded seal (*Erignathus barbatus*) longissimus dorsi (LD) muscle after staining. The LD muscle was stained for its myosin ATPase activity after basic pre-incubation (A), as well as for its reaction to anti-slow (A4.951) (B) and anti-fast IIA (SC-71) myosin antibodies (C). Labels 1 (type I, slow-twitch), 2 (type IIA - dark, fast-twitch), 3 (type IIA - intermediate, fast twitch), and 4 (type I, slow-twitch) indicate the same fibers in each image.

Results

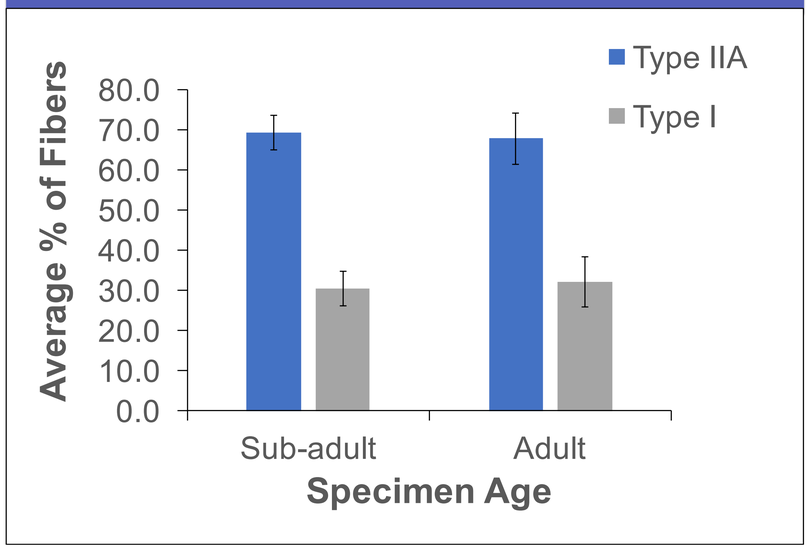

Figure 3. Average percentages of fast-twitch, type IIA, and slow-twitch, type I, in the longissimus dorsi muscle of sub-adult and adult bearded seals (*Erignathus barbatus)*.

- Sub-adult bearded seal LD muscles averaged 69.5% type IIA and 30.5% type I fibers (± 4.3) (**Fig. 3**).
- In comparison, the adult muscles were 67.8% type IIA fibers and 32.2% type I fibers (± 6.3) (**Fig. 3**).
- The average type IIA fiber diameter in sub-adults was 42.7 μm (± 8.9), which was slightly larger than the type I fibers (39.9 μm ± 6.5) (**Fig. 4**).
- In the adult muscles, the type IIA fibers (49 μm ± 9.0), were also slightly larger than the type I fibers (44.1 μm ± 8.4) (**Fig. 4**).

Results Continued

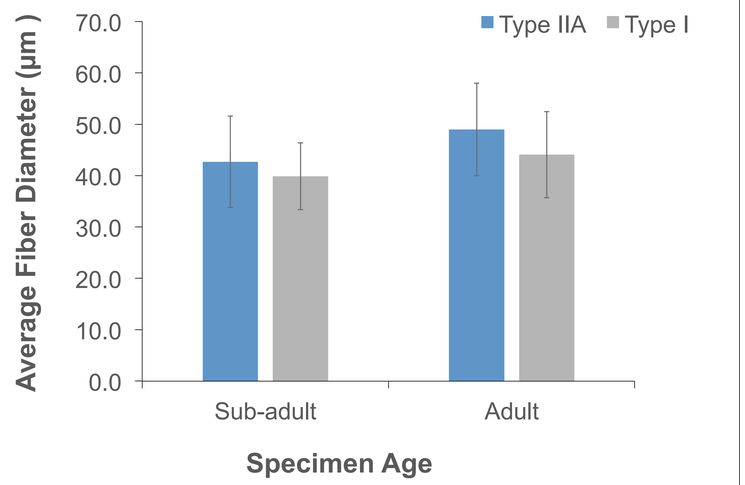

Figure 4. The average diameter (μm) of fast-twitch, type IIA, and slow-twitch, type I, fibers in the longissimus dorsi muscle of sub-adult and adult bearded seals (*Erignathus barbatus).*

Discussion

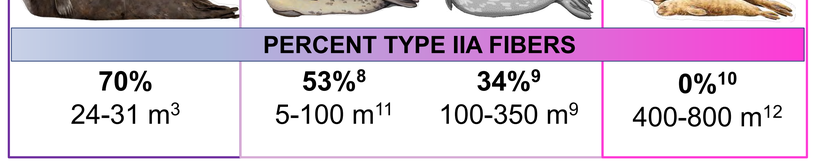

Figure 5. Seal muscle fiber-type profiles and diving depths.

Bearded seal LD muscles are comprised of roughly 70% type IIA fibers, regardless of age (**Fig. 3**). This proportion of type IIA fibers is greater than the proportions found in the muscles of other pinnipeds (**Fig. 5**). This difference in fiber-type profile may be due to the benthic, shallow diving (3) feeding strategy of bearded seals.

The type IIA fibers are slightly larger than the type I fibers, which is a trend seen in both adults and sub-adults, with adults having slightly larger fiber sizes than sub-adults (**Fig. 4**). This trend is consistent among other pinnipeds, such as the Northern Elephant seal (10).

Acknowledgements

The bearded seal LD muscle samples were obtained under NMFS Permit 15324, with a corresponding LOA from the NMFS West Coast Region. We thank the subsistence hunters of Point Hope, Alaska, Lori Quakenbush, the Alaska Department of Fish and Game's Arctic Marine Mammals Program, and the Ice Seal Committee for enabling this research. The authors would also like to thank Lindsey Barrett, Elijah Ballard, Vaneeza Mukhtar, and Sundus Nazar for their assistance in the lab. This project was funded in part by the Hendrix College Odyssey Program.

References

1. Kovacs, KM. 2002. In: Perrin WF, Würsig B, Thewissen JGM, editors. Academic Press. p 84-87.
2. Stroeve, JC, et al. 2012. Climatic Change 110:1005–1027.
3. Hamilton, CD, et al. 2018. Scientific Reports 8:16988.
4. Thometz NM, et al. 2018. J Comp Physiol B 188:177-193.
5. Dearolf, JL. 2003. J Morph 256:79-88
6. Gurley CM. 2011. Pers. comm.
7. Cameron MF, et al. 2010. NOAA Tech. Memo.
8. Watson RR, et al. 2003. J Exp Biol 206:4105-4111.
9. Kanatous SB, et al. 2002. J Exp Biol 205:3601-3608.
10. Moore SE, Huntington HP. 2008. Front Physiol 12: https://doi.org/10.3389/fphys.2014.00217.
11. Eguchi T, Harvey JT. 2006. Mar Mamm Sci 21:283-295.
12. Hindell MA. 2002. In: Perrin WF, Würsig B, Thewissen JGM, editors. Academic Press. p 370-373.